Master's thesis

NTNU
Norwegian University of Science and Technology
Faculty of Engineering
Department of Civil and Environmental Engineering

Merhawi Berhe Geberegergis

Modelling inflow to culverts for E6, Helgeland Sør

Master's thesis in Hydropower Development
Supervisor: Prof. Knut Alfredsen
June 2020

NTNU
Norwegian University of
Science and Technology

Merhawi Berhe Geberegergis

Modelling inflow to culverts for E6, Helgeland Sør

Master's thesis in Hydropower Development
Supervisor: Prof. Knut Alfredsen
June 2020

Norwegian University of Science and Technology
Faculty of Engineering
Department of Civil and Environmental Engineering

NTNU
Norwegian University of
Science and Technology

NTNU
Norwegian University of
Science and Technology

Faculty of Engineering
Science and Technology
Department of Hydraulic and
Environmental Engineering

M.Sc. THESIS IN HYDROPOWER DEVELOPMENT

Candidate: **Merhawi Berhe Geberegergis**

Title: Modelling inflow to culverts for E6, Helgeland Sør.

1 BACKGROUND

The ability to estimate flow in ungauged catchments is one of the major challenges in hydrology. This is particularly an issue in small catchment were few measurements are available and catchment responses are fast and short time steps are needed. A particular issue in small ungauged catchments is related to flood calculations. Today a number of methods are used, e.g. the rational method or the PQRUT flood model. Both of these are event based and have issues related to the antecedent conditions in the catchment at the start of the event.

Over the latest years the ability to use the DDD hydrological model for simulating flow in small ungauged catchments with an hourly time step has been developed and tested in Work Package 2 the Klima2050 centre (http://www.klima2050.no). This will potentially allow us to simulate extremes in a continuous model which can improve the design flood computation and also let us investigate the effects of catchment wetness and other catchment conditions.

In the Klima2050 center a number of pilot projects have been defined to test methods developed in the center on practical cases. One such pilot is the new E6 in the southern part of Helgeland. Here a number of culverts is constructed, and the purpose of this project is to set up DDD and do flood calculations for some of these culverts.

2 MAIN QUESTIONS FOR THE THESIS

The thesis shall cover, though not necessarily be limited to the main tasks listed below. The following main steps will be carried out during the thesis work:

1. A brief overview of the status of flood computations in small ungauged catchments. This should describe methods, data needs and issues related to the computations.

2. The DDD model should be established for a number of the small catchments draining into culverts along this section of E6. Model parameters should be computed using the methods described by Tsegaw (2019a), and the dynamic river network method should be used (Tsegaw 2019b). Rainfall and temperature should be taken from the SeNorge2.0 gridded database. The possibility to evaluate the model should be investigated.

3. For a further evaluation, the model should be set up for a couple of gauged catchments in the same area and the simulated flow using the transfer method described by Tsegaw should be computed. This should then be compared to observations as a control.

4. Design precipitation events should be established for each of the culverts from 2) and peak flood should then be computed using the model with different antecedent conditions. A comparison should be made between the flood computed for a wet catchment, a dry catchment and during snow melt. These should be evaluated against the design floods computed by the consultant on the project.

5. Evaluate the DDD model simulation against other methods for design flood computation, using the findings from 1) to select methods.

6. Report the findings in a thesis and document all model setups and data used. The models with data should all be delivered as a part of the work, and the report should contain the necessary information needed to run them.

3 SUPERVISION, DATA AND INFORMATION INPUT

Professor Knut Alfredsen will be the supervisor the thesis work.

Discussion with and input from colleagues and other research or engineering staff at NTNU, SINTEF, power companies or consultants are recommended. Significant inputs from others shall, however, be referenced in a convenient manner.

The research and engineering work carried out by the candidate in connection with this thesis shall remain within an educational context. The candidate and the supervisors are therefore free to introduce assumptions and limitations, which may be considered unrealistic or inappropriate in a contract research or a professional engineering context.

4 REPORT FORMAT AND REFERENCE STATEMENT

The thesis report shall be in the format A4. It shall be typed by a word processor and figures, tables, photos etc. shall be of good report quality. The report shall include a

summary, a table of content, a list of literature formatted according to a common standard and other relevant references. A signed statement where the candidate states that the presented work is his own and that significant outside input is identified should be included.

The report shall have a professional structure, assuming professional senior engineers (not in teaching or research) and decision makers as the main target group.

All data and model setups should be compiled, documented and submitted with the thesis.

The thesis shall be submitted no later than __ of June 2020.

Trondheim 13th of January 2020

_____

Knut Alfredsen
Professor

DECLARATION OF AUTHORSHIP

I, Merhawi Berhe Geberegergis, declare that I am the sole author of the thesis titled

"Modelling inflow to culverts for E6, Helgeland Sør"

That has been submitted to Norwegian University of Science and Technology (NTNU) on 23rd of June 2020, in partial fulfillment of the requirements of M.Sc. degree in Hydropower Development.

I have duly acknowledged the work of any other authors, in accordance with the standard referencing practices.

ABSTRACT

The estimation of flood peak discharge is a primary and vital step which is required in the design and safety assessment of hydraulic structures. The commonly used methods for estimating the flood peaks in small ungauged catchments such as rational method and the Norwegian rainfall-runoff model, PQRUT, are simple event based methods that contain parameters difficult to estimate and/or have an issue related to the pre-event antecedent moisture conditions. The continuous hydrological models for estimating the design flood discharges have been getting more attention recently. In this study, the DDD continuous hydrological model on an hourly time step is applied for estimating the 200-year flood peak discharges for seven small ungauged catchments located in Norway. The DDD model parameters have been determined by regionalization methods, the combination of the multiple-regression method and the pooling group-based physical similarity method. The DDD model performance was tested in another two gauged catchments at around the same area prior to flood peak estimation for the study catchments. The regionalized DDD model simulation reproduced the observed discharges satisfactorily ($0.5 \leq KGE \leq 0.75$) for both test catchments. The study analyzed the effect of pre-event catchment conditions on generating flood peak discharges. Application of the DDD model indicated high sensitivity to the catchment condition. The results show that flood peak estimate produced by a combination of design rainfall and snowmelt condition contributed to the potential flood peaks, whereas the combination of design rainfall with dry catchment conditions gave the lowest flood peak results. The computed flood estimates using the DDD model were compared to an existing design flood estimates by three methods, namely; the rational method, NIFS formula and regional analysis. The DDD model flood peak estimates showed a discrepancy in the catchment size. Robust flood peak estimates using the model produced during the combination of design rainfall and snowmelt condition for the three relatively bigger catchments. In contrast, the DDD model resulted in an underestimation of flood peaks more often in the two tiny catchments.

Keywords: Flood peak discharge, Small ungauged catchments, Design precipitation, Catchment condition, Regionalization, DDD model

ACKNOWLEDGEMENTS

At the very outset, honours with praise to the Almighty God who enabled me to complete my study and for fulfillment of my wishes.

I am extremely grateful to my supervisor Prof. Knut Alfredsen, (NTNU) for his valuable advices, guidance and providing all necessary materials needed during the thesis work.

My heartfelt gratitude to Dr. Aynalem Tsegaw Tasachew for his time and great support with the DDD model.

I would like to thank Mr. Elhadi Mohsen Hassan Abdalla (PhD candidate), NTNU for his support in preparing the climate data.

My deepest thanks to NTNU in cooperation with the Norwegian Agency for Development Cooperation's (NORAD) for the financial support to cover my living expenses during my master's study.

I would like to express my warm thanks to my families and friends for your prayers and encouragements all the time.

TABLE OF CONTENTS

LIST OF FIGURES

LIST OF TABLES

NOMENCLATURE

A	Area
Ac	Critical support area
Ase	Effective lake percentage
B	Bare mountain percentage
C	Runoff coefficient
cea	Degree day factor for evapotranspiration
CFR	Degree day factor for refreezing
CDF	Cumulative distribution function
CN	Runoff curve number
CX	Degree day factor for snowmelting
DDD	Distance Distribution Dynamics (Hydrological model)
DEM	Digital Elivation Model
Dm	Mean hillslopes distance distributions
Dmax	Maximum hillslopes distance distributions
Ea	Actual evapotranspiration
Ep	Potential evapotranspiration
F	Forest percentage
Fc	Critical flux
Gscale	Scale parameter of λ
GscInt	Scale parameter of Λ
Gshape	Shape parameter of λ
GshInt	Shape parameter of Λ
H	Elevation difference in the catchment
HL	Catchment relief
IDF	Intensity–duration–frequency
KGE	Kling–Gupta Efficiency (goodness of fit criteria)
L	Length of a catchment
MAD	Mean Annual Discharge
maxDL	Maximum soil (non-marsh) distance to river networks

maxFL	Maximum river length from the outlet
maxGL	Maximum glacier distance to river networks
maxLbog	Maximum marsh Land distance to river networks
Me	Mean elevation
midDL	Mean soil (non-marsh) distance to river networks
midFL	Mean river length from the outlet
midGL	Mean glacier distance to river networks
midLbog	Mean marsh Land distance to river networks
Mp	Mean annual precipitation
NVE	The Norwegian water and Energy Directorate
OF	Saturation excess overland flow
P	Rainfall depth
Pkorr	Precipitation Correction factor
Pro	Liquid water content of snow
Q	Discharge
Qp	Peak discharge
Rs	River slope
rv	River celerity
Sq	Specific runoff
stdFL	Standard deviation river length from the outlet
stdGL	Standard deviation glacier distance to river networks
tc	Time of concentration
U	Urban percentage
Le	Effective lake percentage
Zbog	Zero fraction for marsh (zero distance to the river)
Zsoil	Zero fraction for soil (zero distance to the river)

1. INTRODUCTION

The determination of design flood is crucial for the design of hydraulic structures and has a large impact on the life of the structures. The flood peak discharge is required for planning, design and management of hydraulic structures such as dams, bridges, levees, and design of storm water drainage systems (Singh, 1988; Pilgrim and Cordery, 1993; N. Vivekanandan et al., 2016; Filipova et al., 2019). The recorded stream runoff data are essentially required to compute the design floods of river basins. However, for small ungauged catchments observed streamflow is available to a low extent (Loukas and Vasiliades, 2014; N. Vivekanandan et al., 2016). Hydrologists have recognized that flow prediction for small ungauged catchment demands modeling techniques to understand the system. Generally, there are two available methods for estimating the design floods; statistical flood frequency analysis based on recorded past events and rainfall-runoff models which require observed rainfall depth (Wilson et al., 2011). The choice of the method for flood peak computation relies on catchment size and data availability.

In the statistical flood frequency analysis, observed flood information is used to estimate the design floods with a certain return period. This method comprises a hydrologic data series either at the desired site (at-site analysis) or from one or several gauged stations within a hydrologically homogeneous region in case of no observed data or insufficient data length (regional analysis) (Wilson et al., 2011). The statistical flood frequency at-site analysis tends to use long term consistent and good quality data to estimate the design discharge produced from a river basin (Chow et al., 1988). The flood events can be analyzed essentially either in an annual maximum series or a partial-duration series (Chow et al., 1988; Filipova et al., 2019). The annual maximum series approach incorporates the maximum flood peak for each year. A partial-duration series or alternatively called peak-over-threshold (POT) is determined by considering flood peaks greater than or equal to a predefined threshold value and it is more appropriate for considering more than one flow data a year (Chow et al., 1988). The basis for defining the threshold value depends upon the investigator and the purpose of the analysis. The regional analysis aims to use flood data from one or more stations with a similar morphological and hydrological region. This approach comprises the normalized regional flood distribution or the growth curve, which is the relationship between a certain return period flood and the mean annual flood (Wilson et al., 2011).

The rainfall-runoff model is an alternative method for determining magnitude of the design floods

by incorporating design precipitations for different return periods. Rainfall-runoff modeling allows further to operate within hydrological behavior mode to establish stream discharge (Da Ros and Borga, 1997). Hydrologists have tried to distinguish and categorize rainfall-runoff modeling approaches based on their characteristics and particular approaches (Refsgaard and Knudsen, 1996; Rientjes, 2004; Beven, 2012; Singh and Woolhiser, 2002). In general, rainfall-runoff models can be classified into three groups, namely; empirical based, conceptual based and physical based methods and depending on their spatial description of catchment processes classified as lumped and distributed (Wood and O'connel, 1985; Refsgaard and Knudsen, 1996; Beven, 2012).

Empirical based modeling approach is associated with a set of equations that resides physical characteristics to simulate based on input-output pattern, that means the method typically incorporates the application of simple equations that link runoff responses to flow at the outlet of the catchment, without involving many references to hydrological processes (Wood and O'connel, 1985; Rientjes, 2004). Conceptual based modeling focuses on the system that deals with the characteristics that represent the hydrologic phenomena in simplified patterns and heuristic mathematical expressions (Wood, and O'connel, 1985; Singh, 1988; Rientjes, 2004). For example, methods such as Hydrologiska Byråns for Vattenbalansavdelning model (HBV) (Bergström, 1995), Topography based hydrologic model (TOPMODEL) (Beven, 1995) and distance distribution dynamics (DDD) (Skaugen and Onof, 2014) model. Physical based model is based on physical laws strongly dependent on the conservation equation of mass, momentum and energy to describe the “real world” physics that governs the nature and could be helpful in changed circumstances (Wood and O'connel, 1985; Rientjes, 2004).

The continuous hydrological models are engaged in a wide scope of areas ranging from water resources investigation to engineering design (Fleig and Wilson, 2013) and they are becoming embedded in flood prediction purposes. Further, the capability of hydrological models to predict stream discharges remains the most essential intention of most models. The continuous hydrological models allow the incorporation of the antecedent moisture condition and snowmelt condition in their simulation process (Filipova et al., 2019). This helps in estimating the potential flood peak discharges produced from the catchments (Stenius et al., 2015; Filipova et al., 2019). The DDD hydrological model is used in this study to estimate a 200-year flood peak discharges of several small ungauged catchments draining into culverts. DDD is a semi-distributed model, that utilizes distributed in its input data (precipitation and temperature) and the snow accumulation and

melting is carried out for each of 10 elevation zones of a catchment, and is lumped in the model parameters (Skaugen and Weltzien, 2016). The DDD model is a parsimonious rainfall-runoff model with few parameters needing regionalization, and most of its other parameters are derived from the topographical catchment characteristics and runoff recession characteristics (Skaugen and Onof, 2014). In this study, a combination of multiple regression and physical similarity through the pooling group, regionalization methods are applied to determine the DDD model parameters. According to the study of Tsegaw et al. (2019a), the DDD model underestimates flood peak events in many cases. However, in the study of Tsegaw et al. (2019b) the possibility for improving the flood peak was investigated and showed that the flood peak discharges had improved by adding the dynamic river network method into the DDD model. Therefore, the dynamic river network routine is also applied in this study.

1.1 Objectives

The first objective of this study is to compute a 200-year flood peak discharges using the DDD model with different catchment states, namely; dry catchment, wet catchment and during snowmelt condition, for several small ungauged catchments. The second objective is to compare and evaluate the DDD flood peak estimates against the existing design flood discharges calculated by Norconsult using the three methods, namely; the rational method, NIFS formula and the regional analysis.

1.2 Outline

The study is organized as follows: The first section comprises an introduction to methods for estimating the design flood discharges, and the objectives of the study. The second section contains a literature review about the methods for flood peak estimation in small ungauged catchments and the regionalization methods. The third section describes the catchment selection and the location of the catchments. The fourth section is devoted to the illustration of the method and data extraction techniques applied in the study, with a focus on describing the essential procedures to establish the DDD model requirements. Section five contains the results of the model performance in regionalization, and results of flood peak discharge simulated by the DDD model and design floods computed by Norconsult, for the study catchments. Section six is focused on the discussion of the model performance and flood peak estimates using the DDD model in comparison to the design flood results from Norconsult. Finally, conclusions are summarized in Section seven.

2. LITERATURE REVIEW

The first part in this section contains a literature review of the methods used for peak flood estimation in small ungauged catchments and previous works using the methods. The second part describes methods of regionalization with their previous regionalization performances.

2.1 Flood computation in small ungauged catchments

Small catchments are defined differently in different countries. In UK, small catchments are defined catchment areas between 20-25 km^2, in New Zealand small catchments are described less than 100 km^2, and in Norway less than 50 km^2 are distinguished as small catchments (Felig and Wilson, 2013; Midttømme et al., 2011). Flood estimation in small catchments is required for the design of culverts, small bridges, causeways, and drainage works (Pilgrim and Cordery, 1993). Estimation of floods in small ungauged catchments is known to be more challenging than the larger catchments (Marshall and Bayliss, 1994). In many cases, flow in small catchments are not measured and recorded, this limiting factor in various places makes it hard to accomplish flood and drought analysis studies (Lorenz et al., 2011; Cisty et al., 2019). The peak flow rate of surface runoff occurs in a local extreme rainfall event which makes it difficult for flood estimation in small catchments (Lorenz et al., 2011) and it is hard to capture the instantaneous peak flows. In different hydrology literature, numerous empirical methods have been developed to estimate the peak discharges produced from small ungauged catchments. The rational method, soil conversation service (SCS) method and Natural hazards-Infrastructure, Floods and Slides (NIFS) formula are commonly used amongst. The first two methods are traditional approaches mainly created in a certain region or for catchments with specific features and the third one has developed recently in Norway for the application of peak flood estimation. Besides, the PQRUT is the rainfall-runoff model used for practical applications in Norway (Wilson et al., 2011).

2.1.1 The rational method

In the history of hydrology, the rational method was the first attempt of the rainfall-runoff process by Mulvany (1850) to obtain the peak flow that could be produced from a rainfall event (Beven, 2012). The rational method has been widely used to estimate design discharge for the design of various hydraulic structures on small drainage basins. It is also well known for practical use in Norway on estimating peak flood in small catchments (Fleig and Wilson, 2013). The rational

method is a simple equation developed to estimate peak discharge for a small catchment. The equation is given as follows:

$$Q_P = C\, i\, A \tag{2.1}$$

Where, Q_P is the peak discharge (l/s), C is runoff coefficient (dimensionless), i is rainfall intensity (l/s/ha) and A is catchment area (ha). In different hydrology literatures, the method might include unit conversion factors. The formula seen in Equation (2.1) is the rational method used in Norway. For the practical application of the rational method, two fundamental ideas are incorporated in the rainfall-runoff process: the runoff coefficient, C, and the rainfall intensity, i. The runoff coefficient is the most uncertain and critical variable in the rational method (Chow et al., 1988). The runoff coefficient relates the fact that not all the rainfall directly converted to runoff, it accounts the integrated effects of catchment losses mainly due to infiltration which relies on the land cover of the catchment (O'Loughlin et al., 1996; Beven, 2012). The type of surface determines how much rainfall ingress into the soil and how much becomes runoff. Further, the selection of the runoff coefficient relies on surface imperviousness, slope, antecedent condition of the catchment and return period (Chow et al., 1988; Beven, 2012). The range of C is between 0 and 1, which implies no response and full response from the catchment respectively. Impervious surfaces such as concrete have high runoff coefficients, while cultivated lands and forests have lower values.

The simple technique to determine C can be the ratio of the total depth of produced runoff to a total depth of precipitation, for runoff produced using hydrological models, for a different set of catchment antecedent conditions. For example, the work of Blume et al. (2007) determined the runoff coefficient (C) as the ratio of an event flow to the total precipitation, for specific events. However, this way of determining C is not consistent throughout all the hydrology literatures. For instance, Young et al. (2009) criticized that this approach of determining C lead to significant underestimation of flow and suggested that C should be a function of land cover. Consistent study was followed by Dhakal et al. (2012) who concluded the volumetric C values (ratio of total runoff to total precipitation) significantly underestimates by 80% than literature-based C values (a function of landcover), for comparisons made for 90 watersheds (area from 0.8 to 440 km^2) in Texas.

For ungauged sites, determining the accurate value of C is suspicious task (Beven, 2012). For ungauged sites, a reasonable value of C can be chosen depending on the land use type and return

period. Nevertheless, for similar land cover conditions, there is a high degree of subjectivity in selecting an individual runoff coefficient value. There are many tables available for the value of C as a function of land use types, described in different hydrology textbooks. For example, typical C values for use in the rational method for various surface types are described in Chow et al. (1988) and Pilgrim and Cordery (1993). For practical use in Norway, C values for different surface types are described in the Norwegian public roads administration handbook (SVV, 2014).

The rainfall intensity, i, is the average rainfall rate over the design rainfall duration. The design rainfall duration is assumed to be equal to the time of concentration (t_c) of the catchment. The basic assumption is the peak runoff occurs at the time of concentration, t_c, when all parts of the catchment is contributing to runoff at the outlet (Chow et al., 1988). The rainfall intensity is thus selected as a function of time of concentration, t_c, and a return period, T.

The time of concentration, t_c, is the time required for a drop of water from the farthest distance of the catchment to the outlet. There are numerous empirical methods for estimating $\mathrm{t_c}$, suggested by several authors such as for urban, rural and agricultural catchments. To mention some, Kirpich (1940), Hathaway (1945), California Culverts Practice (1955), SCS (1975), and in Norway, the t_c for practical purposes from the Norwegian public roads administration handbook (SVV, 2014) is described in Section 4.7.

The relationship between the rainfall duration and the rainfall intensity is represented by intensity-duration-frequency (IDF) curves, which gives the probabilistic rainfall input for the rational method, using the return period as the measure of frequency (O'Loughlin et al., 1996). The return period, T, is the average length of time between events of similar size that equal or exceed the design magnitude. For example, a 200-year return period has an exceedance probability of 1/T percent, which is 0.5% chance of being equaled or exceeded in any one year. The return period relies on the importance of the intended end-use.

In the rational method, the rainfall intensity is assumed to be constant over the entire catchment throughout the rainfall event. This can be the main limitation for the application of the rational method for larger catchments as stated in different literature. For example, in the study of Jainet Pj (2018), the performance of rational method provided adequate match on the estimation of the peak discharge to the "kinematic wave theory" of the HEC-HMS (Hydrologic Engineering Corps

- Hydrologic Modeling System) model for small areas up to 0.8 km^2, and rational method provided greater flood peak than kinematic wave model hydrograph for catchment area above 0.8 km^2.

The performance of the rational method is not consistent in different countries and throughout different literature. For instance, Genereux (2003) found that the rational method provided lower peak discharge value than the SCS method, for a 50-year return period flood produced from 15.8 ha of watershed area in North Carolina, U.S.A. In the work of Rahman et al. (2011), the rational method gave lower peak flood than quantile regression technique (QRT), for comparisons performed for 107 catchments (areas from 8 to 1010 km^2) in Australia. On the other hand, the rational method yielded higher flood peak discharges than the NIFS formula and the regional analysis, for most of the small ungauged catchments involved in E6 Helgeland Sør project in Norway (Norconsult, 2018).

The biggest advantage of the rational method lies in its simplicity and ease of application. The application of the rational method is known to vary from place to place. For example, Pilgrim and Cordery (1993) specified that it can be applied for small (Area ≤ 25 km^2) to medium (Area ≤ 550 km^2) size catchment areas, while in Norway, according to the SVV (2014) the rational method is not recommended for catchment area larger than 5 km^2.

2.1.2 Soil Conservation Service Curve Number Method (SCS-CN)

The Soil Conservation Service Curve Number (SCS-CN) method was published in 1956 by the United States Soil Conservation Service and has since been revised several times (Mishra and Singh, 2003). It is the most widely used for computing magnitude of a flood of a certain return period for a certain rainfall event of the same return period, produced from a small ungauged watersheds (Pilgrim and Cordery, 1993). The SCS-CN utilizes the runoff curve number (CN), to relate runoff depth and rainfall during a flood event. The SCS-CN runoff equation is given in the following equation.

$$Q = \frac{(P - I_a)^2}{(P - I_a) + S} \tag{2.2}$$

In which, Q is runoff depth (mm), P is rainfall depth (mm), S is potential maximum retention after the runoff begins (mm) and I_a is initial abstraction (mm). It is valid for P > I_a, otherwise, runoff is null. The initial abstraction, I_a, accounts losses before the runoff starts. It includes losses by interception, evaporation, infiltration and surface depression. I_a is given empirically as $I_a = \lambda S$.

Where, λ is dimensionless initial abstraction coefficient. $I_a = 0.2S$ has been used empirically for many watersheds in US. Local empirical values can replace λ. S is linked to the dimensionless curve number (CN) is by the following equation.

$$S = \frac{25400}{CN} - 254 \tag{2.3}$$

The CN is a function of land cover type, soil type and antecedent moisture conditions. The land cover type accounts specified hydrological surface conditions in poor, fair and good condition. The soil types are classified by four classes (high, moderate, slow, very slow infiltration). The antecedent moisture conditions are specified into three (dry, average and wet conditions). The range of CN is from 0 (null runoff) to 100 (full runoff response) depending on catchment characteristics. The standard CN can be estimated from the SCS handbook (SCS, 1972) or tables published by the SCS in the technical report 55 (Technical Report - 55, 1986). The peak flood in the SCS-CN method is given in the following equation.

$$q_p = \frac{0.208\ A\ Q}{0.5\ D + 0.6\ t_c} \tag{2.4}$$

Where, q_p is the peak discharge (m^3/s), Q is runoff depth (mm), A is drainage basin area (km^2), D is rainfall duration (hr.) and t_c is time of concentration (hr.). The time of concentration can be determined by several general empirical equations, a designer is free to choose the method (Pilgrim and Cordery, 1993).

As mentioned earlier, the SCS-CN method is widely used and its applicability lies on explicit considerations of different soil type, land cover, hydrologic surface condition and antecedent watershed moisture. However, the slope of the watershed is not considered in the CN estimation. Some authors have been tried to consider a slope factor into the CN parameter to perceive the effect. For example, Haggard et al., (2002) found that surface runoff increased "logarithmically" with the slope, up to a slope of 15%, for a demonstration on a small plot of 1.5 m x 3 m on a silty loam soil group with slopes ranging from 0 to 28%. Huang et al., (2006) found that runoff increased to a large extent with slope, and the standard CN overestimates small runoff events and underestimated large runoff events, for an 11-year experiment conducted in China for sites with range of slopes covering from 14 to 140%. Garg et al., (2013) modelled in a watershed level for three different CN slope-adjusted estimation approaches and concluded that the slope factor

significantly increased the surface runoff for all the slope-adjusted CN approaches, for Solani watershed in India.

The SCS-CN method is easy to apply and useful for ungauged catchments. However, the performance of the method is highly sensitive on the curve number (CN). The study performed by Hoesein et al., (1989) can be a good example, the study compared CN values estimated form conventional SCS handbook and CN values derived from observed data for 96 watersheds in Australia. The former gave very poor estimates of CN value. Similarly, Ponce and Hawkins, (1996) suggested that the performance of the SCS-CN method relies on CN values, and recommended that the application of the SCS-CN method is generally limited for catchments up to 250 km^2.

2.1.3 The NIFS formula

The NIFS formula has been developed by Glad et al., (2015). This method makes use of three main catchment characteristics: area, specific runoff and effective lake percentage to estimate floods in ungauged catchments. The NIFS formula is given by growth curve and mean annual flood empirical relationships. These two components of NIFS formula have been developed by fitting a regression analysis on the results yielded from regional flood frequency analysis on annual maximum discharges in 165 small catchments in Norway (Glad et al., 2015). The growth curve is given in the following equation.

$$\frac{Q_T}{Q_M} = 1 + \frac{0.308 * q_N^{-0.137} [\Gamma(1+K)\Gamma(1-\mathrm{K}) - (T-1)^{-K}]}{K} \quad (2.5)$$

Where, Q_T is flood with return period, T, (m^3/s), Q_M is mean annual flood (m^3/s), q_N is specific runoff ($l/s.km^2$), Γ is gamma function, K is constant, T is return period (years). The mean annual flood (Q_M) and the constant (K) are given in Equation 2.6 and Equation 2.7 respectively.

$$Q_M = 18.97\ [0.001\ q_N\ \mathrm{A}]^{0.864} e^{-0.251\sqrt{A_{se}}} \quad (2.6)$$

$$\mathrm{K} = -1 + \frac{2}{1 + e^{0.391 + 1.54\ A_{se}/_{100}}} \quad (2.7)$$

Where, A is catchment area (km^2) and A_{se} is effective lake percentage.

The NIFS formula is most favored for small unregulated catchments and less urbanization percentage. It is unfavorable or highly uncertain if the study area is out of the recommended

catchment size (0.2 – 50 km^2) and degree of uncertainty increases with the increase in return period (Stenius et al., 2015).

2.1.4 Rainfall-runoff modelling

Rainfall-runoff modelling depends heavily on the rainfall data as input. This is due to longer precipitation data and/or rainfall records are often widely available than runoff or when precipitation shows reliable uniformity in the neighboring stations (Wilson et al., 2011). Rainfall-runoff model utilizes a rainfall event with a specified hyetograph to estimate the design discharge. In small catchments, models using sub-daily temporal resolution is required for an appropriate modeling to capture the dynamics of the catchment response (Fleig and Wilson, 2013), in Norway typically 1- to 3-hourly time step is needed for catchments less than 100 km^2 (Midttømme et al., 2011). For the large catchments, the daily time step can yield satisfactory results; the spatial distribution in inputs is perceiving than temporal variation (Beven, 2012). Runoff-rainfall models have been used widely to generate runoff statistics in ungauged sites. Most of the rainfall-runoff models need to be calibrated against locally available precipitation and observed flow. However, in most small catchments, observed flow information is not available or is poorly available (Loukas and Vasiliades, 2014). Such sites are treated as ungauged catchments. Nevertheless, for the ungauged sites, several methods can be applied to estimate model parameters using regionalization techniques such as Regression, Physical similarity, and Spatial proximity methods (He et al., 2011; Parajka et al., 2013) prior to statistical streamflow prediction and flood estimation. The regionalization methods are described in Section 2.2. The Norwegian rainfall-runoff models such as PQRUT is used for flood calculations in small ungauged catchments in Norway.

PQRUT has been developed by Andersen et al., (1983) and can be used to estimate flood discharges of a certain return period by utilizing a rainfall event. It is a simple three parameter model, lumped, event-based rainfall-runoff model and in principle the PQRUT model is a simplified version of the widely used HBV model (Wilson et al., 2011). The HBV hydrological model is used operationally for flood forecasting in Norway, not essentially for flood estimation in small catchments; the PQRUT is intended to model storm hydrographs at hourly time step for small catchments (Wilson et al., 2011; Fleig and Wilson, 2013). PQRUT is a single “bucket” with two outlets that represent fast and slow runoff in response to a rainfall event, upper and lower outlet respectively (Figure 2.1). The three model parameters (two runoff constants and the one threshold parameter for fast runoff) can be calibrated against observed discharge or can be

estimated based on catchment characteristics such as for ungauged catchments. As illustrated in Figure 2.1, the outflow (q) relies on the updated water content, H, relative to a threshold value, T. If the updated H surpass or equal the threshold value T, thus q occurs at a faster flow rate (K_1*(H-T)) and slower flow rate (K_2*T); if the updated H is less than the threshold value T, no fast response will be generated, q occurs only at slower (K_2*H). A conceptual relation can represent graphically for the model parameters to the high and low slopes of the recession curve and their boundary from a two-component hydrograph separation (Andersen et al., 1983), illustrated in Figure 2.1.

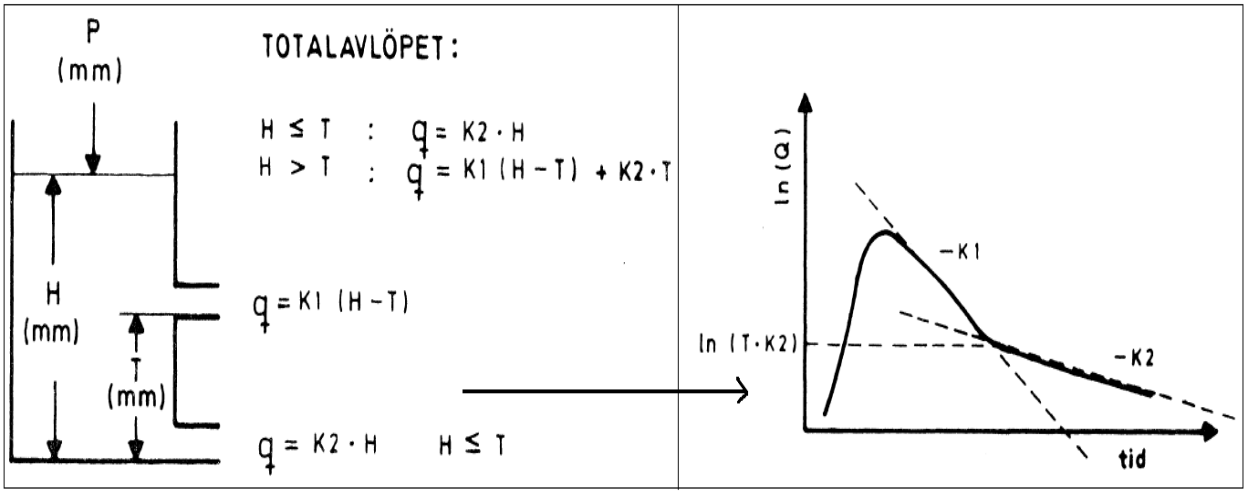

Figure 2.1: PQRUT model structure (left) and corresponding hydrograph (right) (Andersen et al., 1983).

Andersen et al., (1983) has developed empirical formulas that describe the three model parameters linked with the catchment characteristics. The formulas are given in the following equations.

$$K_1 = 0.0135 + 0.00268 * H_L - 0.01665 * \ln(A_{se}) \quad (2.8)$$

$$K_2 = 0.009 + 0.21 * K_1 - 0.00021 * H_L \quad (2.9)$$

$$T = -9.0 + 4.4 * K_1^{-0.6} - 0.28 * Q_N \quad (2.10)$$

Where, H_L is catchment relief (m/km), A_{se} is effective lake percentage, and Q_N is specific runoff (l/s/km^2). The constant parameters K_1 and K_2 are estimated per time step, and T is estimated in mm for the initial tank content. These empirical equations are appropriate for small catchments and do not perform well for large catchments (Wilson et al., 2011). The parameters are highly sensitive to effective lake percentage, A_{se} (Wilson et al., 2011).

The issue in PQRUT model is the difficulty to set the initial saturation level, and PQRUT is used

particularly in areas where snowmelt combined floods are minor importance (Wilson et al., 2011). The study of Wilson et al. (2011) noticed that the performance of PQRUT varied relative to the size of the catchment; the bigger the catchment area the higher flood magnitudes produced than the flood frequency analysis.

2.2 Regionalization methods

The need for prediction of streamflow in ungauged catchments is extensively enlarging as countless infrastructure development projects are related to ungauged sites. For instance, most likely, small catchments connected to crossroad culverts are ungauged sites. There are several approaches for the simulation of discharges in ungauged catchments or in the absence of observed data. Hydrological models have been used widely to generate streamflow in ungauged sites (Loukas and Vasiliades, 2014). Most of the hydrological models need to be calibrated against locally available observed discharge data. However, observed discharges are not available or are insufficient in length, in many desired sites (Loukas and Vasiliades, 2014). Such catchments are considered as ungauged sites. For these ungauged catchments, the streamflow need to be predicted with the help of regionalization methods to estimate the model parameters (Oudin et al., 2008; He et al., 2011; Parajka et al., 2013). Estimation of model parameters and generating streamflow statistics in ungauged catchments are challenging and are associated with a high degree of uncertainties (He et al., 2011).

Several authors define the meaning of regionalization that is slightly different in various literature (He et al., 2011). Regionalization can be defined as "the process of transferring information from comparable catchments to the catchment of interest" (Blöschl and Sivapalan, 1995) for generating streamflow in ungauged sites. This implies to transfer model parameters from gauged (donor) to ungauged (target) catchments upon diagnosed conditions of possibility. The most common approaches of regionalization are; Regression, Physical similarity, and Spatial proximity methods (Oudin et al., 2008; He et al., 2011).

2.2.1 Regression

This method incorporates catchment characteristics to estimate the model parameters with a regression function. Regression method is the most widely used among the regionalization approaches (Oudin et al., 2008). Regression can be classified as one step and two-step regression. The two-step regression is the most popular approach of the regionalization method (He et al.,

2011). It essentially follows two steps; deriving the calibrated parameter sets from all modelled gauged sites and creating a linkage between calibrated model parameters and catchment characteristics. That means, the approach plays first with improving the goodness of fit between observed and simulated discharges and then moving to get an optimal correlation between model parameters and catchment descriptors. This method sounds simple and effective for estimating model parameters in ungauged catchments, but the developed regression functions provided poor results in many cases when compared with the physical similarity and spatial proximity methods. For example, Yang et al., (2020) concluded that the regression method yielded weaker results than the other regionalization approaches for 86 catchments in Norway using four different hydrological model. Similarly, the study of Oudin et al., (2008) concluded that the regression method performed worst of the three regionalization methods studied for 913 catchments located in France using two different hydrological models. On the other hand, Young, (2006) studied 260 catchments in UK and the regression method performed better than the spatial proximity method. Similarly, the study of Tsegaw et al., (2019a) found that the multiple regression provided a satisfactory result for 41 catchments in Norway using a parsimonious DDD hydrological model. However, many authors argued that the performance of the regionalization method relies on the study area and the hydrological model employed (Parajka et al., 2013). In using the regression method, Oudin et al., (2008) recognized that models that utilize a lesser number of model parameters perform better than with a greater number of parameters (overparametrized). This can make to pay attention for using parsimonious models in regression applications.

2.2.2 Physical similarity

This method transfers the entire set of parameters from similar gauged to the ungauged catchment. In this method, the catchment similarity assessment is carried out between the donor gauged catchments and ungauged catchment by using the catchment characteristics. There are two approaches commonly used for similarity assessment: single donor and pooling group method. In the single donor method, all the donor catchments are ranked based on their descriptors with the most similar descriptor ranked foremost, followed by the second most similar, and so on. In case two or more donor catchments provide the same catchment descriptor value, they will be assigned the same rank (Tsegaw et al., 2019a). Each donor catchment will be ranked differently for every descriptor. For each donor catchment, all rank values are accumulated. Thus, the catchment with the smallest accumulated rank is selected as the most similar catchment. In the pooling group

method, a number of similar donor catchments are considered, and weighted average of the corresponding parameters is taken. The pooling group physical similarity is described in detail in Section 4.6.2. In the study of Tsegaw et al., (2019a), pooling group physical similarity provided satisfactory performance for 41 catchments in Norway using a parsimonious DDD hydrological model. In the same study, Tsegaw et al., (2019a) found that the combined regionalization method (multiple regression and physical similarity through pooling group) performed slightly better than the other regionalization approaches.

2.2.3 Spatial proximity

This method relies on the assumption of similar hydrological behavior in the neighboring region, and variation in parameters relies on the spatial distances only. This method establishes spatial interpolation methods on the gauged parameters in the same region to estimate the model parameters. For example, “Kriging” and “inverse distance weighting” methods (He et al., 2011). In several studies, spatial proximity outperformed the other two regionalization methods. For instance, Merz and Blöschl (2004) found that the spatial proximity method yielded a better result than the regression method for 308 catchments in Australia using HBV hydrological model. Similar result found by Oudin et al., (2008), spatial proximity provided the best result than the other regionalization approaches.

3. STUDY AREA

This section explains the ground for study catchment selection and location of the catchments.

3.1 Background for the catchment selection

The E6 Helgeland Sør highway is owned by Norwegian public roads administration (*statens vegvesen*) (https://www.vegvesen.no/). There are several culverts constructed along the E6 Helgeland Sør, roadway. The culverts belong to the small tributaries passing beneath the highway. Norconsult is a consulting company in Norway running multidisciplinary planning and design works (https://www.norconsult.no/). Norconsult has reviewed the design basis for culverts along the E6 Helgeland Sør based on builder notification 089, in a document entitled "E6 Helgeland sør, Dimensjoner stikkrenner BHM 089 (NO-RIVA-901 v.J01)" (Norconsult, 2018). The design flood calculations have been checked and assessed whether the culverts have sufficient capacity for a 200-year flood (Norconsult, 2018). Furthermore, Norconsult (2018) has done new design flood calculations and capacity assessment for 86 culverts using the rational method, the regional analysis and the NIFS formula. Consequently, 59 culverts appeared to have sufficient capacity, 18 culverts out of the remaining 27 found with insufficient capacity at the inlet but have enough culvert capacity, and the last nine culverts showed insufficient capacity (Norconsult, 2018). Out of the nine insufficient culvert capacity, seven culverts are selected by the Norwegian public roads administration aiming to assess a 200-year flood using the DDD model in cooperation with NTNU. Therefore, the culverts corresponding to the study catchments involved in this paper are among the nine culverts that have insufficient capacity.

3.2 Study area location

Seven ungauged catchments used in this study are located at E6 Helgeland Sør, in Norway. The other two gauged catchments used to test the DDD model performance are located near to the E6 Helgeland Sør. The study catchments are very small and located close to each other, thus the NVE Atlas online ArcGIS platform (https://atlas.nve.no/) has been used to display them visible as shown in Figure 3.1, that shows the exact location of the study catchments along the E6 Helgeland Sør. In Figure 3.1 the study catchments are labelled with the culvert number from the Norconsult (2018) culvert design document. Table 3.1 shows the geographical location and size of the test catchments and the study catchments, their coordinates described in Universal Transverse Mercator (UTM) Easting (m) and Northing (m), and the altitude is measured above the mean sea level (a.m.s.l). The

coordinates indicate the location at the outlet of the respective catchments.

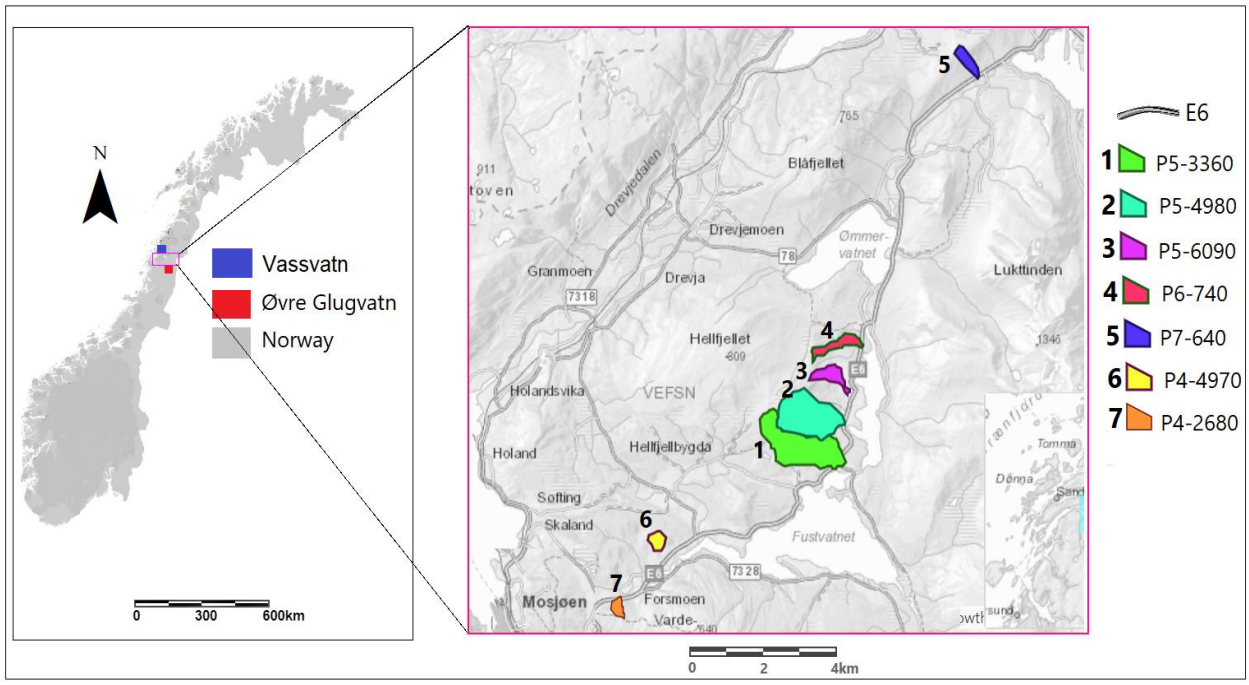

Figure 3.1: Location of the test catchments and the study catchments.

Table 3.1: Geographical location in UTM zone 33 and catchment size, for all catchments.

S.N	Catchment Id	Latitude (E)	Longitude (N)	Altitude (m)	Area (Km^2)
	Test catchments				
1	Vassvatn (157.3)	418511.14	7365335.12	107.8	16.4
2	Øvre Glugvatn (151.13)	433107.3	7283660.06	399.6	60.7
	Study catchments				
1	P5-3360	427207.39	7312610.45	38.4	2.8
2	P5-4980	427524.93	7314050.99	38.6	2.5
3	P5-6090	427653.22	7315145.79	61.2	0.7
4	P6-740	428239.56	7316547.02	40.9	0.7
5	P7-640	432249.35	7325321.54	152.7	0.3
6	P4-4970	421306.68	7309921.42	68.8	0.3
7	P4-2680	419923.65	7308284.36	38.3	0.2

4. METHOD AND DATA

This section illustrates the model used in the study, the data acquisition approaches and the essential procedures to run the model with their process data are presented. The methods of regionalization used, and the design precipitation approach applied, for this study are described.

4.1 The DDD model

The DDD model is a conceptual rainfall-runoff model which is recently developed in Norway by Skaugen and Onof, (2014), and it is written in the programming language R (http://www.r-project.org). At this time, the DDD model runs operationally at daily and sub-daily time steps at the flood forecasting subdivision of the Norwegian Water Resources and Energy Directorate (NVE) (Skaugen and Mengistu, 2016). The DDD model is parsimonious model, which means the model possesses few calibrated parameters and most of its model parameters are estimated from the catchment descriptors and the observed runoff characteristics (Skaugen et al., 2015; Skaugen and Weltzien, 2016).

4.2 The DDD model structure

The overall structure of the DDD model is presented in Figure 4.1. The model has three basic modules: the snow, subsurface and runoff dynamics. The snow routine is handled by distributing into 10 elevation zones, in a similar way to HBV (Bergström, 1995). The subsurface routine is divided between saturated and unsaturated storage zones. The runoff dynamics routine is derived from the observed catchment features. In many conditions the DDD model underestimates simulation in the flood peak events (Tsegaw et al., 2019a), to improve this underestimation, a dynamic river network accounting method was proposed by (Tsegaw et al., 2019b), and it is practiced in this study as an additional module to the above mentioned three routines.

4.2.1 Precipitation, temperature and snow

The central inputs to the DDD model are areal precipitation and temperature. Catchments are divided into 10 elevation zones. As the method used by (Skaugen and Weltzien, 2016), the areal precipitation and temperature are calculated for each elevation zone by averaging gridded input data that are located within the zone. For the very small catchments that has no gridded input in the zone, it is directly assigned to the same input values of the closer zone in elevation. As presented in Figure 4.2, the catchment is classified into 10 elevation zones and the distributed gridded locations for precipitation and temperature within the catchment.

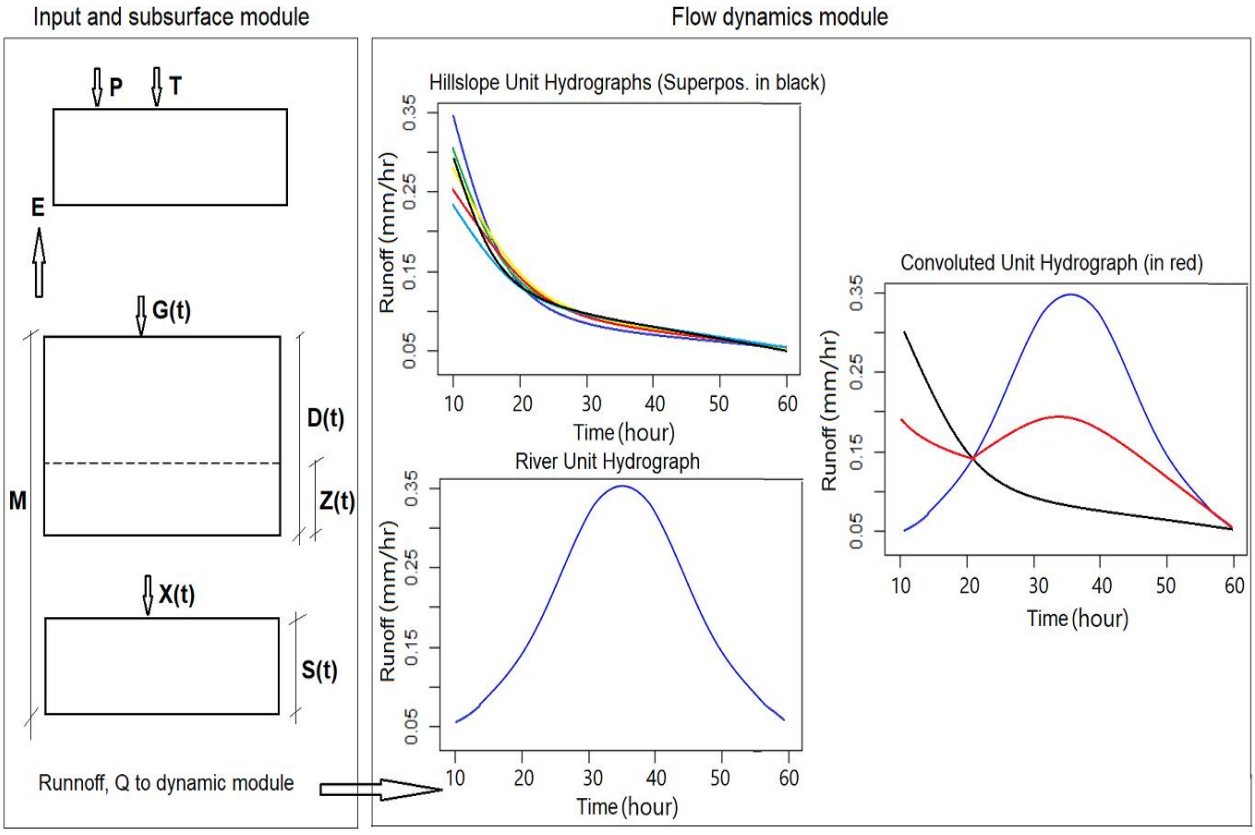

Figure 4.1: Structure of the DDD model adapted from (Skaugen and Onof, 2014), input and subsurface module (left) and flow dynamics module (right).

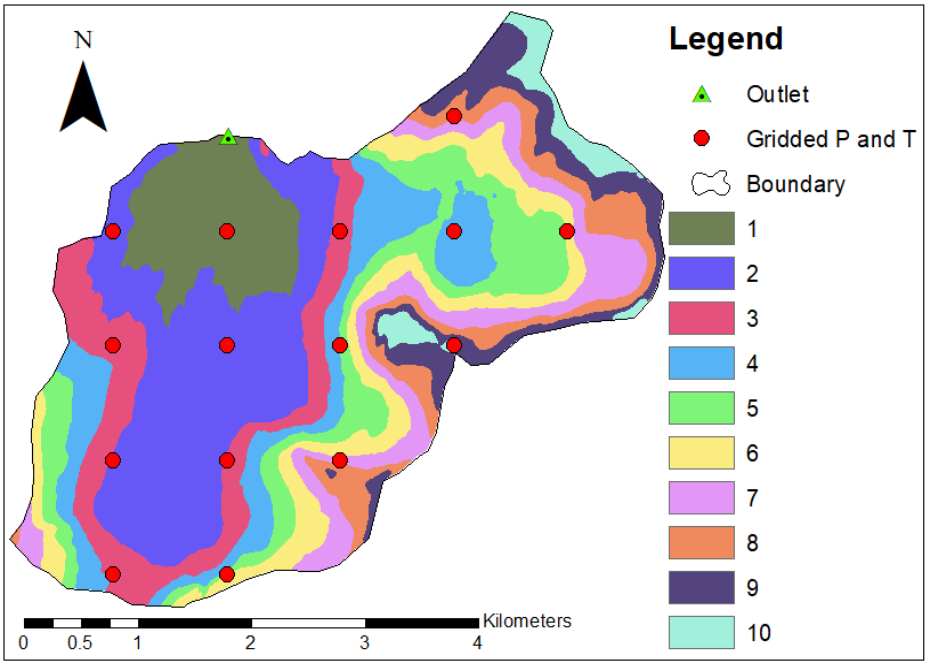

Figure 4.2: Gridded precipitation (P) and temperature (T) distributed across the 10 elevation zones, for Vassvatn catchment.

The snow and snowmelt are handled separately for each elevation zone. The snow routine in the DDD model makes use of a degree-day model for snow melting and refreezing, the same as the HBV model (Bergström 1995). In the DDD model the parameters T_x and T_s are fixed to 0.5 ^{0}C and 0 ^{0}C respectively to minimize the calibrated parameters in the snow routine (Skaugen and Mengistu, 2016).

4.2.2 Subsurface routine

The overall illustration for rain input and the subsurface module is presented in Figure 4.1 (left). The input from the rain and snowmelt, G(t), is the amount of water that goes into the subsurface routine. The subsurface module holds a tank, M (mm), shared between a saturated (groundwater zone, S (mm)) and unsaturated (soil moisture zone, D (mm)). The actual moisture available in the unsaturated zone, D, is described as Z (mm). The subsurface state variables are updated after evaluating the existing soil moisture, Z(t), together with the input from snow routine, G(t), in the event that it exceeds the field capacity threshold, R, of 30% of D(t) (Skaugen and Onof, 2014). If this condition satisfied, the excess water X(t) is added to S(t). The potential evapotranspiration, Ep, is estimated as a function of degree-day factor, Cea (mm ^{0}C^{-1}h^{-1}), which is positive for positive temperature (T) and zero for negative temperature. Cea is the only regionalized parameter in this module. The actual evapotranspiration, Ea(t), which is computed as a function of potential evapotranspiration (mm day^{-1}) and the level of storage. To summarize:

Input: $$G(t) = P(t) + Sm(t) \quad (4.1)$$

Potential evapotranspiration: $$Ep(t) = Min(Cea \times \mathrm{T(t)}, 0) \quad (4.2)$$

Actual evapotranspiration: $$Ea(t) = Ep(t) \times \frac{S(\mathrm{t})+Z(\mathrm{t})}{M} \quad (4.3)$$

Excess water: $$X(t) = MAX\left\{\frac{G(t)+Z(t)}{D(t)} - R, 0\right\} \quad (4.4)$$

Groundwater: $$\frac{\mathrm{d\,S}}{\mathrm{dt}} = \mathrm{X(t)} - \mathrm{Q(t)} \quad (4.5)$$

Soil water content: $$\frac{\mathrm{d\,Z}}{\mathrm{dt}} = \mathrm{G(t)} - \mathrm{X(t)} - \mathrm{Ea(t)} \quad (4.6)$$

Soil water zone: $$\frac{\mathrm{d\,D}}{\mathrm{dt}} = -\frac{\mathrm{d\,S}}{\mathrm{dt}} \quad (4.7)$$

Where, Q(t) is runoff. The variability of the hydrograph is dependent on M to a great extent, increment in amplitude of the hydrograph is associated with the storage capacity. The catchment-scale fluctuation of storage is related to runoff recession and its distribution, hence the storage dist-

ribution is considered as a scaled version of the recession (Skaugen and Mengistu, 2016).

4.2.3 Runoff dynamics

The parameters in the runoff dynamics feature (i.e., the hillslope routing and river routing) of DDD are entirely derived from the catchment characteristics and recession analysis of the observed runoff (Skaugen and Onof, 2014). The principal technique for creating the runoff dynamics for a catchment is the distance distributions derived from the topographic features of the catchment by using the Geographical Information System (GIS). The distances are measured for marsh and non-marsh (soil) of the catchments from points in the catchment hillslopes to the nearest river reach and distances between points in the river network and outlet. As presented in Figure 4.3, the exponential distribution fits well to the cumulative distribution functions (CDF) of the distances of the hillslopes and the normal distribution describes well to the CDF of the river networks in the catchment (Skaugen and Onof, 2014; Skaugen and Mengistu, 2016). The distances in combination with the celerity values can be transformed to concentration times (the required time to pass water from point in the catchment to the closest river network). Skaugen and Onof (2014) applied the CDF of the concentration time to derive runoff hydrographs of the hillslopes and the unit hydrograph of the flow in the river is determined from the distances of points in the river networks to the outlet.

In the DDD dynamics model, the transportation of the water from the points in the catchment to the closest river stream is by waves with celerity determined by the actual storage, S(t), in the catchment (Skaugen and Onof, 2014; Skaugen and Mengistu, 2016). The celerity corresponding to different levels of the subsurface storage is calculated by assuming exponential recession with parameter Λ in the following equation.

$$Q(t) = Q_0 \Lambda e^{-\Lambda(\mathrm{t}-t_0)} \tag{4.8}$$

Where, Q_0 is the peak discharge immediately before recession starts, t_0 is time of input and Λ is the slope of change per time (t) of the recession in the log-log space, determined by the following equation.

$$\Lambda(\mathrm{t}) = \frac{log(Q(t)) - log(Q(t + \Delta t))}{\Delta t} \tag{4.9}$$

The celerity, v (ms^{-1}), is estimated as a function of Λ using the equation below.

$$v = \frac{\Lambda\, d_{mean}}{\Delta t} \tag{4.10}$$

Where, d_{mean} is the mean of the distances from points in the catchment to the nearest river reach. The subsurface water reservoir is divided into five equal storage levels, each level corresponding to the quantiles of the distribution of Λ based on the assumption that the higher the storage, the higher the value of Λ. The lowest storage level starts filling water and the degree of saturation increase correspondingly from the bottom to the top level. Each storage level i contains a unit hydrograph with the parameter λ_i, estimated such that the runoff from several storage levels will provide a unit hydrograph to the exponential unit hydrograph with parameter Λ_i. Different celerity for each storage level hence attributes a celerity described in the equation below.

$$v = \frac{\lambda_i\ d_{mean}}{\Delta t} \tag{4.11}$$

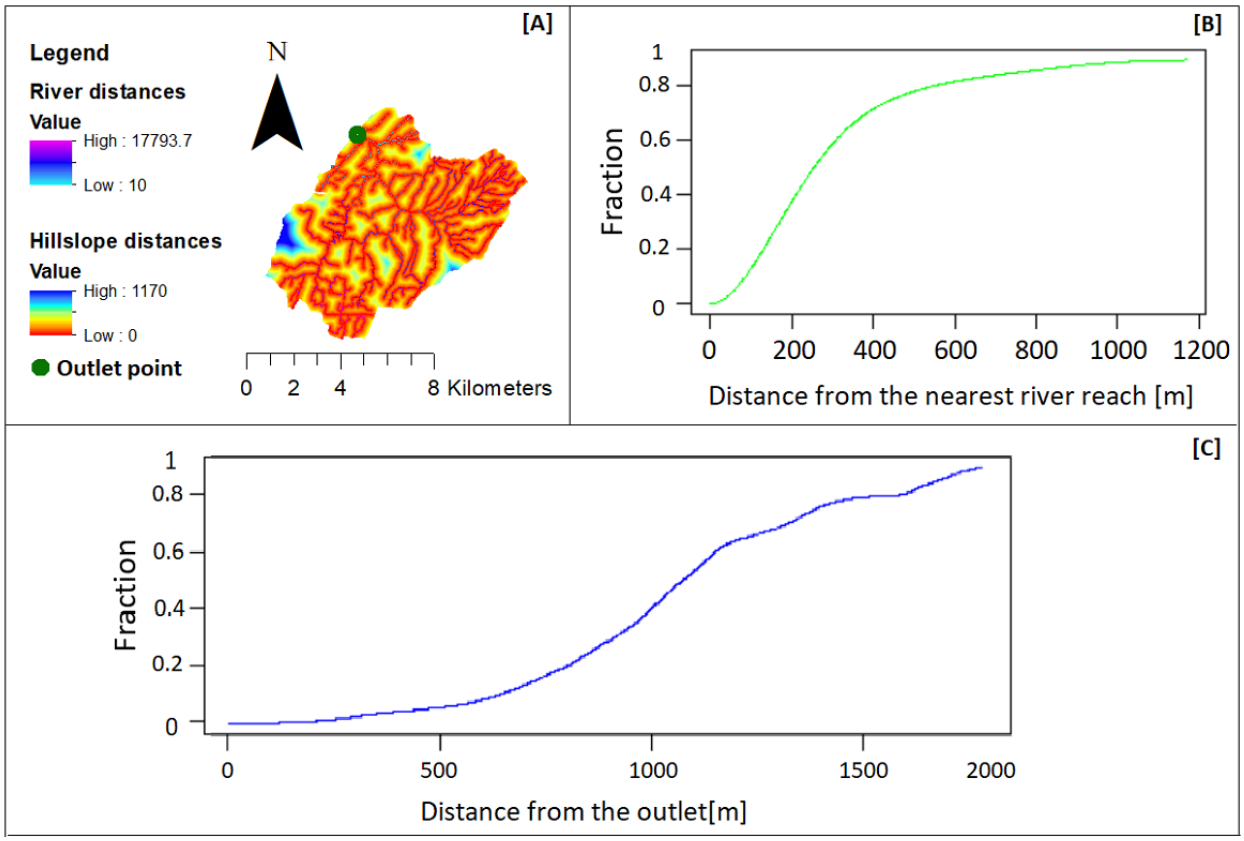

Figure 4.3: The river distances and hillslope distances [A], CDF between points in the catchment to the nearest river reach [B], CDF between the river networks to the outlet [C], for Øvre-Glugvatn catchment.

In the DDD model, when the subsurface is fully saturated (i.e., S = M), the overland flow occurs and the saturated zone of the subsurface reservoir is estimated as a function of the released runoff and the parameter Λ described in the following equation.

$$S(t) = \frac{Q(t)}{1 - e^{-\Lambda(t)}} \tag{4.12}$$

The unit hydrograph of the hillslope, UHs, is described in the model by using exponential distribution as shown in the equation below.

$$\mathrm{UH}_i(t) = \lambda_i e^{-\lambda_i (t - t_0)} \tag{4.13}$$

Where, t_0 is the time of input, λ_i is the parameter of the exponential distribution determined from recession analysis for each level, as a shape and scale parameter denoted as $Gshape$ and $Gscale$, respectively. These couple of parameters are derived from the recession analysis of the observed runoff. As explained earlier, the parameter Λ is obtained from the recession and its distribution can be modelled using two parameter gamma distribution, $Gs\mathrm{hInt}$ and $Gsc\mathrm{Int}$, the shape and scale parameters of Λ respectively (Skaugen and Mengistu, 2016).

For the river network, the celerity of the streamflow, rv, is considered in order to transform the distance distribution of the stream network into a distribution of travel times and hence the river unit hydrograph of the river network (UH).

As presented in Figure 4.1 (right), the final unit hydrograph that describes the catchment is then determined by convoluting the hillslopes-UHs and the river-UH. The runoff generated from the catchment Q(t) is estimated from the X(t) and convoluted UH.

4.2.4 The dynamic river network routine

The DDD model accounts five storage levels with corresponding five-UHs. Four storage levels are subsurface and the fifth one is an overland flow level with unlimited volume (Skaugen and Onof, 2014; Skaugen and Mengistu, 2016). Tsegaw et al. (2019b) latterly introduced the idea of dynamic river network into the DDD model, in such a way that the four subsurface UHs remain constant and the scale of the overland unit hydrograph (OUH) is dynamic during the simulation time. The shape of the travel time distribution in a hillslope is assumed to be constant and the scale is dynamic to create dynamic OUHs (Tsegaw et al., 2019b). Depending on the saturation level of the subsurface, the dynamic OUHs are turned on and off in the DDD model, hence providing a

dynamic travel time distribution. Different assumptions have made to consider the parameters related to the dynamic river network (details can be found in (Tsegaw et al., 2019b)).

To establish the OUH, three parameters need to be computed: the mean (D_m) and maximum (D_{max}) of the hillslopes distance distributions, and the mean overland flow celerity, v_{OF}. The D_m and D_{max} are derived from the catchment features by using GIS, and v_{OF} is estimated in the DDD model for the celerity derived from the recession analysis (Skaugen and Onof, 2014). The basic theory by Tsegaw et al., (2019b) describes the D_m of a river network is a function of overland flow (OF) which has an effect to create a stream with critical flux (F_c). The F_c lead to create the dynamic critical support area, A_c (the minimum area from which the produced runoff is enough to initiate and maintain river development). The A_c is determined after the F_c is introduced as shown in the following equation.

$$F_C(\mathrm{m^3/h}) = \mathrm{A_c(m^2)} * \mathrm{OF(m/h)} \tag{4.14}$$

Where, OF is saturation excess overland flow. The OF is computed from the DDD model output at each simulation time step. The dynamic river network is activated when the subsurface is saturated, that means when the OF > 0 and the corresponding A_c is calculated using Equation 4.14. The saturation excess overland flow, OF, controls the contraction and expansion of the stream network (Tsegaw et al., 2019b). Expansion of the observed stream network starts when the subsurface potential is fully saturated and there is enough overland flow. The relationship between D_m and A_c is given as described in the equation below.

$$D_m = aA_c^b \tag{4.15}$$

The coefficients *a* and *b* are unique for different catchments and are determined from a regression curve fitted to the relation between mean distance distribution, D_m, and critical support area, A_c. The A_c determined from Equation 4.14 is then used to estimate D_m by using Equation 4.15. If the D_m calculated using Equation 4.15 is greater than the D_m of the observed river network, the dynamic river network degenerates to the observed river network (Tsegaw et al., 2019b).

4.3 DDD model parameters

The DDD model accounts many parameters derived from catchment features and a small number of regionalized parameters. In this study, the model parameters are tabulated in to two categories depending on their mode of estimation. The parameters listed in Table 4.1 are acquired by through

regionalization. The snow routine regionalized parameters are Pro, Cx, and CFR. The snow routine in DDD model has another two non-regionalized parameters, the shape parameter (a0) and the decorrelation length (d) of gamma distribution of snow and snow water equivalent (Skaugen and Weltzien, 2016) are determined from the previously calibrated 84 catchments (Appendix A) in Norway (Skaugen et al., 2015). The subsurface routine and the dynamic flow routine have only one regionalized parameter each, Cea, rv, respectively. In this study, the five parameters (Pro, Cx, CFR, Cea, and rv) are regionalized from recently calibrated 41 small catchments (Appendix B) in Norway (Tsegaw et al., 2019a), the regionalization detail description is given in Section 4.6. For the dynamic river network routine, the F_c is the only parameter that need to be regionalized. As shown in Table 4.1, the respective estimation intervals are set according to different literatures and experiences brought into play the DDD model (Skaugen and Mengistu, 2016**)**. The parameters listed in Table 4.2 are obtained from observed hydro-meteorological data and geographical features of the catchment. These parameters are unique for each of the study catchments.

Table 4.1: DDD model parameters that require regionalization.

Parameters	Description	Lower bound	Upper bound	unit
pro	Liquid water content of snow	0.03	0.1	fraction
cx	Degree day factor for snowmelt	0.05	1	mm $^0C^{-1}$ h^{-1}
CFR	Degree day factor for refreezing	0.001	0.01	mm $^0C^{-1}$ h^{-1}
cea	Degree day factor for evapotranspiration	0.01	0.1	mm $^0C^{-1}$ h^{-1}
rv	River flow celerity	0.5	1.5	m s^{-1}
F_c	Critical flux	Positive real number		m^3 h^{-1}
Gshape	Shape parameter of λ	Positive real number		-
Gscale	Scale parameter of λ	Positive real number		-
GshInt	Shape parameter of Λ	Positive real number		-
GscInt	Scale parameter of Λ	Positive real number		-

4.4 Data preparation approach

The DDD model requires climatic input data (precipitation and temperature), discharge data and catchment features data.

Table 4.2: DDD model parameters derived from observed precipitation data and geographical data.

Parameters	Description	Method of estimation
a0	Shape parameter for the spatial distribution of SWE	Spatial distribution of observed precipitation
d	Decorrelation length for the spatial distribution of SWE	Spatial distribution of observed precipitation
MAD	Mean annual discharge	Long term recorded annual discharge data
Area	Catchment area	ArcGIS
midFL	Mean river length from the outlet	ArcGIS
stdFL	Standard deviation river length from the outlet	ArcGIS
maxFL	Maximum river length from the outlet	ArcGIS
midLbog	Mean marsh Land distance to river networks	ArcGIS
maxLbog	Maximum marsh Land distance to river networks	ArcGIS
Zbog	Zero fraction for marsh (zero distance to the river)	ArcGIS
bogfrac	The marshland areal fraction from the total landcover	ArcGIS
midDL	Mean soil (non-marsh) distance to river networks	ArcGIS
maxDL	Maximum soil (non-marsh) distance to river networks	ArcGIS
Zsoil	Zero fraction for soil (zero distance to the river)	ArcGIS
midGL	Mean glacier distance to river networks	ArcGIS
maxGL	Maximum glacier distance to river networks	ArcGIS
stdGL	Standard deviation glacier distance to river networks	ArcGIS
a and b	Coefficients for computing the dynamic D_m of the hillslope distance distributions	ArcGIS and requires separate python script

4.4.1 Precipitation, Temperature, and discharge data

Hourly temporal resolution precipitation and temperature from seNorge2 data base are utilized in this study. The precipitation and temperature comprises 1 km ×1 km gridded data set of the Norwegian Meteorological Institute (https://thredds.met.no/thredds/catalog.html). The time series hourly resolution data is available covering the period from 2010 up to the present. In this study,

hourly precipitation and temperature data from 2010 to 2016 is used as a distributed input for the analysis in the DDD model for the 10 elevation zones of the hypsographic curve. The gridded climatic data (precipitation and temperature) is available as network common data form (NetCDF) files of Norway, and it has been extracted for the desired catchments by using R script. From the NetCDF files, the coordinates of the grids within the shape of desired catchment and their respective precipitation and temperature are extracted by R script. For example, 15 grid points have been obtained within the catchment for the first test catchment (Vassvatn), (seen in Figure 4.4). The acquired grids within the respective catchments are shown in Figure 4.5 for Øvre Glugvaten, P5-3360, P5-4980, P5-6090 and P6-740. As shown in Figure 4.4 and Figure 4.5 the number of grid points within each catchment are different. The number of grids relies on the coverage area and shape of the catchment. However, the three tiny catchments namely P7-640, P4-4970 and P4-2680 which covers areas of 0.3 km^2, 0.3 km^2 and 0.2 km^2 respectively, do not contain any grid point within their catchment area. These catchment areas are less than the 1 km^2 grid coverage, and there is no grid point touching on these catchments. But this occasion is not consistent for the other two tiny catchments that are P5-6090 and P6-740 which covers area of 0.7 km^2 each. Regardless of their area, but due to the relatively broad in shape, two grids and a single grid have found on P5-6090 and P6-740 catchments respectively (see Figure 4.5). For the three catchments that do not contain any grid, approximately 1 km^2 imaginary area around the respective catchments was considered to seek for at least a single nearest grid point. Thus, one nearby grid point that holds precipitation and temperature data was found for the individual catchment, shown in Figure 4.6, and have been considered as climatic input for further processes based on the assumption that the catchments are represented by the closest grid.

As explained earlier in Section 4.2.1, the gridded precipitation and temperature are distributed across the 10 elevation zones of the catchment hypsographic distribution. This has been done by R script which assigns each grid point to the elevation zone it belongs, based on the coordinates of the grids and the DEM (Digital Elevation Model) of the catchment.

The time series hourly discharge data for the two test catchments have been for evaluation of the model performance and it has been obtained from the Norwegian Water Resources and Energy Directorate (NVE) HYDRA II database. The discharge data underwent missing data inspection and few gaps were found and were filled by station interpolation.

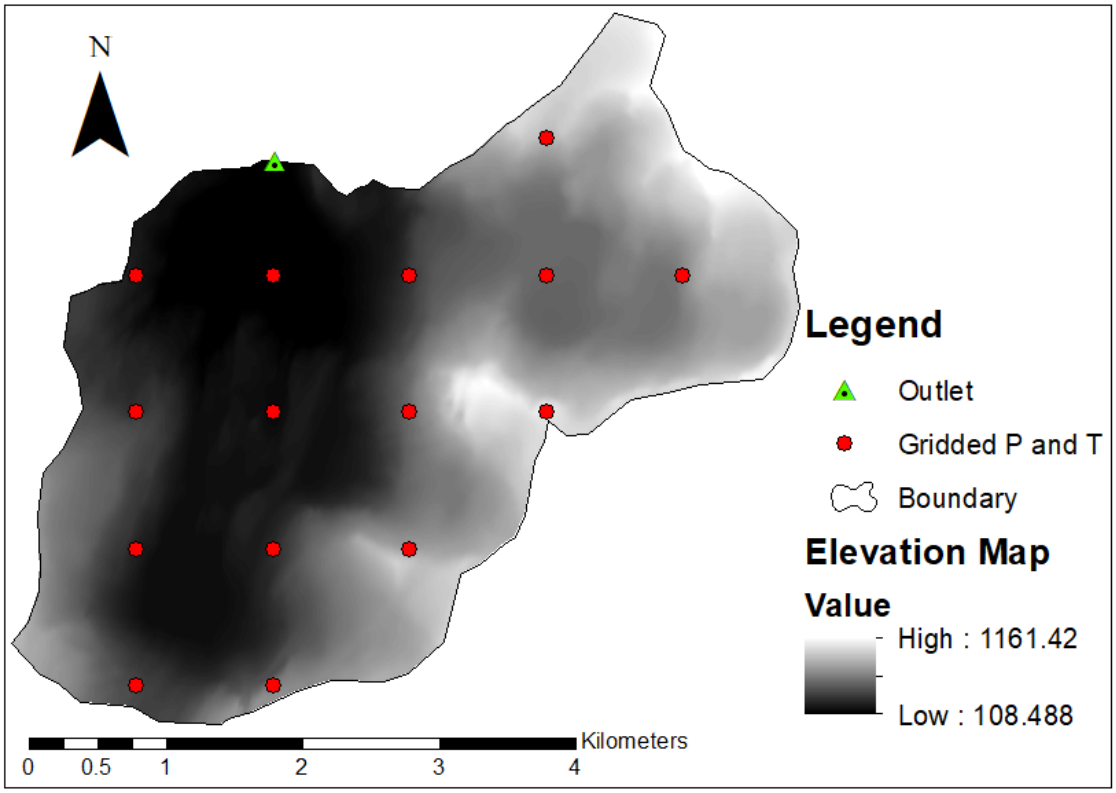

Figure 4.4: Extracted gridded precipitation and temperature, for Vassvatn test catchment.

4.4.2 Precipitation correction (Pkorr)

The correction factor for precipitation (Pkorr) is aimed for water balance correction in DDD model. The Pkorr has been considered as the ratio of long-term mean annual discharge to mean of the initially simulated discharge $(\overline{Q}_{sim})$, described in Equation 4.16. The long-term mean annual discharge (MAD) was considered from NEVINA (MAD = Specific runoff x catchment area).

$$Pkorr = \begin{cases} MAD/\overline{Q}_{sim}, & \text{for } MAD/\overline{Q}_{sim} > 1 \\ 1, & \text{for } MAD/\overline{Q}_{sim} \leq 1 \end{cases} \quad (4.16)$$

4.5 Catchment features extraction

Many of the DDD model parameters are derived from topographical, hydro-meteorological and land cover data for the catchments. The catchment features are essential for physical similarity evaluation, besides, to use as model parameters. Some of the catchment features are gathered from NEVINA and most of the DDD model requirements are derived by using ArcGIS tools.

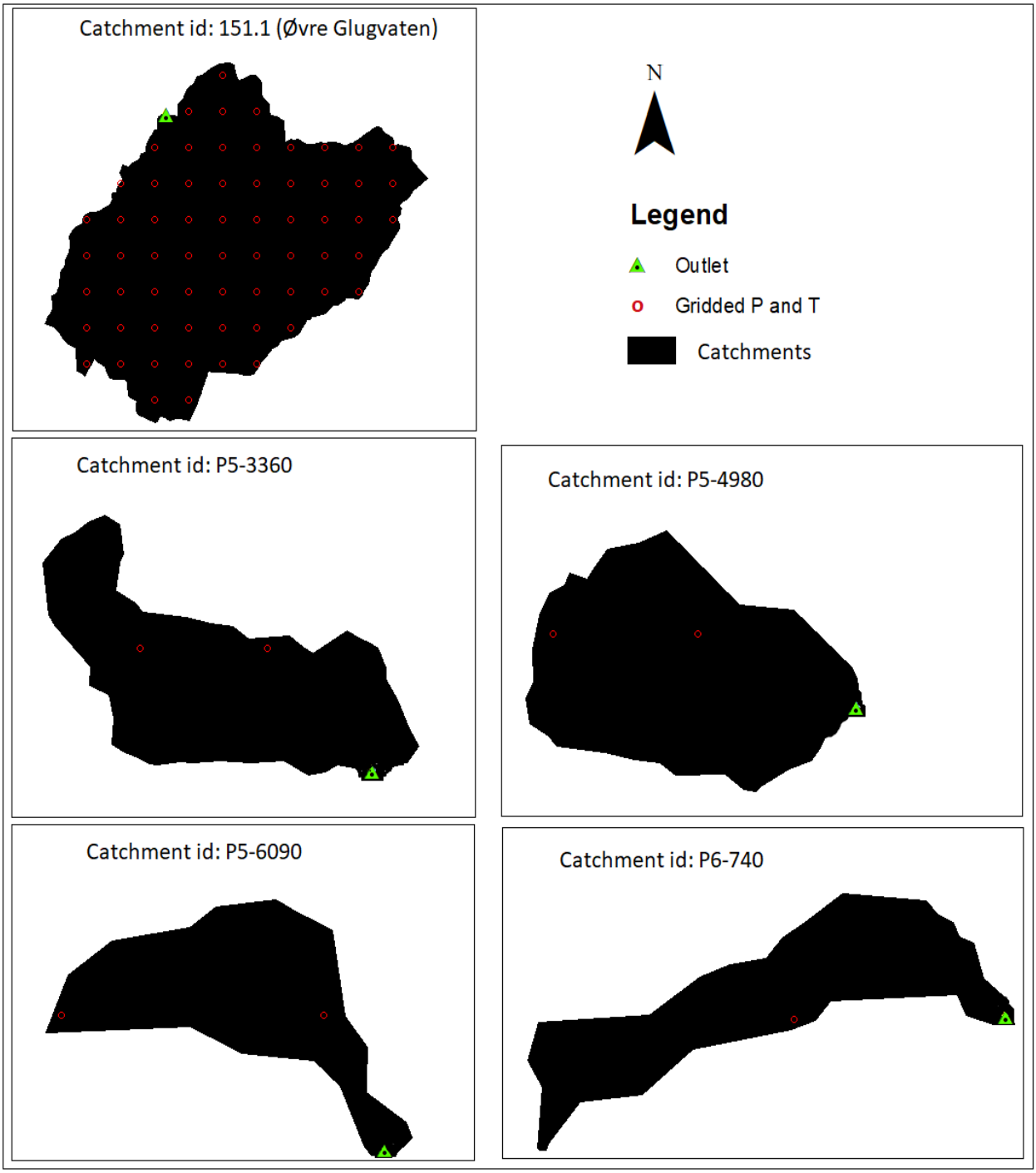

Figure 4.5: Extracted gridded precipitation and temperature within the catchment, for Øvre Glugvaten test catchment, and the study catchments for P5-3360, P5-4980, P5-6090 and P6-740.

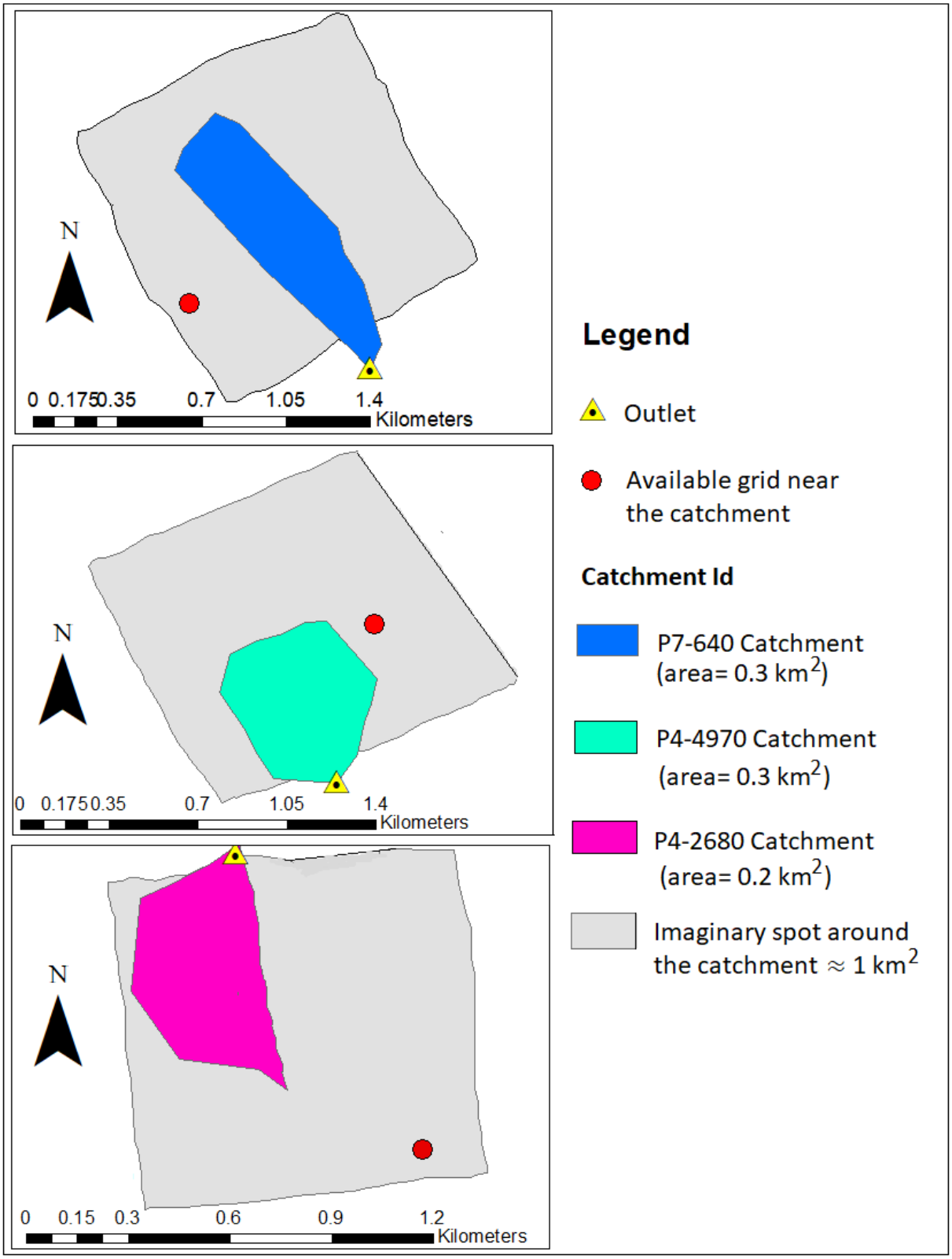

Figure 4.6: The grid point available near to the respective tiny catchment and the boundary of the imaginary spot considered for seeking the nearby grid, for P7-640, P4-4970 and P4-2680 study catchments.

NEVINA is a tool that runs operationally online at NVE (http://nevina.nve.no/) in Norway. This interactive map-based service is a user friendly application to delineate the catchment at the site of interest and provide important information like catchment area, long term specific runoff, hypsographic curve, effective lake percentage and land cover percentage. In this study, the catchment properties are extracted as a summary report as shown in Figure 4.7 and as a shapefile for further analysis in ArcGIS. The catchment characteristics extracted from NEVINA such as topographic data, hydro-meteorological data and land use data are given in Table 4.3, Table 4.4 and Table 4.5 respectively.

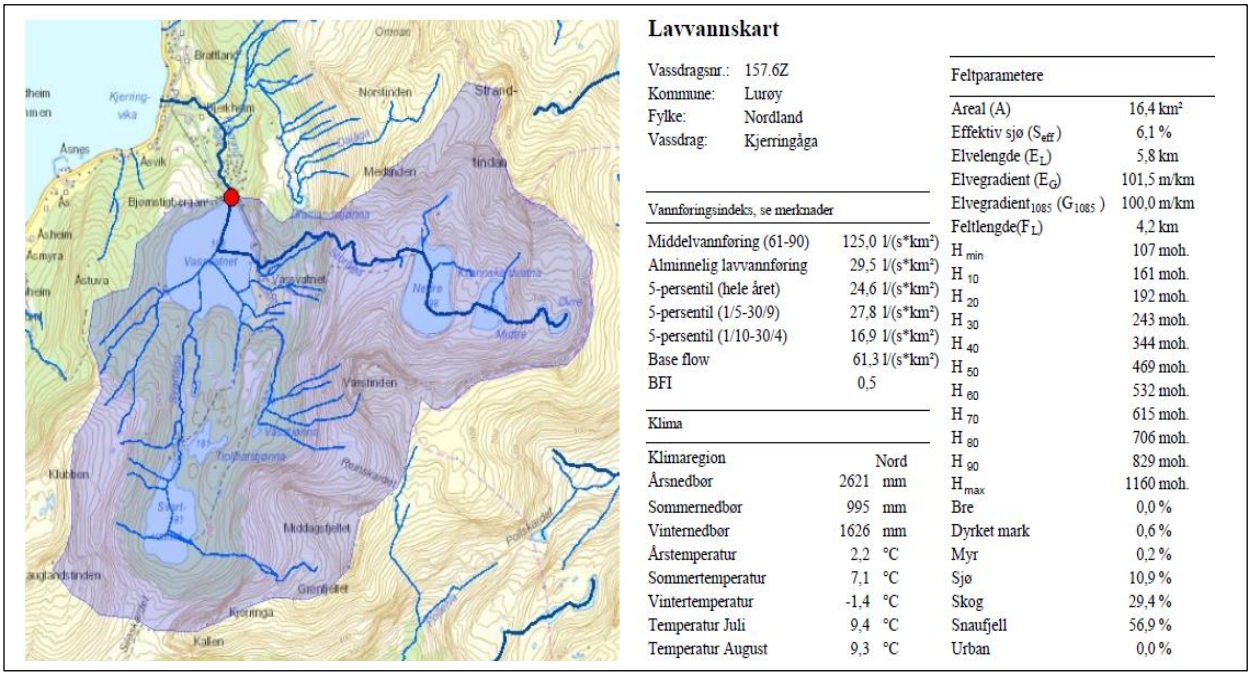

Figure 4.7: Catchment properties produced from NEVINA for Vassvatn catchment

ArcGIS play an important role to extract the geographical data that are useful to set as model parameters prior to running the DDD model. To derive the catchment characteristics, 10 m × 10 m resolution DEM and observed river networks for the catchment have prepared in the first place in this study. The DEM for Norway is readily available at the Norwegian Mapping Authority (http://www.statenskartverk.no/) and the observed river networks have been obtained from (https://kartkatalog.nve.no/) which is owned by NVE. The land cover data has been downloaded from (https://www.nibio.no/) which is controlled by the Norwegian Institute of Bioeconomics (NIBIO).

Table 4.3: Topographic data derived from NEVINA, for the test and study catchments.

Catchments Id	Area (km^2)	Mean elevation (m)	River length (km)	River slope (m/km)
Test Catchments				
Vassvatn (157.3)	16.4	461.0	5.8	101.5
Øvre Glugvatn (151.13)	60.7	581.0	17.4	15.9
Study Catchments				
P5-3360	2.8	163.0	3.9	82.1
P5-4980	2.5	200.0	2.0	79.0
P5-6090	0.5	143.0	1.3	87.5
P6-740	0.5	102.0	1.3	31.8
P7-640	0.3	340.0	0.6	207.8
P4-4970	0.3	143.0	0.2	84.4
P4-2680	0.2	147.0	0.3	77.2

Table 4.4: Hydro-meteorological data derived from NEVINA, for the test and study catchments.

Catchments Id	Mean annual precipitation (mm)	Mean annual temperature (^0C)	Specific runoff ($l/s/km^2$)
Test Catchments			
Vassvatn (157.3)	2621	2.2	125.0
Øvre Glugvatn (151.13)	1315	0.2	61.5
Study Catchments			
P5-3360	1661	2.8	45.3
P5-4980	1643	2.8	48.2
P5-6090	1701	3.1	45.7
P6-740	1723	3.1	43.3
P7-640	1885	2.5	56.3
P4-4970	1646	3.1	42.7
P4-2680	1679	2.8	40.8

Table 4.5: Land use data derived from NEVINA, for the test and study catchments.

Catchment Id	Effective Lake (%)	Bare mountain (%)	Forest cover (%)	Urban land (%)	Marsh land (%)	Cultivated land (%)	Glacial cover (%)
Test Catchments							
Vassvatn (157.3)	6.1	56.9	29.4	0	15.3	0	0
Øvre Glugvatn (151.13)	4.7	29.4	41.5	0	0.2	0.6	0
Study Catchments							
P5-3360	0.33	0	91.9	0	1.1	5.6	0
P5-4980	0	0	95.8	0	0.3	1	0
P5-6090	0	0	89.1	0	3.1	8.4	0
P6-740	0	0	91.4	0	8.8	0	0
P7-640	0	24.2	76.1	0	0.4	0.2	0
P4-4970	0	0	96.9	0	2.2	0	0
P4-2680	0	0	100	0	0	0	0

4.5.1 Stream network distance distributions

The distance distributions of the river network have been obtained using ArcMap 10.7 in this study. The DEM, shapefile, observed river network and land use data prepared initially from the sources mentioned earlier. The following procedures are applied by the tools found in *ArcToolbox* and *ArcHydroTools*, in the ArcMap.

i. *Mosaic To New Raster*: Depending on the spatial coverage of the needed DEM, it could be downloaded as split to different raster data and must be merged by this tool. If there is only a single raster data for the study of interest, this step is skipped.
ii. *Clip*: From the *ArcTool* box under the *Data Management tools*, the raster is trimmed to the study catchment with respect to the shapefile obtained from NEVINA.
iii. *DEM reconditioning*: From the *ArcHydro* toolbox the DEM is re-conditioned in order to fit with the naturally occurring river networks in the catchment using this tool.
iv. *Fill*: From the *spatial analyst tools* under the *hydrology* toolbox, the sinks (holes) of the elevation surface of the re-conditioned DEM are filled, regardless of the depth.
v. *Clip*: From the *Geoprocessing* on the main menu in ArcMap, the land use feature is trimmed to the study catchment with respect to the shapefile of the study catchment by using the clip tool.

vi. *Polygon to Raster*: The land use data is a polygon feature and is converted to a raster dataset by using the polygon to raster tool. The input is the trimmed land use and the value filed must be area type (*artype*). According to NIBIO, the code classification for the different land cover types are given as: 10 for urban, 20 for agriculture, 30 for forest, 50 for land with vegetation cover that is not forest, 60 for marsh, 70 for glacier, 81 for rivers and lakes, and 82 for ocean.

vii. *Reclassify*: The raster land use data is reclassed to marsh lands, non-marsh (soil) lands and glacier lands. The input is raster land use data.

viii. *Polyline to Raster*: The observed river network is a polyline feature and is converted to a raster dataset by using this tool.

ix. *Extract by Mask*: The raster dataset of the observed river network is extracted corresponding to the shape of the study catchment and let this is the stream raster for a catchment. The inputs used are the converted raster polyline and shapefile of the catchment.

x. *Euclidian distance*: The total Euclidean distance (i.e., the shortest distance to the stream network for the marsh and non-marsh part of the hillslope) is calculated by this tool. It utilizes the stream raster as input.

xi. *Extract by Mask*: The Euclidean distance is calculated with some span out of the study catchment, it needs to be extracted corresponding to the shape of the catchment, using the calculated Euclidean distances and shapefile of the catchment as input.

xii. *Zonal Statistics as Table*: The distance distributions statistics (the mean, maximum, and standard deviation) for each reclassified land covers are determined by using this tool, for the respective reclassified land cover.

Eventually, the tool (*Extract by Mask*) is used to determine the zero fraction for each reclassified land cover types. The inputs are the reclassified land cover raster and stream raster.

The overview illustration of the stream networks distance distributions is presented in Figure 4.8, for the first test catchment (Vassvatn). The illustration for stream networks and land cover types is clearly presented in Figure 4.9. The model distance distribution parameters for the stream networks acquired by the *Zonal Statistics as Table* tool is presented in Table 4.6, for the test and study catchments.

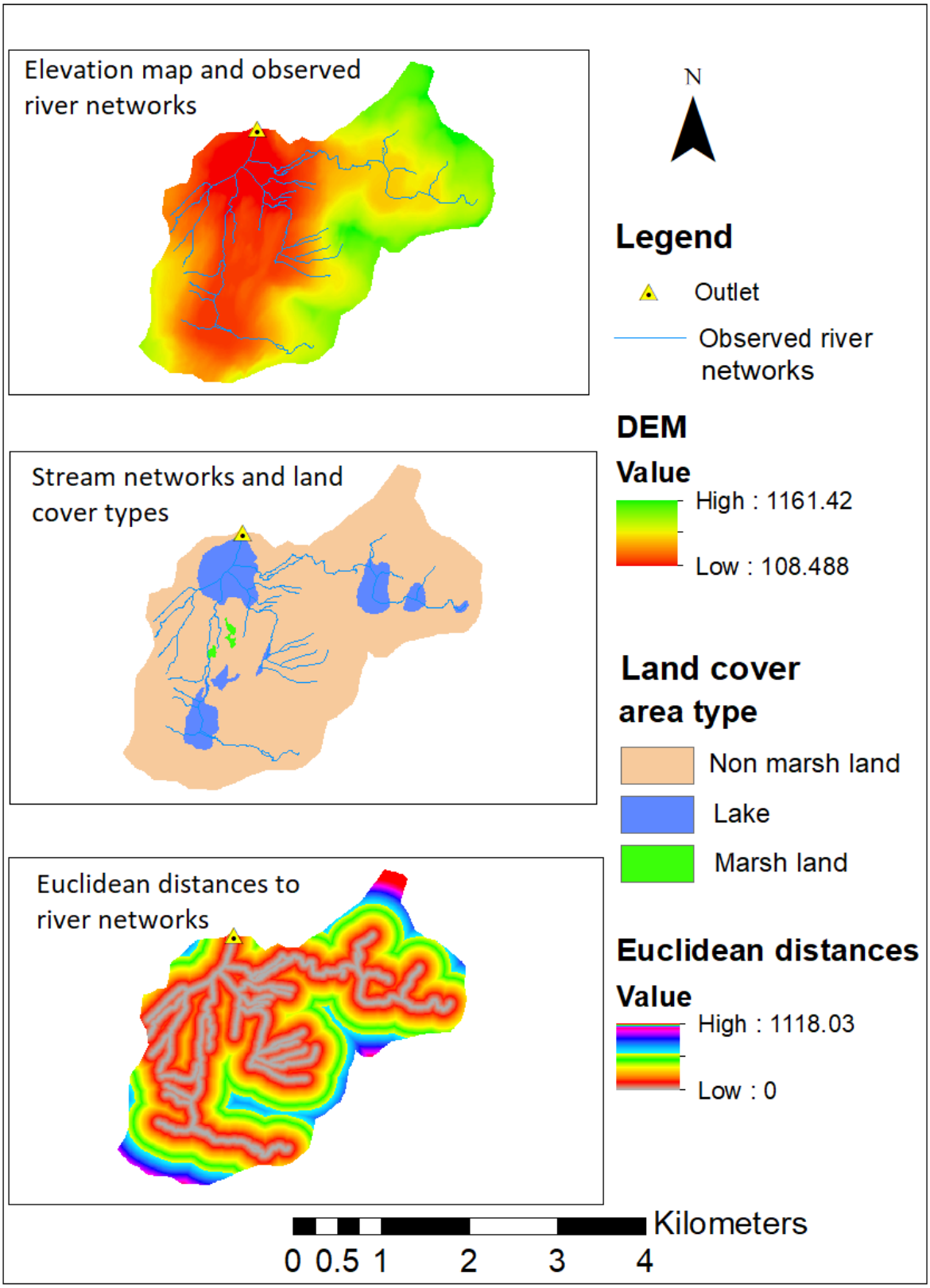

Figure 4.8: The overview illustration of the stream networks distance distributions, for Vassvatn catchment.

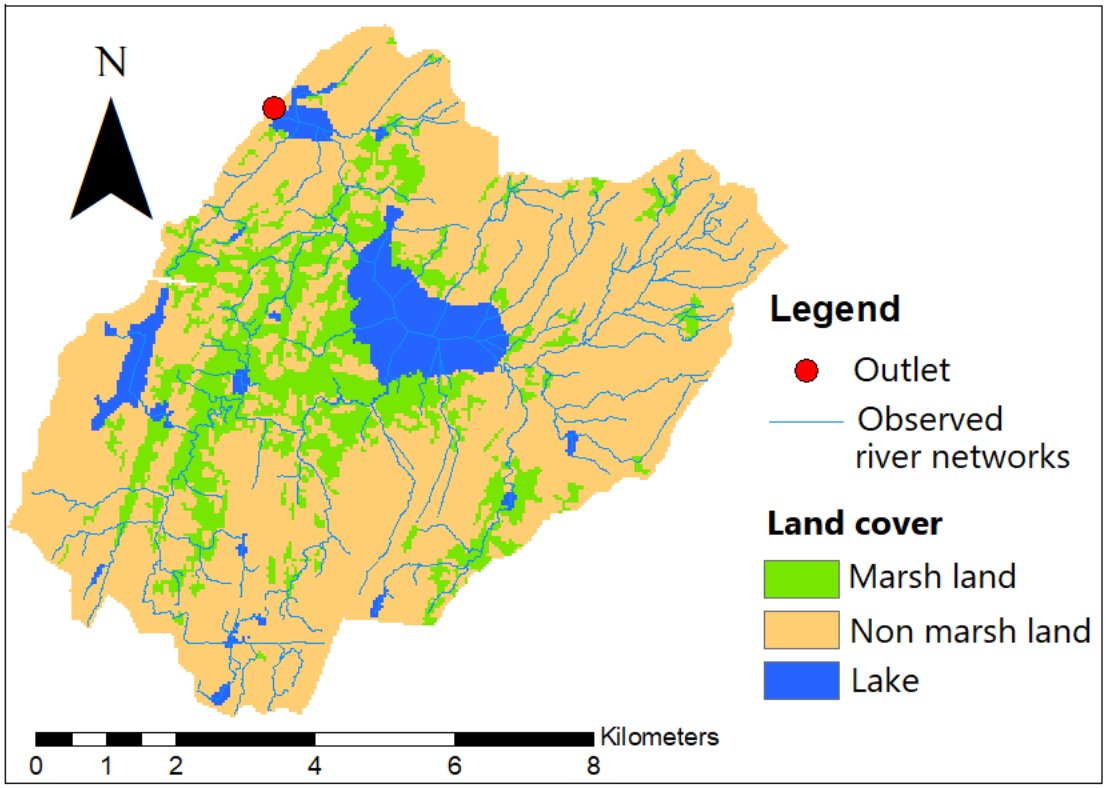

Figure 4.9: Stream networks and land cover types, for Øvre Glugvatn test catchment.

Table 4.6: Distance distribution parameters, for the marsh land and soil (non-marsh) portion of the hillslope: Mean marsh land distance to the river networks (midLbog), maximum marsh land distance to the river networks (maxLbog), mean soil distance to the river networks (midDL) and maximum soil distance to the river networks (maxDL), for the test and study catchments.

Catchment Id	Hillslope Marsh		Hillslope Soil (Non-marsh)	
	midLbog (m)	maxLbog (m)	midDL (m)	maxDL (m)
Test Catchments				
Vassvatn (157.3)	127.07	240.83	254	1118.03
Øvre Glugvatn (151.13)	129.65	761.57	156.48	1149.34
Study Catchments				
P5-3360	202.11	580.34	195.98	712.53
P5-4980	214.57	398.5	253.4	910.7
P5-6090	88.98	208.08	151.63	563.2
P6-740	88.46	240.83	316	1012.42
P7-640	57.34	60.83	266.7	694.62
P4-4970	372.28	455.41	207.86	438.63
P4-2680	0	0	232.44	629.36

4.5.2 River distance distributions

From the stream network distance distributions explained above, steps from *i* to *iv* are kept the same and the following additional steps are applied to determine the river distance distributions.

i. *Flow direction*: Cell to cell flow direction to the eight surrounding cells is computed by using this tool. The input is Filled raster.

ii. *Flow length*: The distances from each cell in the catchment to the outlet is determined by using this tool. It utilizes flow direction to calculate the distances.

iii. *Extract by Mask*: The distances of the river networks are extracted from the total flow length of the catchment by using extract by mask tool. As a control, the maximum flow distance of the river must be similar to the maximum river length found in NEVINA (see Table 4.3). The inputs are flow length and stream raster.

Eventually, the tool (*Zonal Statistics as Table*) is used to determine the distance distribution statistics (the mean, maximum, and standard deviation) of the river network from each cell to the outlet.

The river distance distribution illustration is presented in Figure 4.10, for Vassvatn test catchment. The model distance distribution parameters for the river distances acquired by the *Zonal Statistics as Table* tool is presented in Table 4.7, for the test and study catchments.

4.5.3 Dynamic river network coefficients determination

The coefficients *a* and *b* to account the dynamic river network are practically determined in the following procedures. From the stream network distance distributions explained earlier, all steps are kept the same, and from river distance distributions step i is kept the same.

i. *Flow accumulation*: The accumulated flow map for all cells flowing into each downslope cell is prepared by using this tool. It uses flow direction as an input raster.

ii. Prepare shapefile of the non-marsh lands (i.e., erase the marsh lands from the land cover of the catchment by using the *Erase tool*).

iii. Apart from the ArcGIS, a separate python script is used to loop the thresholds of the flow accumulation (A_c) and create stream networks. Hence, the D_m is computed from the created stream networks. The inputs are flow accumulation map and the shapefile of the non-marsh lands.

Eventually, a power regression curve is fitted to the relation between the derived mean distance distribution, D_m, and critical support area, A_c, to determine *a* and *b* coefficients (see Figure 4.11).

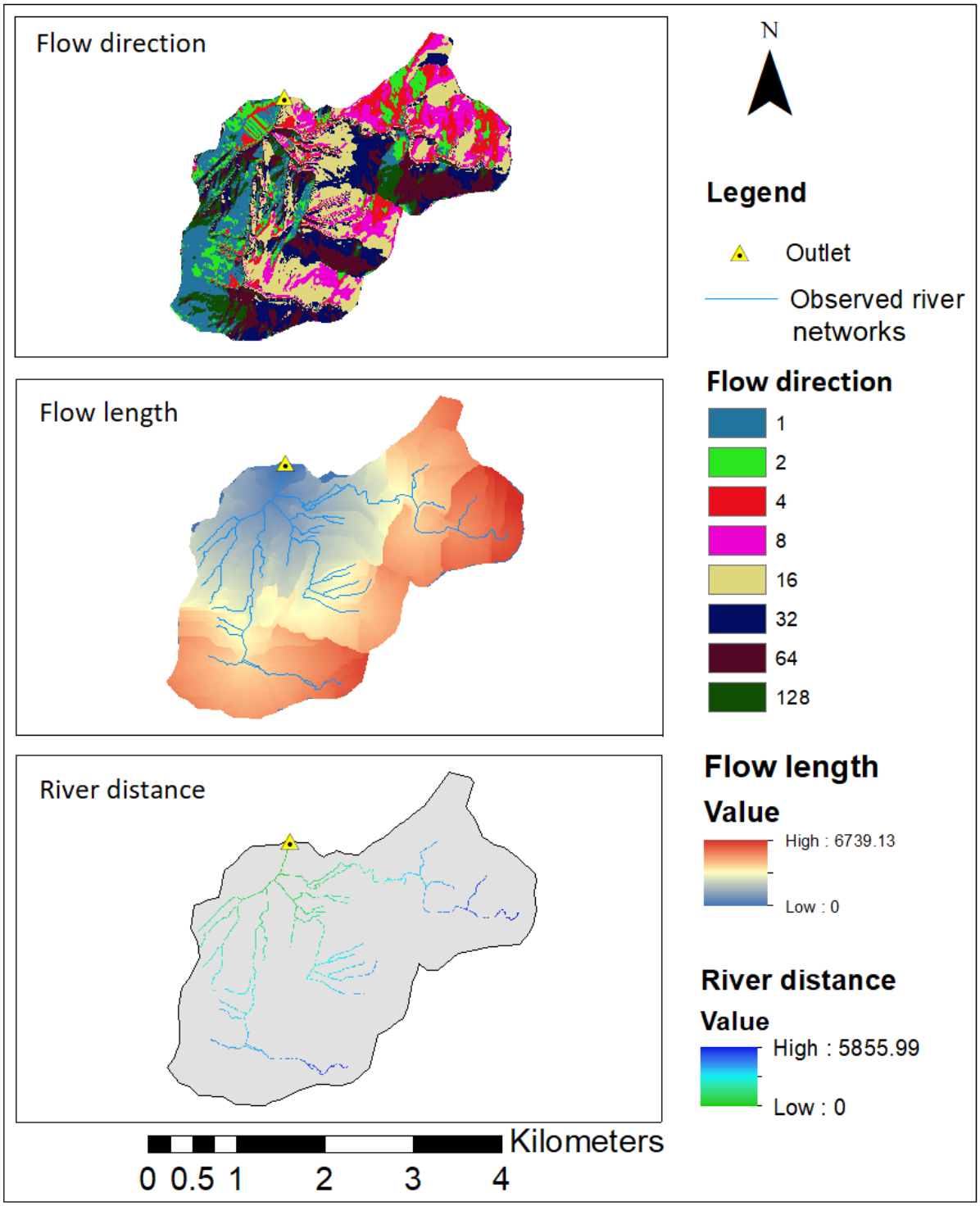

Figure 4.10: Illustration for the river distance distributions, for Vassvatn test catchment.

The illustration for the *a* and *b* coefficients determination is shown in Figure 4.11 for the test catchments and presented in Appendix C for the study catchments. The dynamic river network model parameters are presented in Table 4.8, for all catchments.

Table 4.7: Distance distribution parameters, for the river distance: Mean river distance from the outlet (midFL), maximum river distance from the outlet (maxFL), standard deviation of the river distances (stdFL), area with zero distances to the river (zero fraction) for the marsh (Zbog) and area with zero distances to the river for the soil (Zsoil), for the test and study catchments.

Catchment Id	River distance statistics			Zero fraction	
	midFL (m)	maxFL (m)	stdFL	Zbog	Zsoil
Test Catchments					
Vassvatn (157.3)	2754.53	5855.99	1266.6	0.0134	0.0239
Øvre Glugvatn (151.13)	8666.39	17793.67	3934.5	0.0363	0.0294
Study Catchments					
P5-3360	1859.78	3957.17	1196.7	0.0523	0.0217
P5-4980	1041.5	2068.23	526.05	0.0365	0.0208
P5-6090	656.75	1301.24	373.11	0.0641	0.0315
P6-740	666.15	1336.4	391.6	0.0276	0.0327
P7-640	300.82	615.26	182.54	0	0.0225
P4-4970	115.6	228.99	67.46	0	0.0107
P4-2680	147.4	273.13	80.75	0	0.0153

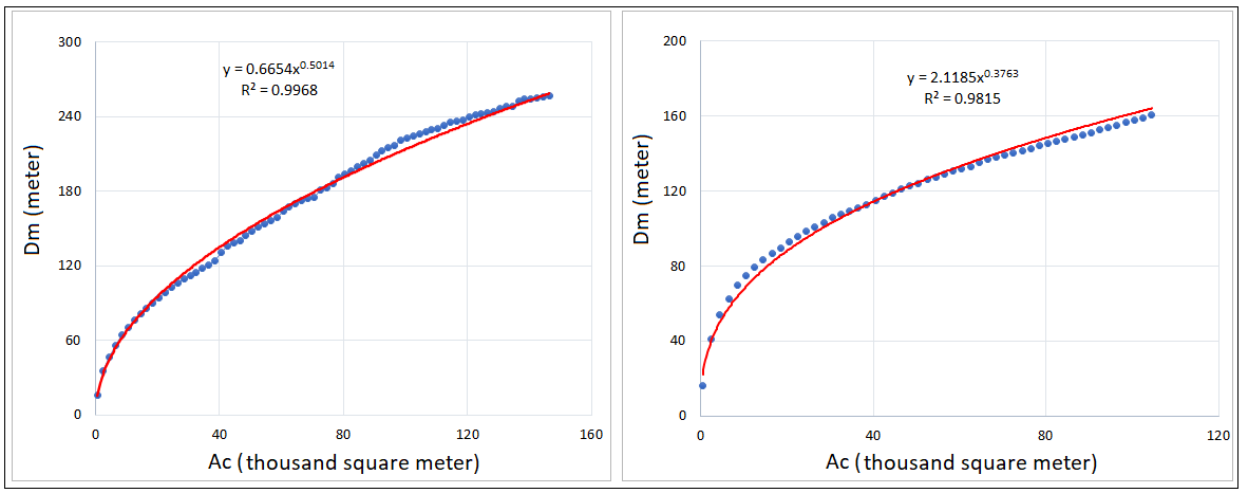

Figure 4.11: Curves fitted to the relation between the mean distance distribution of hillslope (D_m) and critical support area (A_c), for the relation $D_m = aA_c^b$, for the Vassvatn test catchment (left) and Øvre Glugvatn test catchment (right).

Table 4.8: Dynamic river network parameters: The coefficients a and b of the general power relation between D_m and A_c, given as $D_m = aA_c^b$, and their coefficient of determination (R-squared), for the test and study catchments.

Catchment Id	a	b	R^2
Test Catchments			
Vassvatn (157.3)	0.6654	0.5014	0.99
Øvre Glugvatn (151.13)	2.1185	0.3763	0.98
Study Catchments			
P5-3360	0.5912	0.4967	0.99
P5-4980	0.5978	0.4881	0.99
P5-6090	0.3359	0.5583	0.97
P6-740	0.4146	0.5319	0.96
P7-640	0.2714	0.6264	0.98
P4-4970	0.2774	0.5977	0.97
P4-2680	0.1541	0.6631	0.96

Table 4.9: Catchment descriptors used in the physical similarity assessment (for all catchments).

Catchment descriptor	Unit	Minimum	Maximum	Mean
Area (A)	Km^2	0.2	60.7	9.3
Mean soil (non-marsh) distance (midDL)	m	151.6	316.0	226.0
Mean marsh land distance (midLbog)	m	0.0	372.2	142.2
Mean river distance (midFL)	m	115.6	8666.3	1800.9
Effective lake (Le)	%	0.0	6.10	1.2
Forest (F)	%	29.4	100.0	79.1
Bare mountain (B)	%	0.0	56.9	12.2
Urban (U)	%	0.0	0.0	0.0
Mean elevation (Me)	m	102.0	581.0	253.3
Mean annual precipitation (Mp)	mm	1315.0	2621.0	1763.7
Specific Runoff (Sq)	$l/s/km^2$	40.8	125.0	56.5
River slope (Rs)	m/km	15.9	207.8	85.2

4.6 Regionalization methods for DDD model parameters estimation

All the study catchments involved in this paper are small ungauged catchments (area from 0.2 km^2 – 2.8 km^2) and the hourly streamflow needs to be predicted by using the DDD model in order to test the model performance besides to further flood computation for the study culverts. The explanation for the three most known regionalization methods is given in Section 2.2. In this study, the combination of multiple regression and physical similarity (pooling group method) has been applied to estimate the DDD model parameters needing regionalization. In the work of Tsegaw et al. (2019a) the combination method yielded satisfactory performance on an hourly basis for small catchments in Norway. The DDD model parameters were estimated using regionalization methods and model performance was evaluated for two gauged test catchments (comparing simulated runoff against observed runoff).

4.6.1 Regression method

In this approach, it utilizes catchment descriptors to estimate the model parameters using empirical relationships. The physically important empirical formulas that drive between the catchment descriptors and model parameters are described in Equation 4.17, Equation 4.18, Equation 4.19, Equation 4.20. These formulas have been developed in the study by Tsegaw et al. (2019a), and Equation 4.21 developed in Tsegaw et al. (2019b). The catchment descriptors incorporated in this regression approach are due to their significant correlations with the model parameters (Tsegaw et al., 2019a). In this paper, the recession characteristics ($Gscale$, $Gshape$, GshInt and GscInt) are parameters which aimed to predict using multiple regression and critical flux (F_c) using a single regression. The predictor catchment descriptors contain specific runoff, S_q (l/s/km^2), mean elevation, M_e(m), mean annual precipitation, M_p(mm), effective lake, L_e(%) and bare mountain, B(%). The regressed values of the parameters are presented in Table 4.10. The recession characteristics are unitless (positive real numbers), and the critical flux is described as flow in each time step (m^3/h).

$$Gscale = exp(-5.12 - 0.12L_e + 0.22\,ln(S_q) + 0.3\,log(M_e)) \quad (4.17)$$

$$Gshape = 0.82 + 0.0005M_P - 0.009S_q \quad (4.18)$$

$$GshInt = 2.047Gshape - 0.658 \quad (4.19)$$

$$GscInt = 0.49Gscale - 0.0014 \quad (4.20)$$

$$F_c\ (m^3/h) = 160.7 - 1.4 * B \quad (4.21)$$

Table 4.10: DDD model parameters estimated by regression: Scale parameter of λ ($Gscale$), shape parameter of λ ($Gshape$), scale parameter of Λ (GscInt), shape parameter of Λ (GshInt) and the critical flux (F_C), for the test and study catchments.

Catchment Id	$Gscale$	$Gshape$	$GshInt$	$GscInt$	F_C (m^3/h)
Test Catchments					
Vassvatn (157.3)	0.018	1.006	1.400	0.008	81.04
Øvre Glugvatn (151.13)	0.019	0.924	1.233	0.008	119.54
Study Catchments					
P5-3360	0.026	1.243	1.886	0.011	160.7
P5-4980	0.028	1.208	1.814	0.012	160.7
P5-6090	0.026	1.259	1.920	0.012	160.7
P6-740	0.025	1.292	1.986	0.011	160.7
P7-640	0.031	1.256	1.913	0.014	126.82
P4-4970	0.026	1.259	1.919	0.011	160.7
P4-2680	0.026	1.292	1.987	0.011	160.7

4.6.2 Physical similarity method

In this method, the entire model parameters are transferred from most physically similar gauged catchments to the ungauged catchment. In this study, five DDD model parameters (Pro, Cx, CFR, Cea, and rv) are the parameters which aimed to predict using physical similarity. In this study, the pooling group (parameter sets of many similar catchments) based physical similarity have been used to predict the model parameters of the desired catchments. According to the study by Tsegaw et al. (2019a), catchment descriptors which involves topographic features, land uses and characteristics describing runoff dynamics, have used to perform a similarity assessment in this study. 12 catchment descriptors that have been used for similarity assessment are catchment area, mean soil (non-marsh) distances to the river networks, mean marsh land distances to the river networks, mean of river distances from the outlet, effective lake percentage, forest percentage, bare mountain, urban percentage, mean elevation, mean annual precipitation, specific runoff and river slope. The catchment descriptors were prepared for each of the catchments (Table 4.3 to Table 4.7, and summary statistics for the similarity assessment in Table 4.9).

The model parameters of the ungauged study catchments have been estimated by a pooling group method for the calibrated parameters of the 41 small catchments (Appendix B) in Norway that were studied and calibrated in Tsegaw et al., (2019a). The pooling group physical similarity assessment was carried out according to Kay et al. (2006), firstly by considering similarity distance ($dist_{a,b}$) in a space of catchment descriptors between the gauged and ungauged sites as described in Equation 4.22. The smaller value of similarity distance ($dist_{a,b}$) indicates the most similar catchment.

$$dist_{a,b} = \sqrt{\sum_{j=1}^{J} \left(\frac{X_{a,j} - X_{b,j}}{\sigma_{X,j}} \right)^2} \tag{4.22}$$

Where, j represents one of a total of J catchment descriptors, $X_{a,j}$ is the value of catchment descriptor at the ungauged catchment (a), $X_{b,j}$ is the value of catchment descriptor at the gauged catchment (b) and $\sigma_{X,j}$ is the standard deviation of the catchment descriptor for the whole catchments.

(Kay et al., 2006) suggests that 10 most similar donor catchments to form a pooling group, but seven closest neighbors (minimum distances) can optimally provide appropriate site similarity as suggested by Tsegaw et al. (2019a). Therefore, in this study, seven closest neighbors are selected to create a pooling group.

According to Kay et al. (2007), after creating the pooling group, the estimate α_a^{PG} of the model parameter at the desired site (a) is determined as a weighted average of the corresponding parameters from the catchments in the pooling group. It is described in Equation 4.23 as a weighted average of the estimated parameter values, α_m, over all catchments. The weights of the pooling group members are determined by Equation 4.24, which indicates the most similar catchments are given higher weights. Nevertheless, catchments that are not member of the pooling group are assigned a weight (h_{am}) equal to zero.

$$\alpha_a^{PG} = \frac{\sum_{m=1}^{N} h_{am} \alpha_m}{\sum_{m=1}^{N} h_{am}} \tag{4.23}$$

$$h_{am} = 1 - S_{am} \tag{4.24}$$

$$S_{am} = \begin{cases} dist_{a,b} \ / dist_{a,max} & for\ linearly\ decreasing\ weights \\ \left(dist_{a,b}/dist_{a,max}\right)^2 & for\ quadratically\ decreasing\ weights \end{cases}$$

The $dist_{a,max}$ is set to be 10% larger than the maximum distance of a pooling group member, and linear weight assigning method was used in this study.

The seven most similar catchments used in the pooling group for the two test catchments are presented in Table 4.11 and for the study catchments presented in Appendix D. The donor catchments selected for the pooling group are ordered as the most similar catchment on the top, followed by the second most similar catchments and so on.

Table 4.11: Selected pooling group members and their similarity distances for the test catchments: Vassvatn and Øvre Glugvatn.

Vassvatn (id: 157.3)			Øvre Glugvatn (id: 151.13)		
Station name	Station Id	$dist_{a,b}$	Station name	Station Id	$dist_{a,b}$
Hellaugvatn	41.8	2.82	Valen	117.4	2.28
Lauvastøl	36.32	3.11	Røykenes	55.4	2.93
Fjellanger	63.12	3.12	Ånesvatn	186.2	2.97
Havelandself	68.2	3.37	Storvatn	153.1	3.23
Baklihøl	42.6	3.39	Viertjern	16.127	3.51
Nessedalselv	79.3	3.51	Djupevad	42.2	3.71
Djupevad	42.2	3.59	Lakså bru	168.3	3.74

The corresponding model parameters (Pro, Cx, CFR, Cea, and rv) of the pooling group members were derived from the calibrated parameters of the 41 small catchments in Norway, followed by the weighting average procedures explained earlier, in order to transfer the model parameters to the test and study catchments. The derived model parameters by pooling group-based physical similarity for all catchments are presented in Table 4.12.

Table 4.12: The DDD model parameters regionalized by pooling group based physical similarity: Maximum liquid water content of snow (Pro), degree day factor for snow melt (Cx), degree day factor for refreezing (CFR), degree day factor for evapotranspiration (Cea) and river flow celerity (rv).

Catchment Id	Pro -	Cx (mm $^0C^{-1}h^{-1}$)	CFR (mm $^0C^{-1}h^{-1}$)	Cea (mm $^0C^{-1}h^{-1}$)	rv m/s
Test Catchments					
Vassvatn (157.3)	0.098	0.140	0.004	0.027	1.183
Øvre Glugvatn (151.13)	0.089	0.082	0.007	0.020	0.998
Study Catchments					
P5-3360	0.063	0.078	0.008	0.015	0.922
P5-4980	0.063	0.078	0.009	0.015	0.932
P5-6090	0.061	0.078	0.009	0.015	0.913
P6-740	0.072	0.078	0.008	0.015	0.987
P7-640	0.087	0.118	0.005	0.022	1.201
P4-4970	0.063	0.077	0.009	0.015	0.927
P4-2680	0.061	0.078	0.009	0.015	0.912

4.7 Design precipitation approach

The design precipitation is established based on the theoretical storm event via the rainfall intensities associated with frequency of occurrence and duration, for peak flood estimation in combination with a hydrological model. The duration of the design precipitation is determined by the catchment time of concentration (t_c), under the assumption of the occurrence of the peak flood corresponds to the t_c.

As explained earlier in Section 2.1.1, the time of concentration (t_c) is determined based on the Norwegian public roads administration handbook (SVV, 2014), for this study. The t_c formula is given for undeveloped and developed areas, in Equation 4.25 and Equation 4.26 respectively.

$$t_c = 0.6 \text{ L H}^{-0.5} + 300\ A_{se} \quad (4.25)$$

$$t_c = 0.02\ L^{1.15} \text{ H}^{-0.39} + 300\ A_{se} \quad (4.26)$$

Where, t_c is time of concentration (min), L is length of catchment (m), H is the elevation difference in the catchment (m) and A_{se} is effective lake percentage, and it is described in Equation 4.27. The

Equation 4.25 and Equation 4.26 assumes a reasonable generalization between t_c and some catchment characteristics. For instance, the introduction of effective lake percentage, A_{se}, affects the t_c to a great extent if the lake is near to the outlet and to low extent if the lake is located far from the outlet. As the lake is located near the outlet, the A_i gets bigger and results higher effective lake percentage, A_{se} (see equation below).

$$A_{se} = \frac{\sum a_i A_i}{A_{tot}^2} \tag{4.27}$$

Where, a_i is lake area, A_i is upstream catchment area contributing to lake a_i and A_{tot} is total catchment area. In general, if the catchment contains several lakes, flow through the catchment dampens, and consequently delayed t_c.

In this study, the t_c formula for undeveloped areas has been used for estimation. The t_c for each of the study catchments is presented in Table 4.13.

Table 4.13: The catchment characteristics: effective lake percentage (A_{se}), catchment length (L), catchment elevation difference (H) and time of concentration (t_c), for the study catchments.

Catchment Id	A_{se}(%)	L (m)	H (m)	t_c (min)
P5-3360	0.33	2900	340	104.3
P5-4980	0	2300	345	74.31
P5-6090	0	1400	245	53.66
P6-740	0	1800	199	76.55
P7-640	0	1200	364	37.74
P4-4970	0	600	131	31.45
P4-2680	0	700	245	26.83

The design precipitation is derived from the intensity–duration–frequency (IDF) curve for a certain duration and return periods. The design precipitation has been prepared for the study catchments only. In this study, two types of intensity-duration-frequency (IDF) curves were applied for determining the design precipitation: local IDF curve (constructed based on the local precipitation dataset of the catchment) and an online IDF tool recently developed by the Norwegian meteorological institute (MET). The local IDF curve is a 200-year return period of IDF estimate that has been developed from the obtained hourly precipitation data of the desired catchment by aggregating into 2-, 3-, 6-, 12- and 24-h storm events, and the statistics performed for the

corresponding temporal resolutions to construct the curve. Figure 4.12 shows the IDF curve for a 200-year return period developed based on the precipitation dataset for P5-3360 study catchment and for the rest of the study catchments presented in Appendix E. This type of IDF curve is denoted as *local IDF* in this study for further use. The online IDF tool has been created by the MET for extracting IDF precipitation statistics at any point in Norway. This is a new user friendly tool presented in the website of the Norwegian climate service center with possibility to download as figures and tables for the point of interest and for the durations 1 minute to 24 hours and with return periods of 2, 5, 10, 20, 50, 100 and 200 years, (https://klimaservicesenter.no/). For durations longer than 24 hours and return periods for more than 200 years, estimates can be ordered from MET (Stenius et al., 2015). Figure 4.13 shows the IDF curves for P5-3360 study catchment and for the rest of the catchments presented in Appendix E. This type of IDF curve is denoted as *online IDF Tool* for further use in this work.

The design precipitation used by the consultant (Norconsult) on the E6 Helgeland Sør project has been transferred from the IDF curve for Sandsli station in Bergen to all study catchments (Norconsult, 2018). This IDF curve has been also considered in this study in order to make a valid comparison with the Norconsult design flood peak estimates. Figure 4.14 shows the IDF curves for Sandsli station and it is denoted as *Sandsli IDF* in this work for further application.

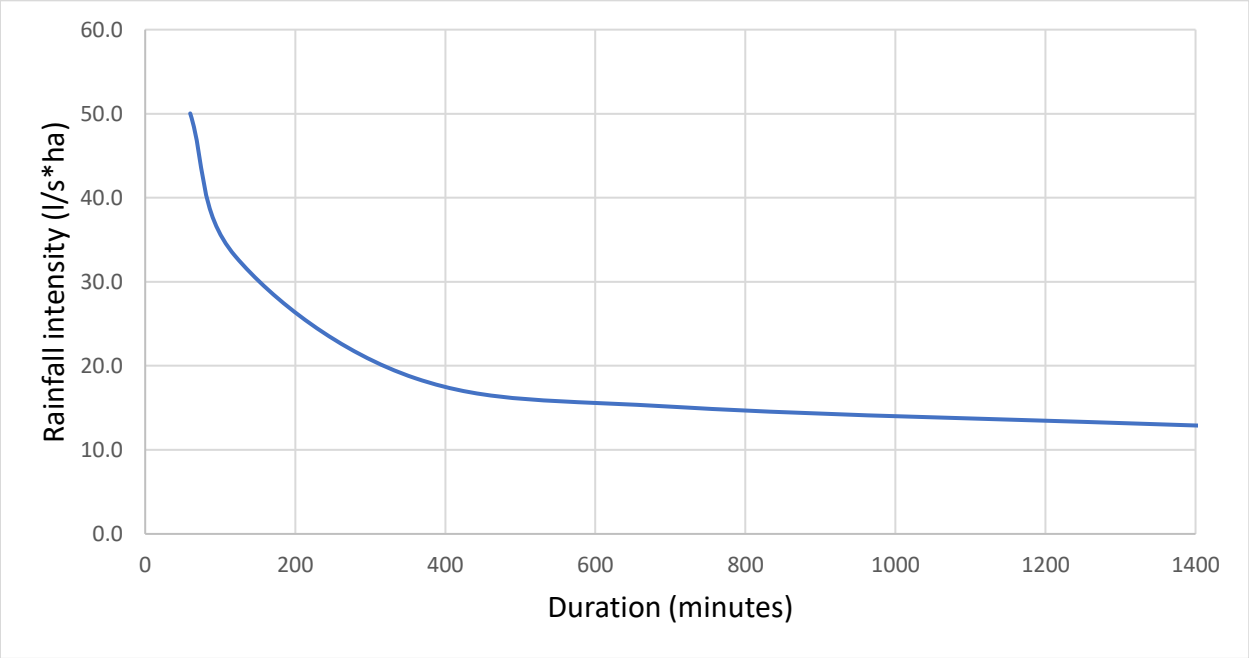

Figure 4.12: The local intensity-duration-frequency (IDF) curve for 200-year return period, for P5-3360 catchemnt.

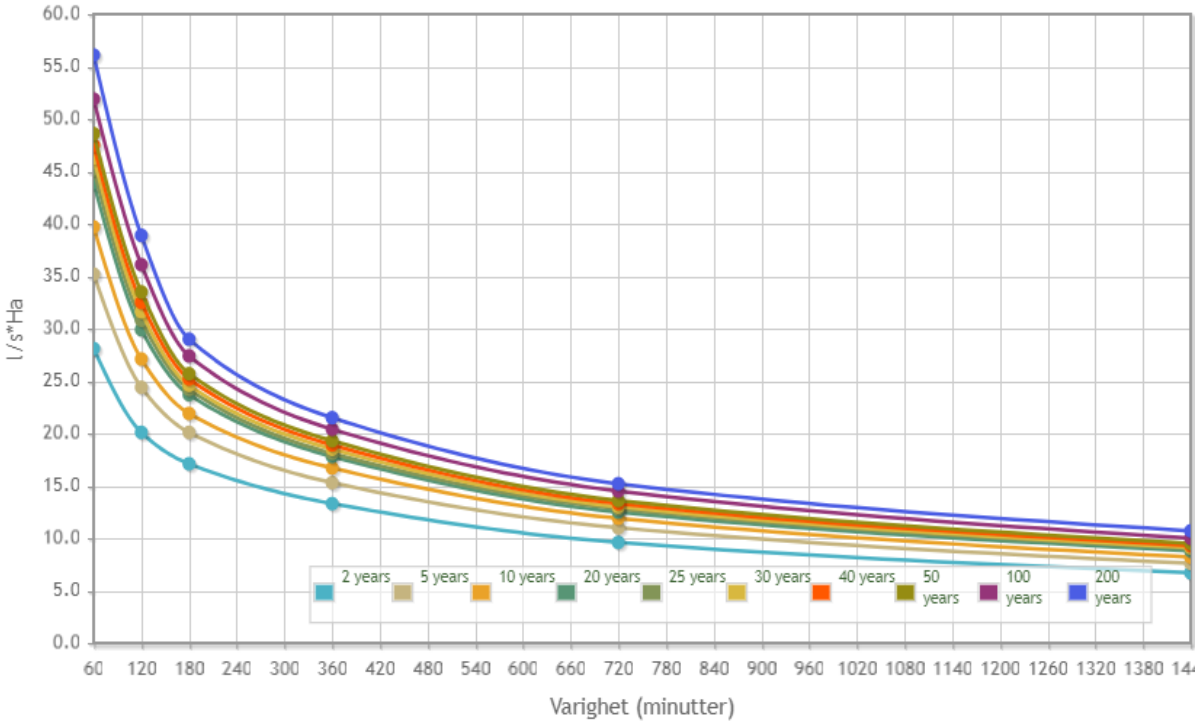

Figure 4.13: The intensity-duration-frequency (IDF) curves downloaded from the Norwegian climate service website (online IDF tool), for 200-year return period marked in blue, for P5-3360 catchment.

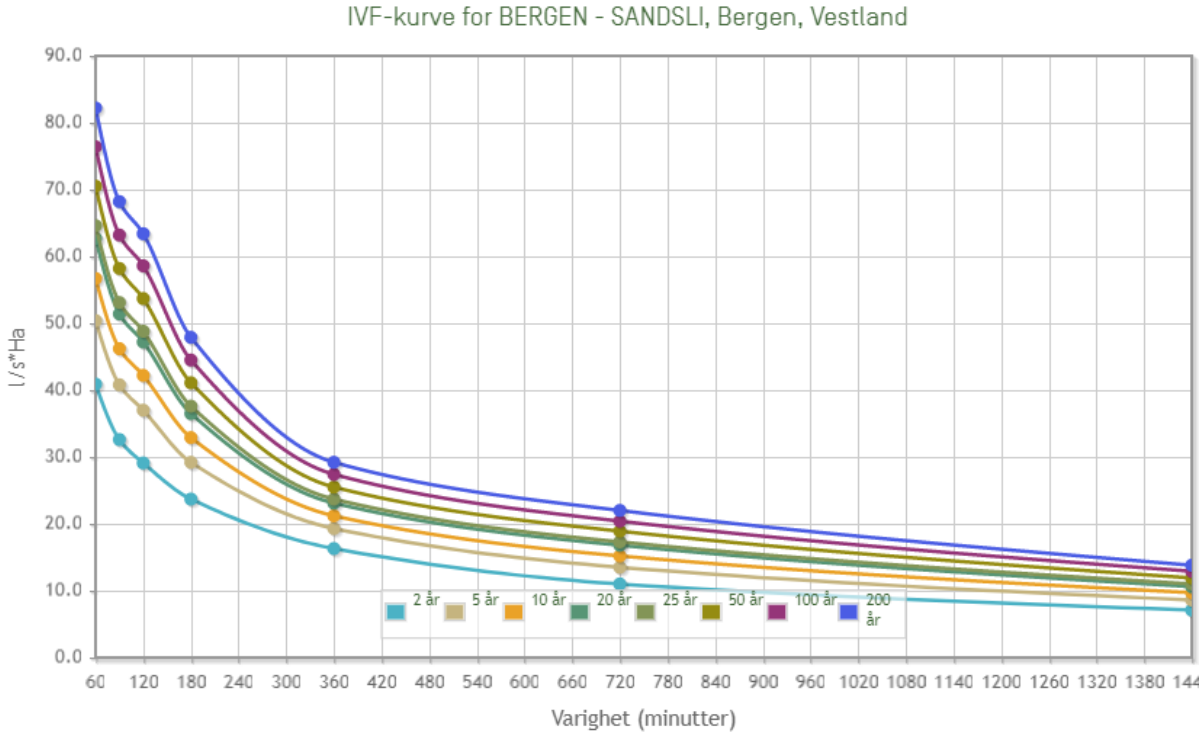

Figure 4.14: The intensity-duration-frequency (IDF) curves for Sandsli station in Bergen, a 200-year return period marked in blue.

The study catchments are very small with short concentration times, and creating an hourly design hyetograph for the corresponding t_c was not convenient for most of the catchments since the DDD model currently runs on hourly temporal resolution and most catchments have t_c close to one hour and less than one hour (Table 4.13). Thus, the design precipitation over a time span equal to t_c of the catchments have been considered as one hour design hyetograph and set into the model as a single event. The magnitude of the rainfall intensity is obtained from the IDF curve as a function of t_c and return period, T. This approach is consistent with the use of the rational method to estimate the peak flood yielded from a small catchment. The 200-year design precipitation used for peak flood computation is given in Table 4.14 for all the study catchments.

The rainfall-runoff model DDD was used for peak flood estimation. The pre-event conditions have been set as a dry catchment, wet catchment and during snowmelt. These conditions have been identified based on the initial model simulation prior to peak flood estimation. That means the model was first tested on simulation with the climatic (precipitation and temperature) input and the required model parameters; then from the first model result, the high soil moisture and snow accumulation periods have been selected over the entire seven years simulation period.

Table 4.14: The time of concentration (t_c) and their corresponding 200-year design precipitation from the three different IDF curves (local IDF, online IDF Tool and Sandsli IDF), for the study catchments.

		Design precipitation (mm) from three IDF curves		
Catchment Id	t_c(minutes)	Local IDF	Online IDF Tool	Sandsli IDF
P5-3360	104.3	24	29	42
P5-4980	74.31	20.5	24	34
P5-6090	53.66	17	20	32
P6-740	76.55	22.5	26	35
P7-640	37.74	16	19.5	26
P4-4970	31.45	13	16	24
P4-2680	26.83	12	14.5	23

5. RESULTS

In the following section, the DDD model performance results for different model states, for both test catchments are presented. The successive sections present the DDD model flood peak estimate results and comparisons with the existing design floods computed by Norconsult.

5.1 DDD model Performance

The DDD model performance was evaluated in regionalization against three simulation conditions. In the first evaluation, simulation without the precipitation correction (Pkorr set to one) and without dynamic river network, was tested. In the second assessment, simulation with precipitation correction (Pkorr value) and without dynamic river network, was carried out to show the goodness of fit from corrected precipitation aspect and/or water balance aspects between the observed and simulated discharges. In the final evaluation, simulation with precipitation correction (Pkorr value) and dynamic river network, was investigated. The predictive accuracy for the regionalization has been described by the Kling-Gupta efficiency (KGE) (Gupta et al., 2009). The evaluation basis for the model performance are KGE, BIAS and visual evaluation of the observed and simulated hydrographs. The best optimal value for KGE and BIAS is 1.

5.1.1 Simulation without precipitation correction and without dynamic river network

The regionalized DDD model parameters without precipitation correction (Pkorr set to one), performs satisfactorily (KGE > 0.5), for both test catchments (Figure 5.1 and Figure 5.2).

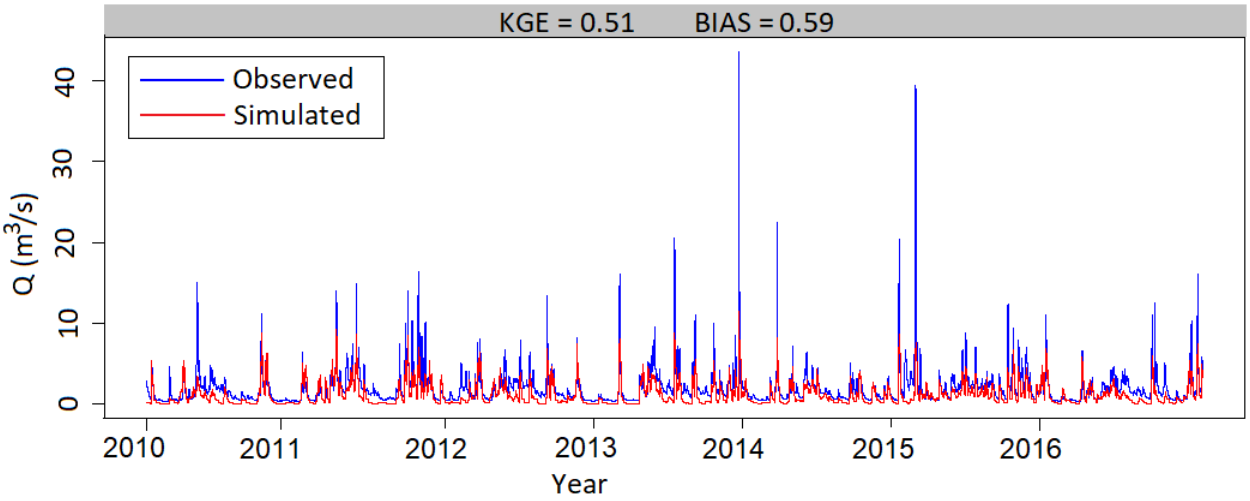

Figure 5.1: Observed and simulated discharges (Q) without precipitation correction (Pkorr set to one) and without dynamic river network, and the model performance, for Vassvatn catchment.

In accordance to the performance classification presented in Thiemig et al. (2013), good (KGE ≥ 0.75), intermediate (0.5 ≤ KGE < 0.75), poor (0.0 < KGE < 0.5) and very poor (KGE ≤ 0.0), the regionalized model simulations show encouraging capacity to predict flows.

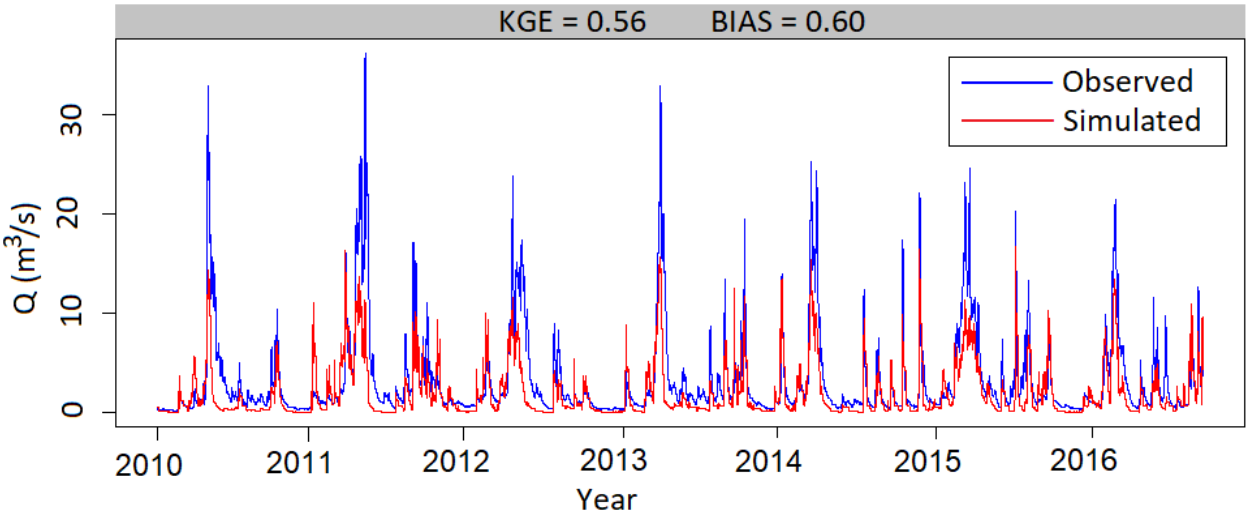

Figure 5.2: Observed and simulated discharges (Q) without precipitation correction (Pkorr set to one) and without dynamic river network, and the model performance, for Øvre Glugvaten catchment.

5.1.2 Simulation with precipitation correction and without dynamic river network

The simulated discharges with corrected precipitation compared to the observed discharges, and the model performance for the test catchments, are presented in Figure 5.3 and Figure 5.4.

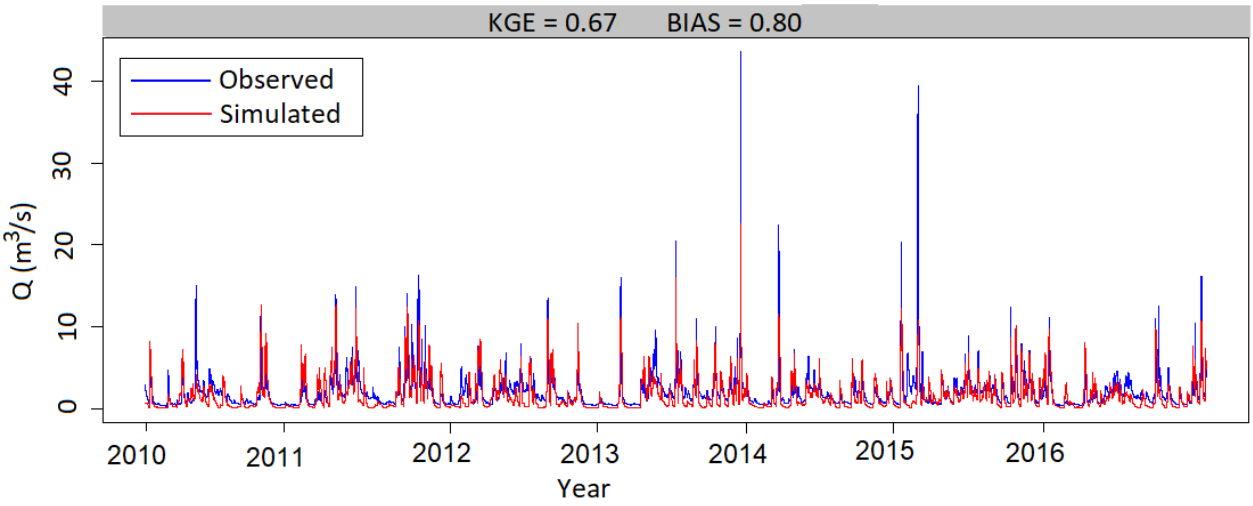

Figure 5.3: Observed and simulated discharges (Q) with precipitation correction, and the model performance, for Vassvatn catchment.

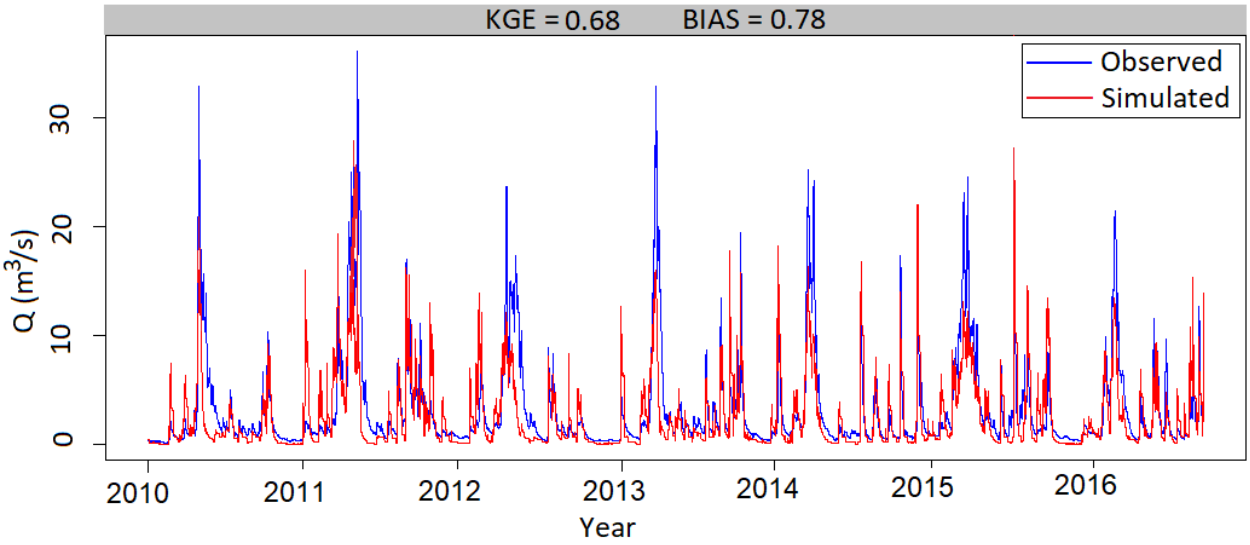

Figure 5.4: Observed and simulated discharges (Q) with precipitation correction, and the model performance, for Øvre Glugvaten catchment.

To improve the precision of the long-term water balance, precipitation correction factor has been applied. The precipitation correction factor (Pkorr) value was considered as the ratio of the long-term mean annual discharge to the mean of the initially simulated discharge. Thus, 1.43 and 1.46 precipitation correction factors have been considered for Vassvaten and Øvre Glugvaten test catchments respectively. As the Pkorr value introduced into the model, the simulation performance of the model has increased. As shown in Figure 5.3, for Vassvaten catchment, the KGE value has improved from 0.51 to 0.67, and BIAS value from 0.59 to 0.80. Similarly, as shown in Figure 5.4, for Øvre Glugvaten catchment, the KGE value has improved from 0.56 to 0.67, and BIAS value from 0.59 to 0.78.

5.1.3 Simulation with precipitation correction and dynamic river network

Besides the precipitation correction value, the dynamic river network was activated in the DDD model. As the dynamic river network introduced, the simulation performance of the model has remained unchanged, i.e., the same KGE and BIAS values with the simulation with precipitation correction and without dynamic river network, in both test catchments. Nevertheless, the flood peak has improved significantly in some events of the hydrograph, clearly shown in both test catchments (Figure 5.5 and Figure 5.6). The simulated discharges using the DDD model including Pkorr value and dynamic river network, the observed discharges and the model performance, for the test catchments are presented in Figure 5.5 and Figure 5.6.

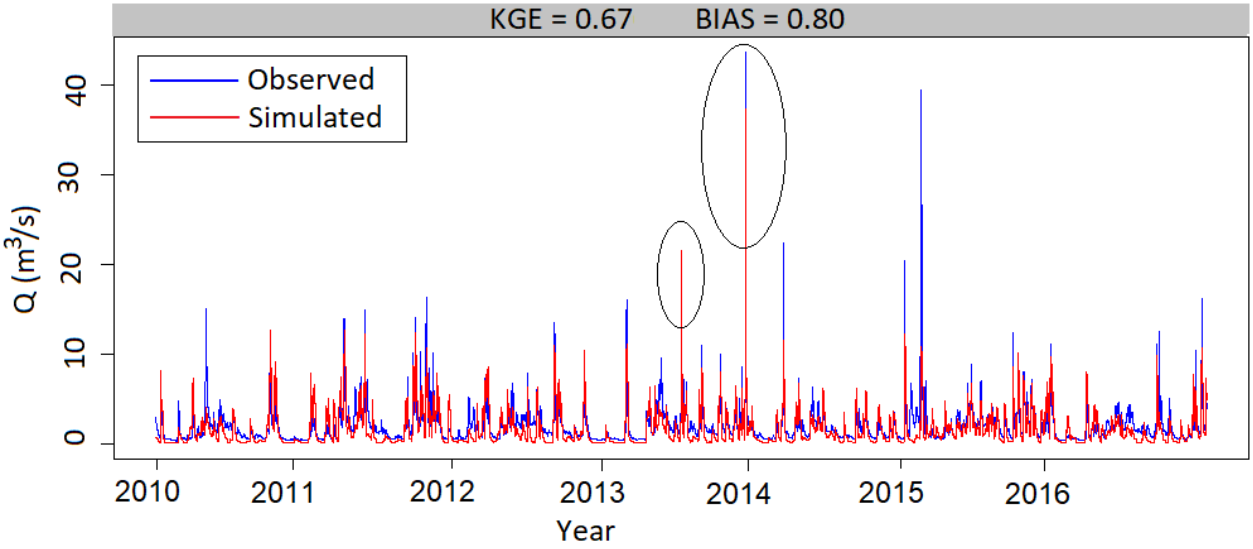

Figure 5.5: Observed and simulated discharges (Q) with precipitation correction and dynamic river network, and the model performance, for Vassvatn catchment.

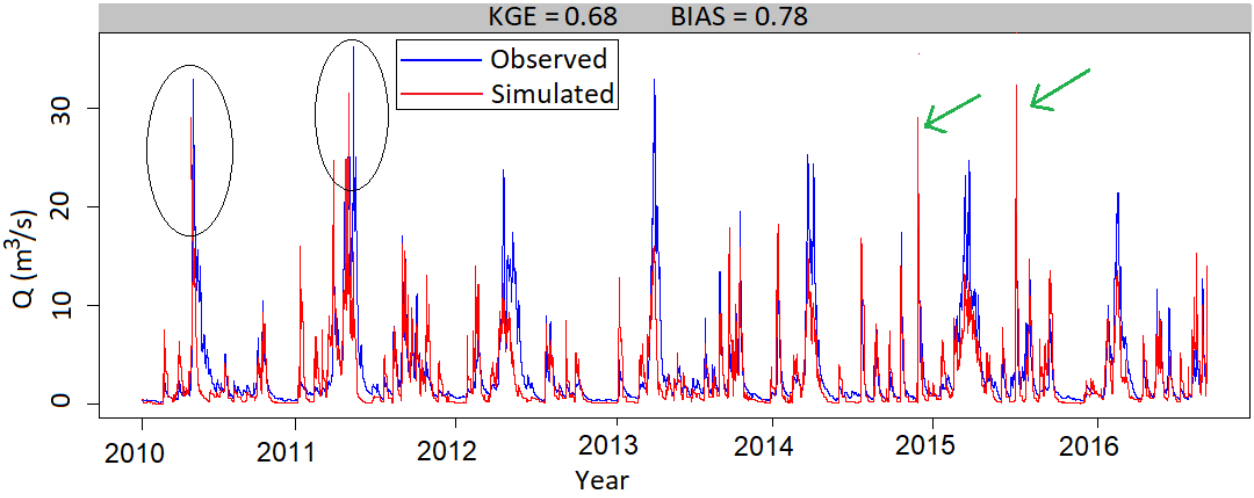

Figure 5.6: Observed and simulated discharges (Q) with precipitation correction and dynamic river network, and the model performance, for Øvre Glugvaten catchment.

5.2 Flood peak estimates using DDD model

For the peak flood estimation of the study catchments, the same routine with the test catchments was followed, i.e., the Pkorr value and the dynamic river network was considered in the DDD model set up. The Pkorr (ratio of long-term mean annual discharge value to mean of the initially simulated discharge) value was resulted as 1.3, 1.1, 1.09, 1.05, 1.13, 1.0, and 1.0 for P5-3360, P5-4980, P5-6090, P6-740, P7-640, P4-4970 and P4-2680 catchment respectively.

The estimation of a 200-year flood peak has been computed using the model for the design precipitation derived from three IDF curves combined with the three different catchment states. The design precipitation estimates have been derived from local IDF, online IDF tool and Sandsli IDF. The three catchment conditions employed are dry catchment, wet catchment and during snowmelt. The three design flood estimation methods used by Norconsult are NIFS formula, regional analysis and rational method.

The estimate of 200-year flood peak using DDD model is presented in Figure 5.7, Figure 5.8, Figure 5.9, Figure 5.10, Figure 5.11, Figure 5.12 and Figure 5.13, for P5-3360, P5-4980, P5-6090, P6-740, P7-640, P4-2680 and P4-4970 catchment respectively, which includes, besides the peak flood estimate using the DDD model, the design flood results of Norconsult.

The results show that the estimated flood peak results using the DDD model were sensitive to the chosen IDF curves. Based on the respective design precipitation inputs; the Sandsli IDF curve yielded the highest flood peak estimate, the online IDF Tool provided the next higher flood peak estimate and the local IDF curve gave the lowest flood peak estimate, this outcome was consistent for all catchments under study.

Based on the flood peak results found, the DDD model results rely on the catchment area. For this reason, the seven study catchments were split according to the catchment size into two bigger catchments (P5-3360 and P5-4980), two smaller catchments (P5-6090 and P6-740) and three tiny catchments (P7-640, P4-4970, P4-2680).

The flood peak estimate using the DDD model for the two bigger catchments (P5-3360 and P5-4980) and one smaller catchment (P6-740) for the design precipitation estimate derived from Sandsli IDF combined with snowmelt condition outnumbered design flood results by Norconsult (see Figure 5.7, Figure 5.8, Figure 5.10). On the other hand, the DDD flood peak estimates for design precipitation combined with dry and wet antecedent conditions yielded lower flood peaks than the Norconsult design floods for the two bigger sizes (P5-3360 and P5-4980) and one smaller catchment (P6-740) (Figure 5.7, Figure 5.8, Figure 5.10). Similarly, for one smaller catchment (P5-6090) and the three tiny catchments (P7-640, P4-2680 and P4-4970), the DDD model flood peak estimates in all conditions provided lower flood magnitudes than the Norconsult design floods (Figure 5.9, Figure 5.11, Figure 5.12, Figure 5.13).

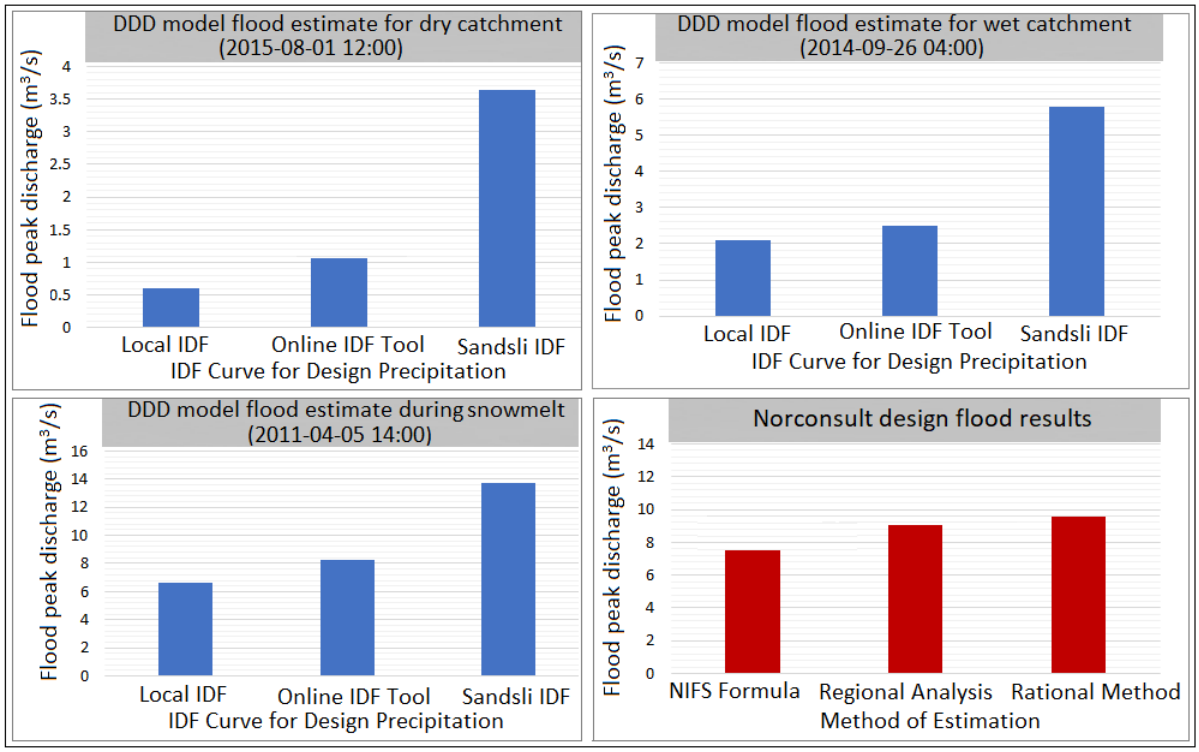

Figure 5.7: Peak flood estimate using the DDD model, for different catchment conditions (dry catchment, wet catchment and during snowmelt) and computed design flood by Norconsult, for P5-3360 catchment.

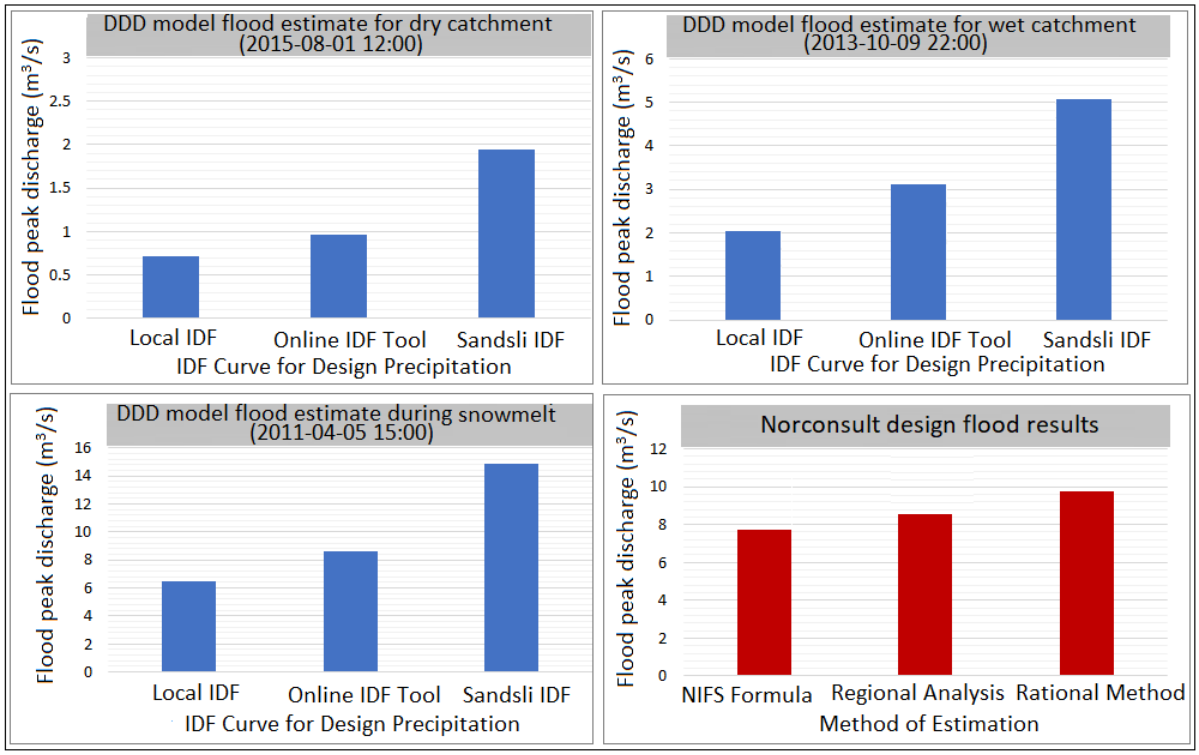

Figure 5.8: Peak flood estimate using the DDD model for different catchment conditions (dry catchment, wet catchment and during snowmelt) and computed design flood by Norconsult, for P5-4980 catchment.

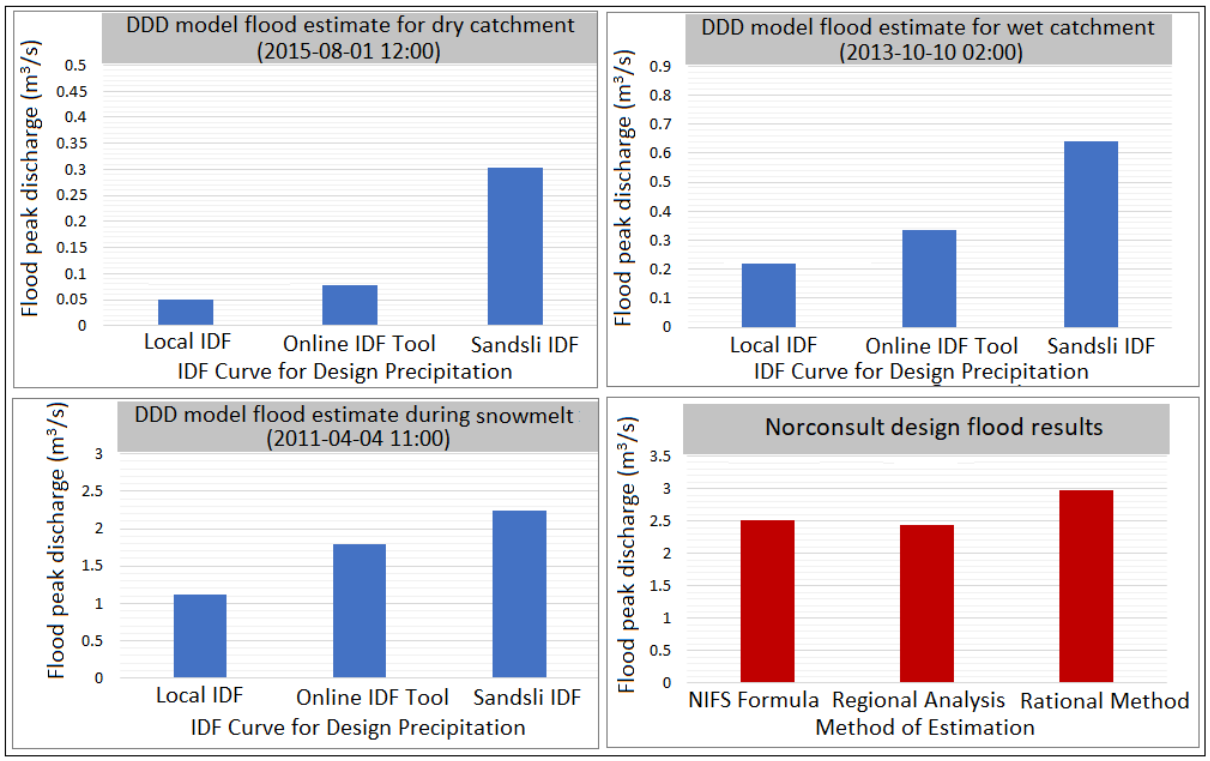

Figure 5.9: Peak flood estimate using the DDD model for different catchment conditions (dry catchment, wet catchment and during snowmelt) and computed design flood by Norconsult, for P5-6090 catchment.

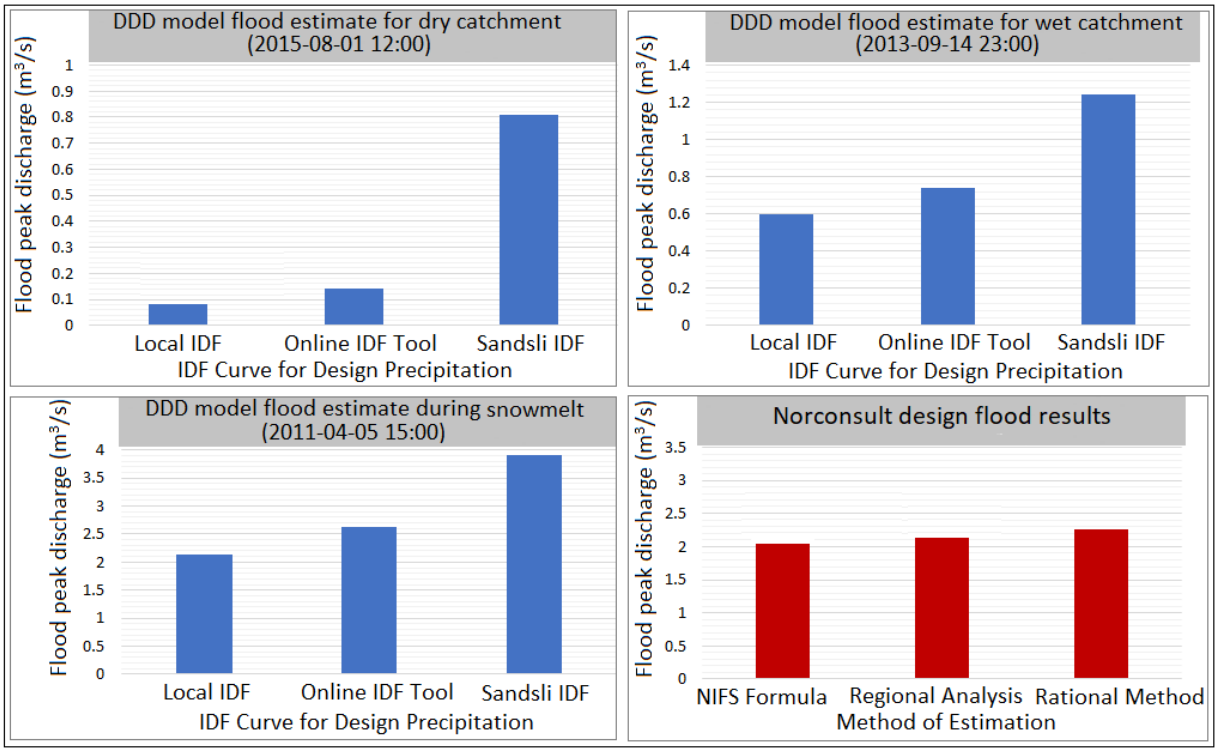

Figure 5.10: Peak flood estimate using the DDD model for different catchment conditions (dry catchment, wet catchment and during snowmelt) and computed design flood by Norconsult, for P6-740 catchment.

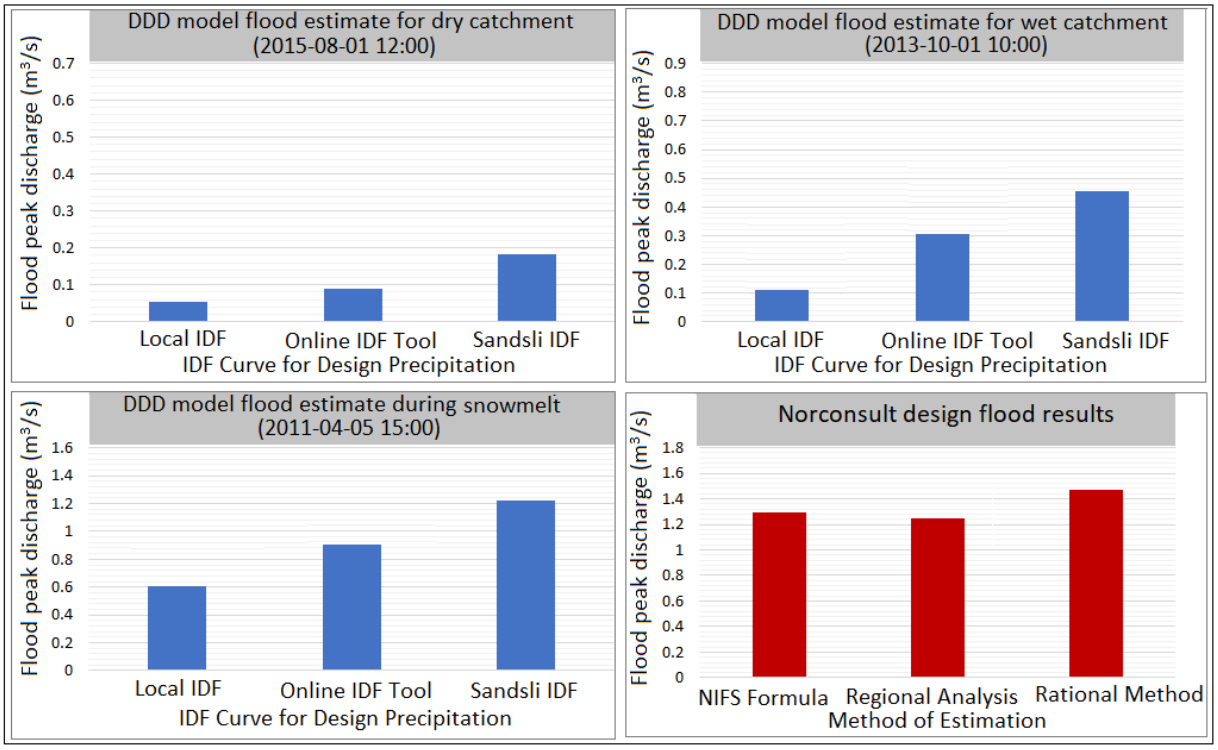

Figure 5.11: Peak flood estimate using the DDD model for different catchment conditions (dry catchment, wet catchment and during snowmelt) and computed design flood by Norconsult, for P7-640 catchment.

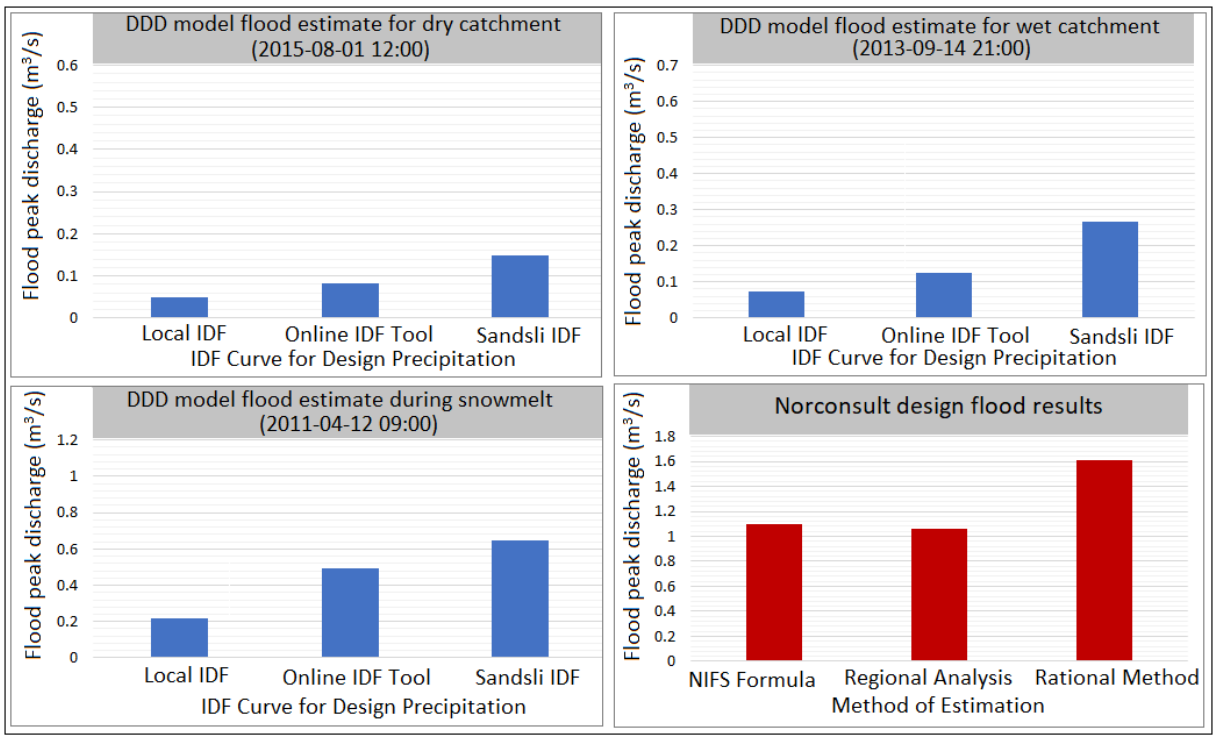

Figure 5.12: Peak flood estimate using the DDD model for different catchment conditions (dry catchment, wet catchment and during snowmelt) and computed design flood by Norconsult, for P4-4970 catchment.

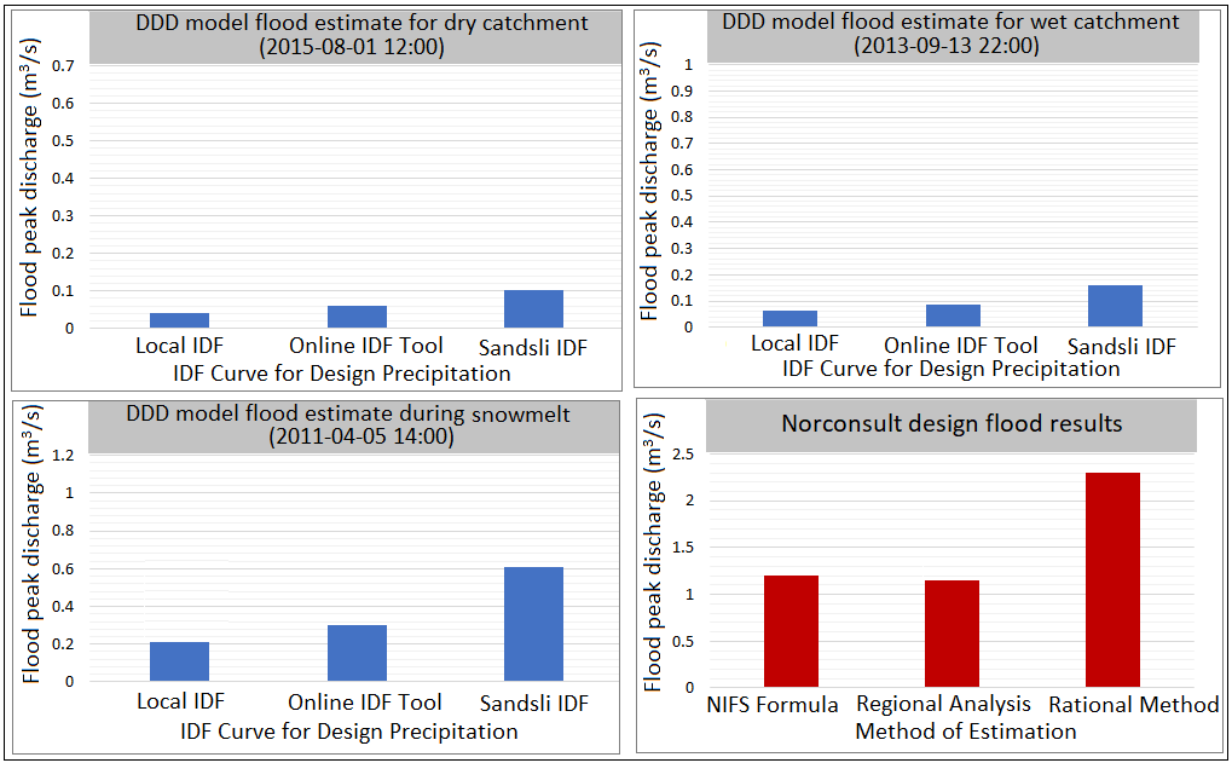

Figure 5.13: Peak flood estimate using the DDD model for different catchment conditions (dry catchment, wet catchment and during snowmelt) and computed design flood by Norconsult, for P4-2680 catchment.

5.3 Flood peak comparisons

The results have been compared to the design flood results of the three different methods computed by Norconsult. The Norconsult design flood results are found from Norconsult (2018) document. The Norconsult document includes a safety factor to the NIFS formula and regional analysis methods, and a climate factor to the average flood peak between NIFS formula and rational method, for each of the catchments. This factor was not considered in the DDD model set up and these factors have been removed from the Norconsult design flood estimates, before comparison with DDD model results, to make a proper comparison.

A relative difference (100 ×(DDD model flood estimate – Norconsult design flood)/ Norconsult design flood), which is a simple statistics between the DDD model flood peak estimates and Norconsult design flood results have been performed to describe the comparison and the results are presented in Table 5.1, Table 5.2 and Table 5.3 for dry catchment, wet catchment and snowmelt condition respectively. In the following tables, the negative relative difference indicates that much lower flood magnitude than the Norconsult results, and the positive relative difference indicates that much higher flood magnitude than the Norconsult results.

Table 5.1: The DDD model flood peak estimates for dry catchment condition and relative difference in comparison to the NIFS formula, regional analysis and rational method.

Catchment id	IDF curves for design precipitation	DDD model flood peak estimate for dry catchment (m^3/s)	Norconsult design flood peak discharges (m^3/s)			Relative difference (%)		
			NIFS Formula	Regional Analysis	Rational Method	NIFS formula	Regional analysis	Rational method
P5-3360	Local IDF	0.60	7.44	9.08	9.53	-92	-93	-94
	Online IDF Tool	1.10				-85	-88	-88
	Sandsli IDF	3.58				-52	-61	-62
P5-4980	Local IDF	0.65	7.88	8.46	9.76	-92	-92	-93
	Online IDF Tool	0.95				-88	-89	-90
	Sandsli IDF	1.84				-77	-78	-81
P5-6090	Local IDF	0.05	2.51	2.48	2.97	-98	-98	-98
	Online IDF Tool	0.07				-97	-97	-98
	Sandsli IDF	0.30				-88	-88	-90
P6-740	Local IDF	0.09	2.15	2.33	2.37	-96	-96	-96
	Online IDF Tool	0.14				-94	-94	-94
	Sandsli IDF	0.80				-63	-66	-65
P7-640	Local IDF	0.05	1.31	1.22	1.47	-96	-96	-97
	Online IDF Tool	0.09				-93	-92	-94
	Sandsli IDF	0.18				-86	-84	-88
P4-4970	Local IDF	0.05	1.12	1.05	1.6	-95	-95	-97
	Online IDF Tool	0.07				-94	-93	-96
	Sandsli IDF	0.14				-87	-87	-91
P4-2680	Local IDF	0.04	1.22	1.19	2.30	-97	-97	-98
	Online IDF Tool	0.05				-96	-96	-98
	Sandsli IDF	0.10				-92	-92	-96

Table 5.2: The DDD model flood peak estimates for wet catchment condition and relative difference in comparison to the NIFS formula, regional analysis and rational method.

Catchment id	IDF curves for design precipitation	DDD model flood peak estimate for wet catchment (m^3/s)	Norconsult design flood peak discharges (m^3/s)			Relative difference (%)		
			NIFS Formula	Regional Analysis	Rational Method	NIFS formula	Regional analysis	Rational method
P5-3360	Local IDF	2.10	7.44	9.08	9.53	-72	-77	-78
	Online IDF Tool	2.50				-66	-72	-74
	Sandsli IDF	5.80				-22	-36	-39
P5-4980	Local IDF	2.05	7.88	8.46	9.76	-74	-76	-79
	Online IDF Tool	3.33				-58	-61	-66
	Sandsli IDF	5.09				-35	-40	-48
P5-6090	Local IDF	0.22	2.51	2.48	2.97	-91	-91	-93
	Online IDF Tool	0.33				-87	-87	-89
	Sandsli IDF	0.64				-74	-74	-78
P6-740	Local IDF	0.60	2.15	2.33	2.37	-72	-74	-74
	Online IDF Tool	0.74				-66	-68	-67
	Sandsli IDF	1.24				-42	-47	-45
P7-640	Local IDF	0.11	1.31	1.22	1.47	-92	-90	-93
	Online IDF Tool	0.30				-77	-74	-80
	Sandsli IDF	0.43				-67	-62	-71
P4-4970	Local IDF	0.08	1.12	1.05	1.6	-93	-92	-95
	Online IDF Tool	0.11				-90	-90	-93
	Sandsli IDF	0.26				-76	-75	-84
P4-2680	Local IDF	0.04	1.22	1.19	2.30	-97	-97	-98
	Online IDF Tool	0.06				-95	-95	-97
	Sandsli IDF	0.17				-86	-86	-93

Table 5.3: The DDD model flood peak estimates during snowmelt condition and relative difference in comparison to the NIFS formula, regional analysis and rational method.

Catchment id	IDF curves for design precipitation	DDD model flood peak estimate during snowmelt (m^3/s)	Norconsult design flood peak discharges (m^3/s)			Relative difference (%)		
			NIFS Formula	Regional Analysis	Rational Method	NIFS formula	Regional analysis	Rational method
P5-3360	Local IDF	6.63	7.44	9.08	9.53	-11	-27	-30
	Online IDF Tool	8.22				11	-9	-14
	Sandsli IDF	13.74				85	51	44
P5-4980	Local IDF	6.50	7.88	8.46	9.76	-17	-23	-33
	Online IDF Tool	8.60				9	2	-12
	Sandsli IDF	14.84				88	75	52
P5-6090	Local IDF	1.12	2.51	2.48	2.97	-55	-55	-62
	Online IDF Tool	1.80				-28	-28	-39
	Sandsli IDF	2.30				-8	-8	-23
P6-740	Local IDF	2.13	2.15	2.33	2.37	-1	-9	-6
	Online IDF Tool	2.62				22	12	15
	Sandsli IDF	3.90				81	67	72
P7-640	Local IDF	0.60	1.31	1.22	1.47	-54	-47	-59
	Online IDF Tool	0.90				-31	-21	-39
	Sandsli IDF	1.26				-4	11	-14
P4-4970	Local IDF	0.22	1.12	1.05	1.6	-80	-79	-86
	Online IDF Tool	0.30				-72	-72	-81
	Sandsli IDF	0.66				-39	-37	-59
P4-2680	Local IDF	0.21	1.22	1.19	2.30	-83	-83	-91
	Online IDF Tool	0.30				-75	-75	-87
	Sandsli IDF	0.62				-49	-48	-73

6. DISCUSSION

In this section, the regionalization model performance and the DDD model flood peak estimates for various catchment conditions in comparison to the existing design floods have been discussed.

6.1 DDD model Performance

6.1.1 Simulation without precipitation correction and without dynamic river network

The regionalization without correction for the precipitation input, the DDD model performance for both test catchments lies in the intermediate range of KGE, $0.5 \leq KGE \leq 0.75$. In this initial simulation, both test catchments yielded satisfactory results. Nevertheless, the visual inspection (Figure 5.1 and Figure 5.2) shows underestimation of flow when compared to the observed flow, in both test catchments. This can be caused due to the gridded precipitation input. In Norway, the gridded dataset is prepared regardless of precipitation correction for losses caused by wind (Tsegaw et al., 2019a). Moreover, due to irregular topography and few precipitation stations in the elevated areas, the gridded precipitation is uncertain, and the correlation between the precipitation and elevation is established only around the station locations, consequently predicted precipitation might potentially create underestimation to the actual precipitation, mostly at higher elevations (Lussana et al., 2018). For instance, a comparison case was conducted in the study of Tsegaw et al. (2019a) between the gridded inputs and precipitation gauges in Norway and discovered that the gridded precipitation provided lower flood estimation value than the precipitation gauges. This highlights that the consideration of precipitation correction factor is important.

6.1.2 Simulation with precipitation correction and without dynamic river network

In this condition, the KGE value lies again in the intermediate range, but show an improved performance relative to the former simulation (Figure 5.3 and Figure 5.4). The results additionally confirmed that the water balance simulation has improved than that of without precipitation correction. Based on the visual inspection, the simulated flow has improved well. However, underestimation of the peak flood events is clearly shown in many parts of the hydrograph, in both test catchments. This agreed with the study of Tsegaw et al. (2019a) who concluded that the DDD model underestimates flood events generated by high precipitation.

6.1.3 Simulation with precipitation correction and dynamic river network

The dynamic river network has been activated in the model and enabled to see how the simulation performance has changed, as well as the influence of dynamic river network to handle the peak

floods. More specifically, for both test catchments, the dynamic river network was first activated without the precipitation correction factor, but it did not affect the flow simulation at all, because excess precipitation is required to expand the observed river network. Thus, a precipitation correction factor was considered to assess the effect of the dynamic river network.

The model yielded equal performance in terms of KGE and BIAS with the previous simulation (Figure 5.5 and Figure 5.6). Based on visual inspection for Vassvaten test catchment the flood peaks have been improved in some parts of the hydrograph (see the marked with an ellipse in Figure 5.5). On the other hand, it shows underestimated flood peak events in some parts of the hydrograph (see Figure 5.5). Similarly, for the Øvre Glugvaten test catchment the flood peaks have been handled in some part of the hydrograph (see the marked with an ellipse in Figure 5.6). In this test catchment, underestimation of flood peaks is clearly shown in several parts of the hydrograph, and in this case, the are some overestimations created due to the dynamic river network (for instance, see the hydrograph part pointed in green in Figure 5.6). Two probable reasons for this overestimation has been pointed out in the work of Tsegaw et al. (2019b): the F_c value may not be the absolute representation for the process of flow generation and the estimated D_m using Equation 4.15 might not represent the actual process during a flood event.

6.1.4 The influence of the dynamic river network

The rational of activating the dynamic river network is to improve the underestimation of the peak flood events. This was required because the main purpose of this study is the computation of the flood peak for several small ungauged catchments using the DDD model. The dynamic river network forcing show an encouraging effect to capture the flood peaks, even though the KGE and BIAS remain unchanged. This agrees with the study of Tsegaw et al. (2019b) who suggested that the KGE and BIAS values yielded when the dynamic river network considered should not be less than the KGE and BIAS values obtained without dynamic river network.

The dynamic river network has shown a significant impact on handling the flood peaks. For example, for the first test catchment (Vassvatn), the observed flood peak over the seven years was 43.53 m^3/s and the simulated flood peak with corrected precipitation and without dynamic river network was 22.57 m^3/s (See Table 6.1), this is can be described by 48% relative difference. When the dynamic river network was activated, the DDD model produced a flood peak of 37.24 m^3/s, which reduce the relative difference to 14.5%. Similarly, the second test catchment (Øvre

Glugvaten) show a relative difference reduction from 22.5% to 7% (Table 6.1). This is a great value for improving the flood peak estimations. The observed peak floods, the simulated peak floods and the KGE and BIAS model performance summarized for the three simulation conditions, for both test catchments presented in Table 6.1.

Table 6.1: Observed and simulated flood peaks using the DDD model, and summary of the corresponding performance of the model, for the test catchments.

				DDD model performance with Pkorr = 1			DDD model performance with Pkorr >1			DDD model performance with Pkorr > 1 and dynamic river network	
Catchment id	Observed flood peak (m^3/s)	Simulation period	Simulated flood peak with Pkorr = 1 (m^3/s)	KGE	BIAS	Simulated peak flood with Pkorr > 1 (m^3/s)	KGE	BIAS	Simulated flood with Pkorr > 1 and dynamic river network (m^3/s)	KGE	BIAS
Vassvatn (157.3)	43.53	7 years	11.52	0.51	0.59	22.57	0.67	0.80	37.24	0.67	0.80
Øvre Glugvatn (151.13)	36.16	7 years	16.66	0.56	0.60	28.04	0.68	0.78	33.62	0.68	0.78

6.2 Flood peak estimates using DDD model for various conditions

As explained earlier, the design precipitation has been derived from three different IDF curves (the local IDF, online IDF Tool and Sandsli IDF). The local IDF and online IDF Tool are at the same location for the respective catchments. However, the Sandsli IDF has been obtained from Sandsli station in Bergen. Since the design precipitation used by Norconsult was derived from Sandsli IDF, it has been considered so as to make a valid comparison. The Sandsli IDF curve provided the highest design precipitation amount. This is due to the Sandsli IDF curve is from a place with a higher amount of rainfall. The online IDF Tool gave higher design precipitation than the local IDF curve. This could be due to the data of the online IDF Tool was created with spatial interpolation of extreme value statistics of the meteorological station. Thus, estimated flood peak follow trend of design rainfall for the respective catchment time of concentration.

The pre-event catchment conditions have been incorporated in the DDD model. The model has been set for 200-year flood peak computations under dry catchment, wet catchment and during

snowmelt, or in different seasons, for analyzing the effect of the pre-event catchment condition on generating flood peaks.

6.2.1 Flood peak in dry catchment condition and comparisons

For the dry catchment condition, the 1st of August 2015 at 12:00 was selected for the event to take place, for all catchments under study. Before this event took place the catchment moisture condition was set to be completely dry (i.e., precipitation input set to zero). The 200-year flood peaks simulated using the DDD model for all conditions of design precipitation show that flood peak estimates for dry catchment provided the lowest flood peak (Figure 5.7 to Figure 5.13). The lowest flood peaks during dry catchment were especially pronounced in the two smaller catchments and the three tiny catchments (Figure 5.9 to Figure 5.13).

In comparison to the design flood peaks computed by Norconsult, flood peak estimates using the DDD model for design precipitation derived from all IDF curves combined with dry catchment condition provided lower results. For example, for P5-3360 catchment, the 200-year flood peak discharge calculated by the Norconsult applying the NIFS formula, regional analysis and rational method were 7.44 m^3/s, 9.08 m^3/s and 9.53 m^3/s respectively. The DDD model estimated 200-year flood peaks of 0.6 m^3/s, 1.1 m^3/s and 3.58 m^3/s for the design precipitation derived from local IDF, online IDF Tool and Sandsli IDF respectively. This shows the DDD flood estimates for dry catchment condition are much lower than the Norconsult design flood results. For all study catchments, the relative difference in comparison to the Norconsult results are presented in Table 5.1. For example, the two bigger catchments show 52 – 94% lower estimate, the two smaller catchments show 63 – 98% lower estimate and the three tiny catchments show 92 – 98% lower estimate, in comparison to the Norconsult design flood results (see Table 5.1). Particularly in the three tiny catchments (P7-640, P4-4970 and P4-2680), the flood peak estimates using the DDD model for design precipitation derived from all IDF curves combined with dry antecedent catchment condition, the differences become much larger (Figure 5.9, Figure 5.11, Figure 5.12, Figure 5.13). This clearly indicates underestimation of floods.

6.2.2 Flood peak in wet catchment condition and comparisons

For the wet catchment condition, the time at which high soil moisture condition attained over the seven years simulation period was selected for the event to take place, under the assumption flood peak occurs at the maximum subsurface storage. Unlike the dry catchment condition, the selected

event date for flood peak estimates for wet catchment condition was different for the respective catchments under investigation (see in (Figure 5.7 to Figure 5.13)). The wet catchment conditions are preceded by small amount rainfall periods. Furthermore, the selected season for wet catchment condition was the period with no snowmelt effect or zero snow storage ensured. The 200-year flood peak estimate using DDD model for design precipitation derived from all IDF curves show that flood peak estimates for wet catchment yielded better than the dry catchment condition in most catchments and lower than the flood peak estimate during the snowmelt condition (Figure 5.7 to Figure 5.11). Nevertheless, the two tiny catchments provided almost similar flood peak results to the dry catchment conditions (Figure 5.12, Figure 5.13). This highlights the underestimation of the model for the tiny catchments.

In comparison with the design flood peaks computed by Norconsult, flood peak estimates of three catchments using the DDD model for design precipitation derived from all IDF curves combined with wet catchment condition provided lower estimates than NIFS formula, regional analysis and rational method (Figure 5.7 to 5.13). The relative difference in comparison to the Norconsult results are presented in Table 5.2. For example, the two bigger catchments show 22 – 78% lower estimate, the two smaller catchments and one tiny catchment show 42 – 93% lower estimate and the rest two tiny catchments show 75 – 97% lower estimate, in comparison to the Norconsult design flood results (see Table 5.2). The DDD flood peak estimate results show closer relative difference especially for the two bigger catchments. But large differences have been more pronounced in the two tiny catchments (Figure 5.12, Figure 5.13).

6.2.3 Flood peak during snowmelt condition and comparisons

For flood peak estimates during snowmelt, the period in which high snow storage condition over the seven years simulation time was selected for the event to took place, under the assumption flood peak occurs upon the melt of high snow storage, and particularly the warmest closest time to the high snow storage that leads to potential melt was selected. As the catchments under study are located near to each other, the high snow storage period is similar for all catchments, which is in March 2011 (Figure 6.1). The selected time for flood peak estimates during snowmelt condition was in April 2011 with different day and hour for the respective catchments under study (see in (Figure 5.7 to Figure 5.13)). The 200-year flood peak estimate using the DDD model for design precipitation derived from all IDF curves show that flood peak estimates during snowmelt condition yielded the highest peak results for all catchments (Figure 5.7 to Figure 5.13). This

considerably indicates that the flood peak events of the catchments are caused by high precipitation combined with the snowmelt event. This agrees with Stenius et. al. (2015), who stated that flood peaks usually occur when rainfall is combined with other adverse conditions, such as snowmelt and saturated soil due to past rainfall. In different hydrology litrature many authors agreed that high precipitation episodes does not always lead to peak floods. However, floods associated with high rainfall and snowmelt lead to large floods.

In comparison to the design flood peaks computed by Norconsult, the DDD model results have found inconsistent. Flood peak estimates of three catchments (P5-3360, P5-4980 and P6-740) using the DDD model for design precipitation derived from Sandsli IDF curve combined with snowmelt condition yielded higher estimates than NIFS formula, regional analysis and rational method; however, the design precipitation derived from the local IDF curve combined with snowmelt condition provided lower estimates (Figure 5.7, Figure 5.8, Figure 5.10). In contrast, flood peak estimates of the rest four catchments (P5-6090, P7-640, P4-2680 and P4-4970) using DDD model for design precipitation derived from all IDF curves combined with snowmelt condition gave lower estimates than the NIFS formula, regional analysis and rational method (Figure 5.9, Figure 5.11, Figure 5.12, Figure 5.13). The relative difference in comparison to the Norconsult results are presented in Table 5.3. For example, for the design precipitation derived from Sandsli IDF, the two bigger catchments P5-3360 and P5-4980, show 85 and 88% higher estimate respectively, in comparison to the NIFS formula, 51 and 75% higher estimate respectively, in comparison to the regional analysis and 44 and 52% higher estimate respectively, in comparison to the rational method (see Table 5.3). In contrast, for example, the two tiny catchments (P4-2680 and P4-4970) show 37 – 91% lower estimate in comparison to the Norconsult design flood results (Table 5.3). The results demonstrate that snowmelt is an important factor, which strongly affects the magnitude of flood peaks for the bigger catchments. On the other hand, the DDD model does not seem promising to estimate potential flood peaks even during snowmelt explicitly for the three tiny catchments and design precipitation derived from the local IDF and online IDF Tool (see Figure 5.11, Figure 5.12, Figure 5.7, and Table 5.3).

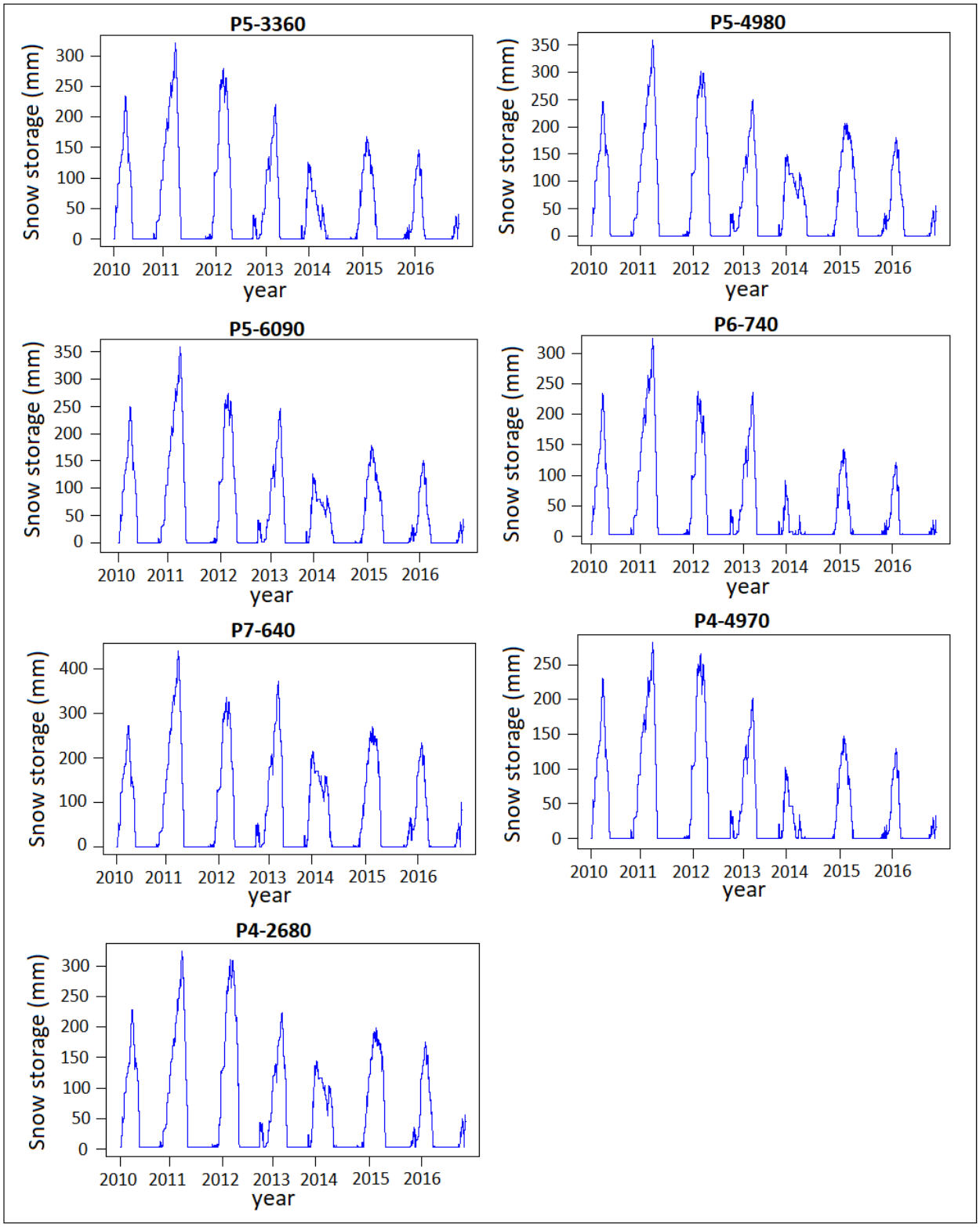

Figure 6.1: The snow storage over the seven years for the seven catchments under study. As per the DDD model snow routine, the highest snow storage is observed in March 2011 for all catchments.

6.3 Model performance in flood peak estimation

The DDD flood peak estimates appeared in a large variability. This variability resulted from different IDF curves and different catchment conditions considered in the modelling. The antecedent moisture conditions and the condition of snowmelt govern the processes by which a catchment responds to rainfall and impact on the flood peak. For the dry catchment condition, the influence of the design precipitation input on flood peak was marginal. The wet moisture condition performed better flood peak responses, as a higher level of subsurface storage is associated with a higher effect on flood peak. The DDD model best possible flood peak estimation was due to the combination of rainfall and snowmelt which contribute to the highest flood peak. As for projects only flood peak is of interest, the flood peak estimate generated from the combination of high precipitation and snowmelt is an important outcome, in a worst case scenario. For example, the capacity of a culvert is fixed based on the best possible estimated flood peak discharge.

Compared to the Norconsult design flood results, most DDD flood peak estimates have provided lower results. Particularly, the DDD model on hourly time resolution seems to be unsuitable for the tiny catchments. The reason could be the current DDD temporal resolution. The DDD model in sub-hourly time step could give better performance, because the concentration time in which the flood peak occurs is less than one hour for the three tiny catchments, i.e., P7-640, P4-2680 and P4-4970 catchments have concentration time of 38 minutes, 31 minutes and 27 minutes respectively (see Table 4.13). So the increased temporal resolution (sub-hourly) could capture the dynamics of the catchment responses, for which the current DDD model hourly resolution is unable to capture.

6.3.1 Evaluation of DDD model against the rational method

To make an absolute comparison and evaluation, the same predictor characteristics and input data must be used. However, the flood peak estimation using the NIFS formula, regional analysis and rational method was not part of the work. The second objective of this study was to compare and evaluate the DDD flood peak estimates with the existing design flood discharges calculated by Norconsult using the three methods. The DDD model flood estimate was compared straightforward with the design flood estimates computed using the three methods applied by Norconsult.

The selection of method has a significant impact on the flood peak values. The Norconsult design

flood results show different flood peak estimates for different methods. As per the Norconsult design flood results, the rational method has provided the highest flood peaks for all the catchments when compared to NIFS formula and regional analysis (Figure 5.7 to Figure 5.13). In comparison with the DDD model, the flood peak estimates using the rational method are higher in most of the catchments, except the flood peak estimate for precipitation derived from Sandsli IDF combined with snowmelt condition for the two bigger catchments (P5-3360 and P5-4980) and one smaller catchment (P6-740).

The morphological and hydrological elements that govern the peak discharge estimation in the rational method are constrained in a few components, which are the catchment area, rainfall intensity and runoff coefficient. In rational method, the antecedent condition of the catchment might not exactly be represented in the runoff coefficient (C) value which leads to the flood peak discharges, even though the runoff coefficient (C) relies on surface imperviousness, slope, antecedent condition and return period. Chow et al. (1988) stated that the runoff coefficient (C) is a highly uncertain variable in the rational method. Furthermore, there is a large degree of subjectivity in selecting C values in an individual flood peak computation. From the comparison perspective with the rational method, the DDD model presents in a more realistic representation of the overall hydrological behavior and more robust flood peak estimations have been achieved during snowmelt conditions for the bigger catchments. Nevertheless, the snowmelt condition can not be incorporated in the rational method. In the DDD model it is highly likely that different flood peak estimates can be obtained for different catchment conditions, while using the rational method only a single flood peak estimate is produced. For countries like Norway where snowmelt has major importance, the DDD model can be valid to estimate the flood peak discharges.

As explained in the literature review part in Section 2.1.1, the runoff coefficient (C) can be determined as the ratio of runoff depth to precipitation depth. This could be a possible technique to compare the C value with the Norconsult have used to calculate the flood peak using the rational method. From Norconsult (2018) report, the C value was used as 0.52 for all catchments and Sandsli IDF was used to obtain the design precipitation for all the catchments under study. In this work, C value was back calculated in order to get a better comparable picture between the DDD model and the rational method. The estimated peak runoff depth using DDD for precipitation derived from the Sandsli IDF curve combined with the wet catchment condition was considered to back calculate the C value. The calculated C (ratio of peak runoff depth to input precipitation

depth) values for P5-3360, P5-4980, P5-6090, P6-740, P7-640, P4-4970 and P4-2680 was determined as 0.18, 0.22, 0.14, 0.26, 0.20, 0.11, and 0.20 respectively. This shows the C value back calculated from the DDD model flood peak estimate is much lower than the C value Norconsult have used to determine flood peak using rational method. This could be the possible reason for larger flood peak estimates using the rational method. The performance of the rational method is highly sensitive to the C value. Furthermore, there could be an overestimation in the design floods calculated using the rational method due to the higher C value used by Norconsult.

The C value back calculated from the DDD flood peak estimate is reasonable, since the land use of the study catchments is dominated by forest cover, in the range of 76 – 100% (see Table 4.5). The runoff coefficient (C) for forest land use is between 0.05 – 0.25 (Pilgrim and Cordery, 1993). It can be noticed that the DDD model results can be considered as more realistic due to the hydrologic responses represented very well, i.e., the interaction between the precipitation and the catchment characteristics is well modelled in DDD model than in rational method.

6.3.2 Evaluation of DDD model against the NIFS formula and regional analysis

The DDD model performed higher flood peak estimates than the NIFS formula for precipitation derived from online IDF Tool and Sandsli IDF combined with snowmelt condition only, for the two bigger catchments (P5-3360 and P5-4980) and one smaller catchment (P6-740). For the rest, one smaller and three tiny catchments design flood peak by NIFS formula was higher than the flood peak produced by the DDD model. This could be due to the higher estimation of the mean annual flood (Q_m) variable in the NIFS formula. According to Glad et al. (2015), the mean annual flood component has been created by fitting a regression analysis on results provided from regional flood frequency analysis on annual maximum discharges for many small catchments in Norway. The long time series annual maximum discharges might have created higher regression linkage with Q_m. The NIFS formula contains a growth curve which relates the flood of a given return period and the mean annual flood. The NIFS formula constituents are limited into three components: catchment area, specific runoff and effective lake percentage. The DDD model can better constitute and produce more realistic flood peak discharges, as the NIFS formula lacks some morphological components, antecedent soil moistures and snowmelt conditions.

As per to the Norconsult (2018) document, the regional analysis showed higher flood peak estimates than the NIFS formula for the bigger catchments (P5-3360 and P5-4980) and with the

majority of the catchments slightly lower than the NIFS formula (Figure 5.7 to Figure 5.13). For E6 Helgeland Sør project, the regional analysis has been carried out from neighboring gauged stations (Norconsult, 2018). The regional analysis is performed based on recorded discharges and requires more data. The most important points that need to address are region selection and the method that controls for pooling the required data. The selected regions may not have the required utmost flood characteristics similarity, especially for the small catchments. However, if local rainfall stations or gridded precipitation data is available, the rainfall characteristics of the desired catchment could have stronger reliability to transform it into a runoff by using a hydrological model. Since runoff is affected by physical characteristics of the catchment including its soils, landform and shape, the merit of DDD model could outweigh regional analysis. In addition, the advantage of the DDD model can produce different flood peak magnitudes of the same design precipitation for various catchment states.

7. CONCLUSIONS

In this work, the DDD model was investigated for estimating the 200-year flood peak discharges in seven small ungauged catchments. The DDD model performance in regionalization was tested for another couple of gauged catchments and yielded satisfactory performance in terms of KGE and BIAS. The results of the test catchments in regionalization methods showed that the DDD model with precipitation correction and without dynamic river network gave an improved KGE and BIAS and better goodness of fit between the observed and simulated discharges. Nevertheless, many flood peaks have been underestimated. The model with both precipitation correction and dynamic river network yielded the same KGE and BIAS, but some of the flood peaks have been improved significantly. Accordingly, the precipitation correction factor and the dynamic river network have been considered in the DDD model to estimate the 200-year flood peak discharges for the seven study catchments.

The DDD model flood estimate results demonstrated that the choice of the IDF curve and catchment condition alters the flood peak estimate significantly. Based on the overall flood peak estimation, the combination of design precipitation derived from the Sandsli IDF curve combined with snowmelt condition yielded the highest flood magnitudes, while the combination of design precipitation derived from the local IDF with dry antecedent condition gave the lowest flood peak results.

Besides, the DDD flood estimates have been compared to the design flood results computed by Norconsult using NIFS formula, regional analysis and rational method. For most of the catchments, the DDD model provided lower flood estimates than the Norconsult design flood results. Potential flood peak estimates using the model have been produced during the combination of design precipitation and snowmelt condition for the two bigger catchments and one smaller catchment. Whereas, the DDD model demonstrated underestimation of flood peaks for the three tiny catchments. Extremely high differences in comparison to the design floods by Norconsult was seen for the last two tiny catchments.

Flood peak estimation using the DDD model should be further investigated on sub-hourly temporal resolution, and future land use change and climate change shall also be investigated.

REFERENCES

Andersen, J. H., Hjukse, T., Roald, L. & Sælthun, N. R., 1983. Hydrologisk modell for flomber-egninger. Rn-2,(83) Oslo. http://publikasjoner.nve.no/rapport/1983/rapport1983_02.pdf

Anne K. Fleig, Donna Wilson, 2013. NIFS - Flood estimation in small catchments. Rn-60-13 Oslo.

Beven, K.J., 2012. Rainfall-runoff modelling: the primer, 2nd ed. ed. Hoboken, NJ.

Beven, K.; Lamb, R.; Quinn, P.R.; and Freer, J. (1995). TOPMODEL. W.R. Publication, 627-688.

Bergstrom, S. (1995). The HBV model. Water Resources Publication, 443-476.

Blume, T., Zehe, E., Bronstert, A., 2007. Rainfall—runoff response, event-based runoff coefficients and hydrograph separation. https://doi.org/10.1623/hysj.52.5.843

Blöschl, G., Sivapalan, M., 1995. Scale issues in hydrological modelling: a review. https://doi.org/10.1002/hyp.3360090305

California Culvert Practice, 1955. Department of Public Works, Division of Highways, 2th edition

Chow, V.T., Maidment, D.R., Mays, L.W., 1988. Applied hydrology, McGraw-Hill, New York.

Cisty, M., Vyleta, R., Soldanova, V., 2019. A Comparison of Methods for Calculating Monthly Flows on Small Catchments. https://doi.org/10.1088/1755-1315/362/1/012102

Da Ros, D., Borga, M., 1997. Adaptive Use of a Conceptual Model for Real Time Flood Forecasting. Hydrology Research 28, 169–188. https://doi.org/10.2166/nh.1997.0010

Filipova, V., Lawrence, D., Skaugen, T., 2019. A stochastic event-based approach for flood estimation in catchments with mixed rainfall and snowmelt flood regimes. https://doi.org/10.5194/nhess-19-1-2019

Fleig, A. K. and Wilson, D., 2013. Flood estimation in small catchments: NVE, Oslo.

Garg, V., Nikam, B.R., Thakur, P.K., Aggarwal, S.P., 2013. The effect of slope on runoff potential of a watershed using NRCS-CN. https://doi.org/10.1504/IJHST.2013.057626

Genereux, D.P., 2003. Comparison of methods for estimation of 50-year peak discharge from a small, rural watershed in North Carolina. https://doi.org/10.1007/s00254-002-0734-5

Glad, P. A., Reitan, T. & Stenius, S., 2015. Nasjonalt formelverk for flomberegning i småned-børfelt. Report no. 13-2015). Oslo.

Gupta, H.V., Kling, H., Yilmaz, K.K., Martinez, G.F., 2009. Decomposition of the mean squared error and NSE performance criteria. https://doi.org/10.1016/j.jhydrol.2009.08.003

Hathaway GA.,1945. Design drainage facility. Trans ASCE 110:697–730

Haggard, B.E., Moore, P.A., Delaune, P.B., 2002. 'Effect of slope, grazing and aeration on pasture

hydrology'Congress, Hyatt Regency, Chicago, IL, USA, Paper Number 022156.

He, Y., Bárdossy, A., Zehe, E., 2011. A review of regionalization for continuous streamflow simulation. Hydrol. Earth Syst. Sci. https://doi.org/10.5194/hess-15-3539-2011

Hoesein, A.A., Pilgrim, D.H., Titmarsh, G.W., Cordery, I., 1989. Assessment of the US Conservation Service method for estimating design floods 11.

Huang, M., Gallichand, J., Wang, Z., Goulet, M., 2006. A modification to the Soil Conservation Service curve number method for steep slopes in the Loess Plateau of China. Hydrol. Process. 20, 579–589. https://doi.org/10.1002/hyp.5925

Jainet Pj, J., 2018. Evaluation of the conceptual basis of the rational method. IJH 2. https://doi.org/10.15406/ijh.2018.02.00145

Jery R. Stedinger, Richard M. Vogel, Efi Foufoula-Georgiou, 1993. Frequency Analysis of Extreme Events. McGraw-Hill, Inc., New York, NY, 9.1–9.42.

Kay, A.L., Jones, D.A., Crooks, S.M., Calver, A., Reynard, N.S., 2006. A comparison of three approaches to spatial generalization of rainfall–runoff models. https://doi.org/10.1002/hyp.6550

Kay, A.L., Jones, D.A., Crooks, S.M., Kjeldsen, T.R., Fung, C.F., 2007. An investigation of site-similarity approaches. https://doi.org/10.5194/hess-11-500-2007

Kirpich ZP, 1940. Time of concentration of small agricultural watersheds. J Civ Eng 10(6):362

Lorenz, P. (Ed.), Gattermayr, W., 2011. Leitfaden – Verfahren zur. Abschätzung von Howasserkennwerten. Wasserhaushalt, Wien, Austria.

Loukas, A., Vasiliades, L., 2014. Streamflow simulation methods for ungauged and poorly gauged watersheds. https://doi.org/10.5194/nhess-14-1641-2014

Lussana, C., Ole Einar, T., & Francesco, U., 2016. seNorge v2.0: an observational gridded dataset of tempperature for Norway. METreport, 108.

Marshall, D.C.W., Bayliss, A.C., 1994. Flood estimation for small catchments, Report / Institute of Hydrology. Institute of Hydrology, Wallingford.

Merz, R., Blöschl, G., 2004. Regionalization of catchment model parameters. J. Hydrol. 287, 95–123. https://doi.org/10.1016/j.jhydrol. 2003.09.028

Midttømme, G., Pettersson, L.E., Holmqvist, E., Nøtsund, Ø., Hisdal, H. & Sivertsgård, R., 2011. Retningslinjer for flomberegninger Report no. 4-2011.

Mishra S.K., Singh V.P., 2003. SCS-CN Method. In: Soil Conservation Service Curve Number

(SCS-CN) Methodology. https://doi.org/10.1007/978-94-017-0147-1_2

Mulvany, T. J. (1850). ‘‘On the use of self-registering rain and flood gauges.’’

Norconsult, 2018. Dimensjonering av stikkrenner. NO-RIVA-901 v. J01. Utgitt 13.04.2018

Nirajan Dhakal, Xing Fang, Theodore G. Cleveland, and Luke J. Marzen., 2012. Estimation of V-olumetric Runoff Coefficients for Texas Watersheds Using Land-Use and Rainfall-Runoff Data. https://doi.org/10.1061/(ASCE)IR.1943-4774.0000368.

N. Vivekanandan, 2016. Statistical analysis of rainfall data and estimation of peak flood discharge for ungauged catchments. ijret 05, 27–31. https://doi.org/10.15623/ijret.2016.0514006

O’Loughlin, G., Huber, W., Chocat, B., 1996. Rainfall-runoff processes and modelling. Journal of Hydraulic Research 34, 733–751. https://doi.org/10.1080/00221689609498447

Oudin, L., Andréassian, V., Perrin, C., Michel, C., Le Moine, N., 2008. Spatial proximity, physical similarity, regression and ungaged catchments: A comparison of regionalization approaches based on 913 French catchments: https://doi.org/10.1029/2007WR006240

Parajka, J., Viglione, A., Rogger, M., Salinas, J.L., Sivapalan, M., Blöschl, G., 2013. Comparative assessment of predictions in ungauged basins – Part 1: Runoff hydrograph studies. Hydrol. Earth Syst. Sci. Discuss. 10, 375–409. https://doi.org/10.5194/hessd-10-375-2013

Pilgrim, D.H. & Cordery, I., 1993. Flood Runoff. In: *Handbook of Hydrology*. (Ed.: Maidment, D.R.). McGraw-Hill, Inc., New York, NY, 9.1–9.42.

Ponce, V.M., Hawkins, R.H., 1996. Runoff Curve Number: Has It Reached Maturity? https://doi.org/10.1061/(ASCE)1084-0699(1996)1:1(11)

Rahman, A., Haddad, K., Zaman, M., Kuczera, G., Weinmann, P.E., 2011. Design Flood Estimation in Ungauged Catchments. https://doi.org/10.1080/13241583.2011.11465381

Refsgaard, J.C., Knudsen, J., 1996. Operational Validation and Intercomparing of Different Types of Hydrological Models. Water Res. 32, 2189–2202. https://doi.org/10.1029/96WR00896

Rientjes, T.H.M. (2004). Inverse modelling of rainfall-runoff relation. Delft University.

SCS., 1972. SCS National Engineering Handbook,Washington, DC.

SCS, 1975. Urban hydrology for small watersheds. Technical Release TR55, Washington, DC

Seija Stenius, P. A. Glad, T. K. Wang, T. Væringstad., 2015. Veileder for flomberegninger i små uregulerte felt. (NVE). Report no. 7-2015). Oslo.

Singh, V.P. (1992). Elementary Hydrology, Prentice-Hall, Inv., New Jersey. U.S.A.

Singh, V.P. (1988). Hydrologic systems. Vol.1. Rainfall-runoff modelling. New Jersey.

Singh, V.P., Woolhiser, D.A., 2002. Mathematical Modeling of Watershed Hydrology. J. Hydrol. Eng. 7, 270–292. https://doi.org/10.1061/(ASCE)1084-0699(2002)7:4(270)

Skaugen, T., Mengistu, Z., 2016. Estimating catchment-scale groundwater dynamics from recession analysis. https://doi.org/10.5194/hess-20-4963-2016

Skaugen, T., Onof, C., 2014. A rainfall-runoff model parameterized from GIS and runoff data: model parameterized from GIS and runoff data. https://doi.org/10.1002/hyp.9968

Skaugen, T., Peerebom, I.O., Nilsson, A., 2015. Use of a parsimonious rainfall-run-off model for predicting hydrological response in ungauged basins. https://doi.org/10.1002/hyp.10315

Skaugen, T., Weltzien, I.H., 2016. A model for the spatial distribution of snow water equivalent parameterizedfrom the spatial variability of precipitation. https://doi.org/10.5194/tc-10-1947-2016

SVV, 2014. Statens vegvesen (SVV): Håndbok N200 Vegbygging.

Technical Report, 1986. Urban hydrology for small watersheds, United States. Second edition.

Thiemig, V., Rojas, R., Zambrano-Bigiarini, M., De Roo, A., 2013. Hydrological evaluation of satellite-based rainfall estimates.. https://doi.org/10.1016/j.jhydrol.2013.07.012

Tsegaw, Alfredsen, K., Skaugen, T., Muthanna, T.M., 2019a. Predicting hourly flows at ungauged small rural catchments using a parsimonious hydrological model. Journal of Hydrology 573, 855–871. https://doi.org/10.1016/j.jhydrol.2019.03.090

Tsegaw, A.T., Skaugen, T., Alfredsen, K., Muthanna, T.M., 2019b. A dynamic river network method for the prediction of floods using a parsimonious rainfall-runoff model. Hydrology Research nh2019003. https://doi.org/10.2166/nh.2019.003

Wilson, D., Fleig, A.K., Lawrence, D., Hisdal, H., Petersson L.E. & Holmqvist, E., 2011. A review of NVE's flood frequency estimation procedures. NVE Report 2011-9.

Wood, E.W.; and O'connel, P.E., 1985. Real-time forecasting. Ed. John Wiley and Sons, 505-558.

Yang, X., Magnusson, J., Huang, S., Beldring, S., Xu, C.-Y., 2020. Dependence of regionalization methods on the complexity of hydrological models in multiple climatic regions. Journal of Hydrology 582, 124357. https://doi.org/10.1016/j.jhydrol.2019.124357

Young, A.R., 2006. Stream flow simulation within UK ungauged catchments using a daily rainfall-runoff model. J. Hydrol. 320, 155–172. https://doi.org/10.1016/j.jhydrol.2005.07.017

Young, C.B., McEnroe, B.M., Rome, A.C., 2009. Empirical Determination of Rational Method Runoff Coefficients. https://doi.org/10.1061/(ASCE)HE.1943-5584.0000114

APPENDIX (A): Calibrated values of shape parameter (a0) and the decorrelation length (d), for 84 catchments in Norway (Skaugen and Weltzien, 2016).

Station ID	a0	d	Station ID	a0	d	Station ID	a0	d
2.11	22.941	240.9	27.24	40.86	559.1	123.31	34.81	258.19
2.145	10.642	128.9	28.7	41.96	629.13	124.2	45.63	645.57
2.265	20.604	224.4	41.1	35.64	485.96	127.11	40.01	449.14
2.268	17.734	373.5	48.1	28.17	458.38	127.13	41.24	529.85
2.279	51.783	429.9	50.1	19.48	349.22	133.7	32.27	489.87
2.291	16.067	569.1	50.13	15.53	399.6	138.1	27.69	547.08
2.32	15.574	145.27	55.4	38.33	505.71	139.15	30.74	587.41
2.323	31.92	384.1	62.5	32.72	485.64	139.35	27.1	422.7
2.604	17.07	215.16	62.10	27.583	497.6	148.2	28.13	580.6
2.614	16.77	140.2	62.18	46.42	639.16	151.15	34.23	670.6
2.634	26.92	340	72.5	24.682	450.4	152.4	41.56	571.8
3.22	45.27	380.5	73.27	28.254	204.7	156.10	0.742	0.95
6.10	42.366	413	77.3	30.35	364.74	157.3	21.22	484.8
8.2	44.28	546.6	79.3	34.69	509.09	162.3	11.71	323.22
8.6	59.978	643.4	82.4	46.775	647.4	165.6	19.015	328.8
12.171	33.47	478	83.2	57.66	607.28	168.2	26.36	456.25
12.178	28.624	367.6	84.11	35.776	530.1	173.8	22.963	344.4
12.192	32.05	294.7	88.4	38.55	436.66	174.3	32.44	330.36
12.193	35.788	425.5	97.1	27.24	481.7	191.2	19.655	229.02
15.53	20.669	262.7	98.4	23.86	379.76	196.35	24.09	544.6
16.66	28.754	237.1	103.1	27.689	441.1	200.4	29.68	458.65
16.132	54.534	596.7	104.23	22.74	299.74	203.2	18.711	393.6
18.10	40.65	546.4	105.1	20.733	296.2	212.10	12.47	147.9
19.107	48.251	711	109.9	12.56	186.89	223.2	8.017	109.4
21.47	23.952	221.2	109.42	17.45	300.89	230.1	12.566	147
22.22	47.16	660.1	112.8	19.96	416.44	234.13	12.84	123.9
25.24	29.21	359.69	122.9	22.75	250.01	247.3	15.41	190.7
26.26	31.155	402.5	122.11	15.94	174.55	311.460	40.766	1133.9

APPENDIX (B): Calibrated values of Pro, Cx, CFR, Cea and rv, for 41 catchments in Norway (Tsegaw et al., 2019a).

S. N	Station	Id	Pro	Cx	CFR	Cea	rv
1	Fura	2.323	0.100	0.052	0.006	0.010	1.221
2	Gryta	6.1	0.030	0.051	0.010	0.017	0.707
3	sæternbekken	8.6	0.030	0.054	0.010	0.020	0.588
4	Rynsa	12.13	0.030	0.071	0.010	0.020	0.504
5	Fiskum	12.193	0.100	0.058	0.001	0.020	0.766
6	Hangtjern	12.212	0.100	0.050	0.010	0.011	0.698
7	Grosettjern	16.66	0.030	0.072	0.010	0.019	0.992
8	Viertjern	16.127	0.099	0.071	0.010	0.015	0.501
9	Lilleelv	19.107	0.100	0.052	0.001	0.010	1.242
10	Jogla	26.26	0.100	0.183	0.010	0.030	1.013
11	Rekedalselv	26.64	0.100	0.062	0.010	0.010	0.769
12	Gramstaddalen	29.7	0.044	0.050	0.010	0.010	1.443
13	Grimsvatn	36.13	0.100	0.112	0.001	0.020	1.464
14	Lauvastøl	36.32	0.100	0.148	0.001	0.025	1.160
15	Kallandsvatnet	39.2	0.099	0.052	0.010	0.010	0.736
16	Hellaugvatn	41.8	0.100	0.071	0.010	0.030	1.467
17	Djupevad	42.2	0.100	0.246	0.001	0.025	1.497
18	Baklihøl	42.6	0.100	0.241	0.001	0.040	1.242
19	Røykenes	55.4	0.100	0.074	0.010	0.020	0.686
20	Kaldåen	61.8	0.100	0.106	0.010	0.040	1.223
21	Fjellanger	63.12	0.100	0.093	0.001	0.030	0.843
22	Havelandself	68.2	0.100	0.103	0.005	0.020	1.036
23	Frostdalen	73.21	0.081	0.073	0.010	0.010	1.499
24	Sula	73.27	0.100	0.072	0.010	0.010	1.347
25	Nysetvatn	74.24	0.030	0.051	0.010	0.020	1.384
26	Krokenelv	75.23	0.100	0.076	0.010	0.020	1.441
27	Feigumfoss	75.28	0.045	0.054	0.010	0.021	1.231
28	Nessedalselv	79.3	0.085	0.089	0.010	0.020	1.036
29	Grasdøla	88.15	0.030	0.066	0.010	0.040	0.852

30	Dalsbøvatn	91.2	0.100	0.069	0.010	0.020	1.497
31	Hareidselv	96.3	0.030	0.057	0.010	0.020	0.503
32	Engsetvatn	101.1	0.030	0.060	0.008	0.020	0.680
33	Morstølbru	103.2	0.100	0.052	0.010	0.020	1.200
34	Valen	117.4	0.099	0.053	0.010	0.020	1.414
35	Svarttjørnbekken	123.29	0.100	0.192	0.001	0.020	1.080
36	Sørra	150.1	0.030	0.076	0.010	0.020	0.888
37	Storvatn	153.1	0.100	0.051	0.001	0.020	1.156
38	Lakså bru	168.3	0.100	0.051	0.003	0.020	1.241
39	Rauvatn	172.8	0.100	0.081	0.010	0.020	1.111
40	Øvstevatn	174.3	0.096	0.060	0.001	0.020	1.146
41	Ånesvatn	186.2	0.031	0.050	0.010	0.020	0.503

APPENDIX (C): Curves fitted to the relation between mean distance distribution of hillslope (D_m) and critical support area (A_c), for the relation $D_m = aA_c^b$, for the study catchments.

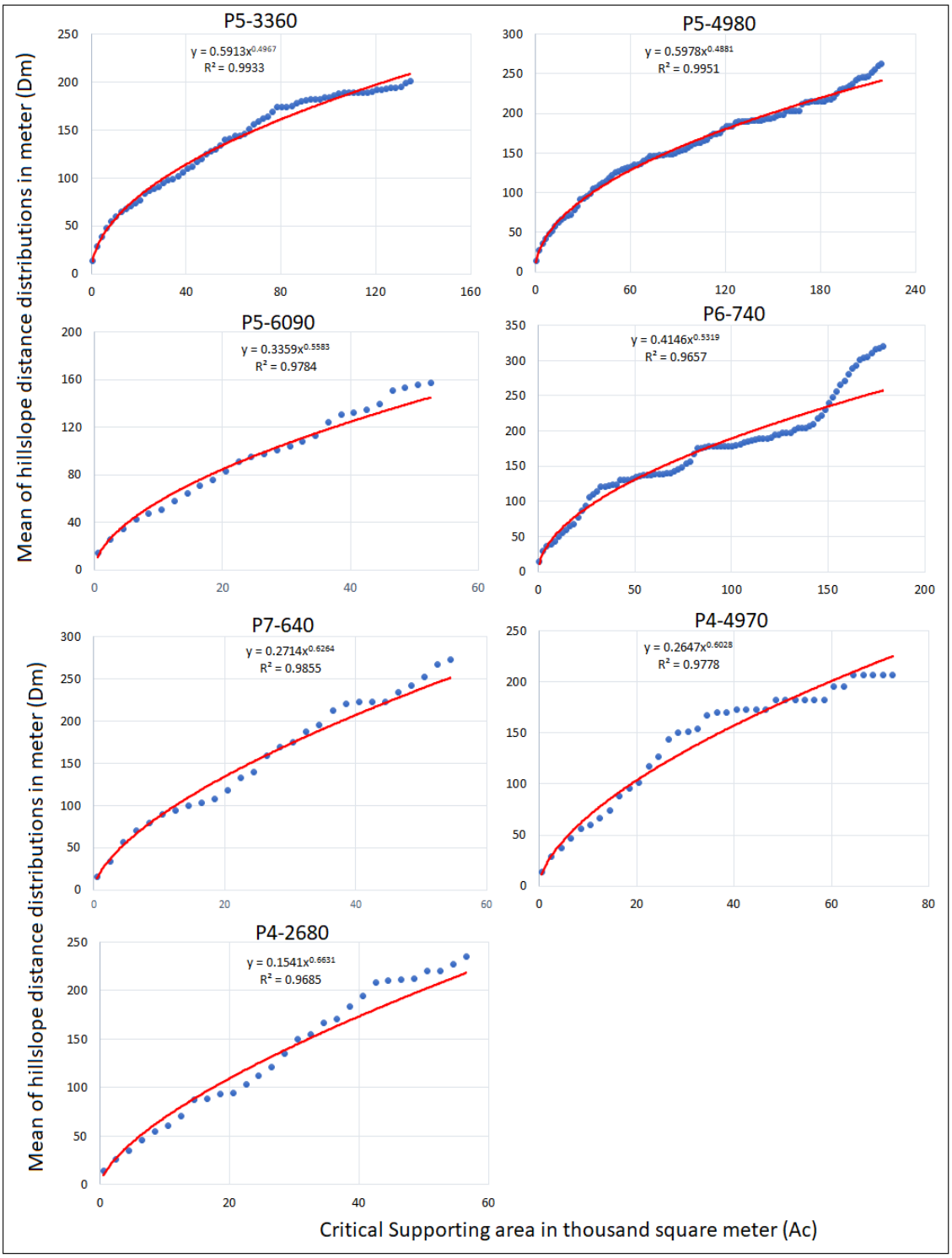

APPENDIX (D): Selected pooling group members and their similarity distances, for the study catchments.

P5-3360		
Station name	Station Id	$dist_{a,b}$
Gramstaddalen	29.7	1.67
Svarttjørnbekken	123.29	1.91
Gryta	6.1	2.25
Hangtjern	12.212	2.65
Rekedalselv	26.64	3.31
sæternbekken	8.6	3.34
Grosettjern	16.66	3.40

P5-4980		
Station name	Station Id	$dist_{a,b}$
Gramstaddalen	29.7	1.30
Svarttjørnbekken	123.29	2.11
Gryta	6.1	2.56
Hangtjern	12.212	2.58
Rekedalselv	26.64	3.51
Grosettjern	16.66	3.60
sæternbekken	8.6	3.64

P5-6090		
Station name	Station Id	$dist_{a,b}$
Gryta	6.1	2.254
Svarttjørnbekken	123.29	2.285
Gramstaddalen	29.7	2.333
sæternbekken	8.6	3.268
Hangtjern	12.212	3.430
Grosettjern	16.66	3.490
Rekedalselv	26.64	3.559

P6-740		
Station name	Station Id	$dist_{a,b}$
Svarttjørnbekken	123.29	2.368
Gryta	6.1	2.695
Gramstaddalen	29.7	2.781
Rekedalselv	26.64	3.103
Hangtjern	12.212	3.243
Grosettjern	16.66	3.617
Lakså bru	168.3	4.003

P7-640		
Station name	Station Id	$dist_{a,b}$
Gramstaddalen	29.7	4.394
Baklihøl	42.6	5.327
Nessedalselv	79.3	5.893
Lauvastøl	36.32	6.030
Morstølbru	103.2	6.170
Svarttjørnbekken	123.29	6.304
Øvstevatn	174.3	6.334

P4-4970		
Station name	Station Id	$dist_{a,b}$
Gramstaddalen	29.7	2.193
Svarttjørnbekken	123.29	2.987
Hangtjern	12.212	3.170
Gryta	6.1	3.496
Rekedalselv	26.64	4.243
sæternbekken	8.6	4.307
Grosettjern	16.66	4.371

P4-2680		
Station name	Station Id	$dist_{a,b}$
Gryta	6.1	2.524
Svarttjørnbekken	123.29	2.629
Gramstaddalen	29.7	2.651
sæternbekken	8.6	3.576
Hangtjern	12.212	3.698
Grosettjern	16.66	3.720
Rekedalselv	26.64	3.859

APPENDIX (E): The local IDF and online IDF Tool curves, for P5-4980, P5-6090, P6-740, P7-640, P4-4970 and P4-2680 study catchments.

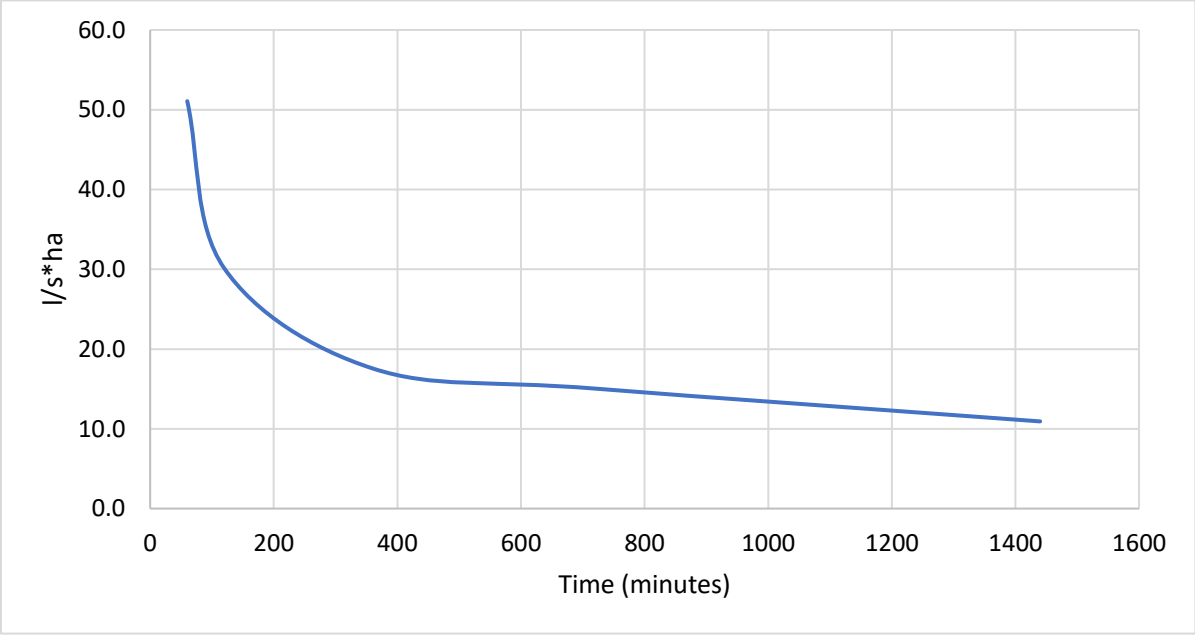

Figure E-1: The local IDF curve for 200-year return period, for P5-4980 catchment.

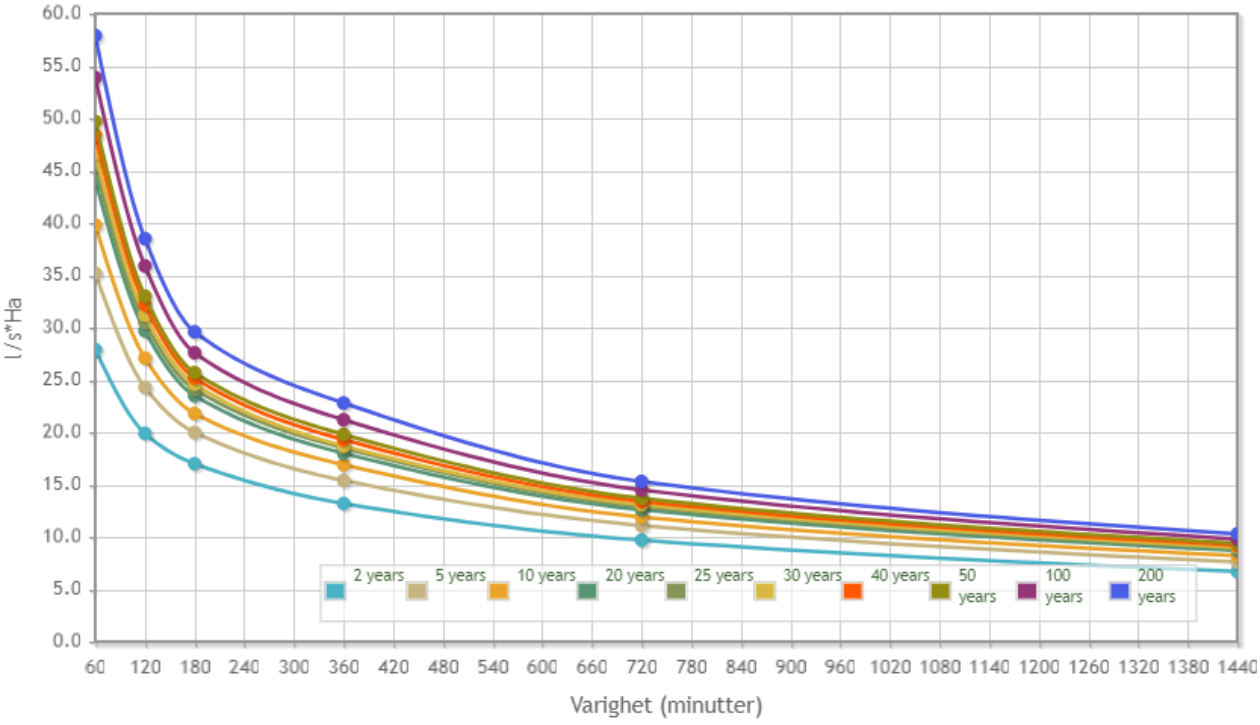

Figure E-2: The online IDF curve, for 200-year return period in blue, for P5-4980 catchment.

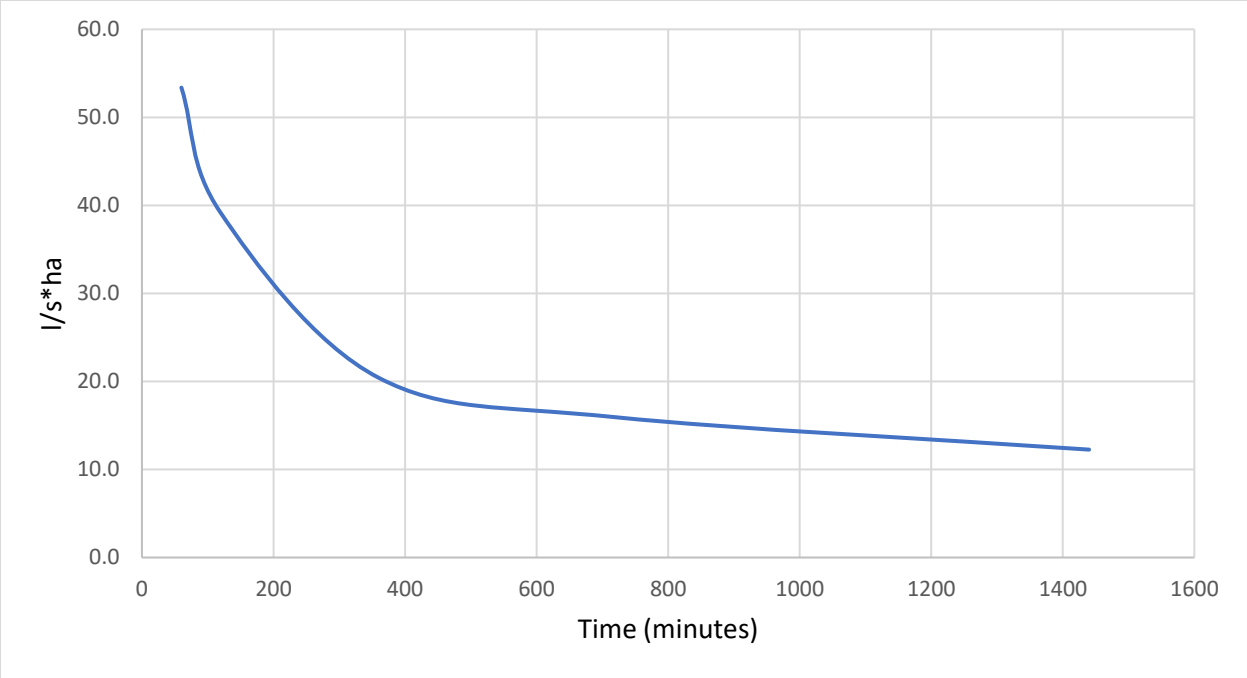

Figure E-3: The local IDF curve for 200-year return period, for P5-6090 catchment.

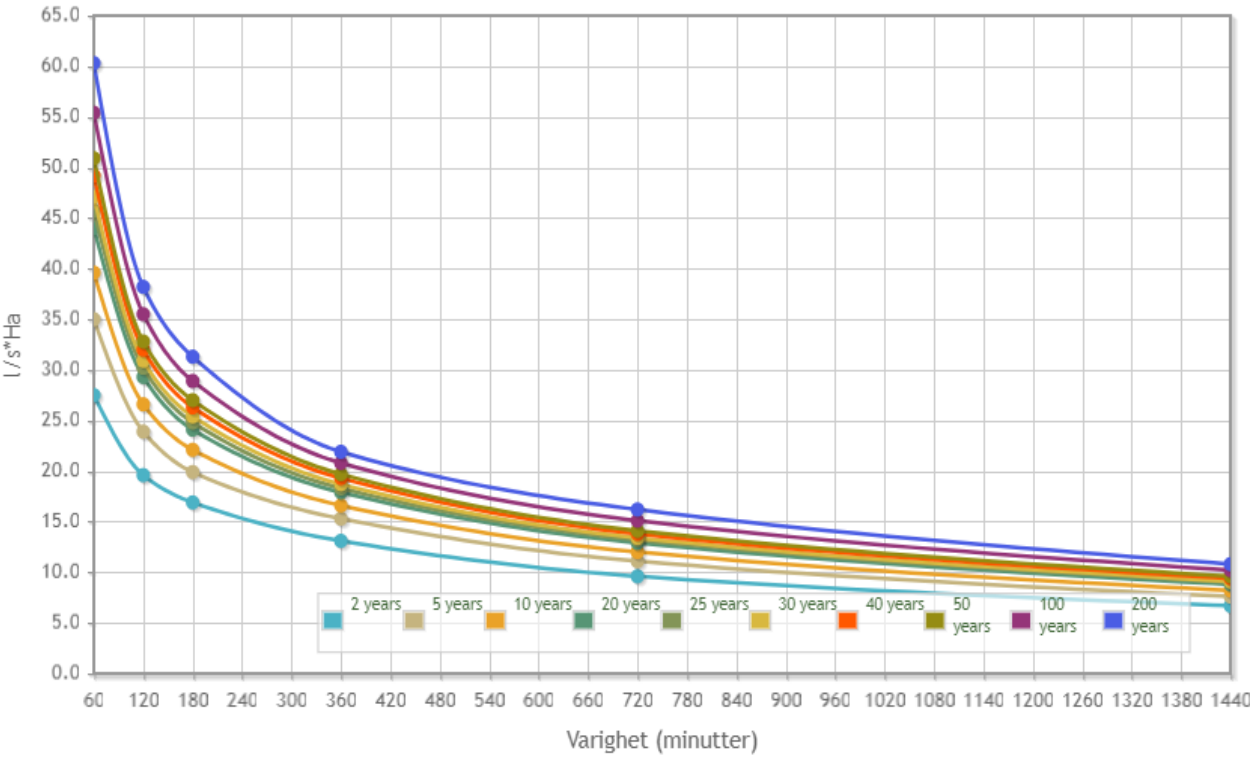

Figure E-4: The online IDF curve, for 200-year return period in blue, for P5-6090 catchment.

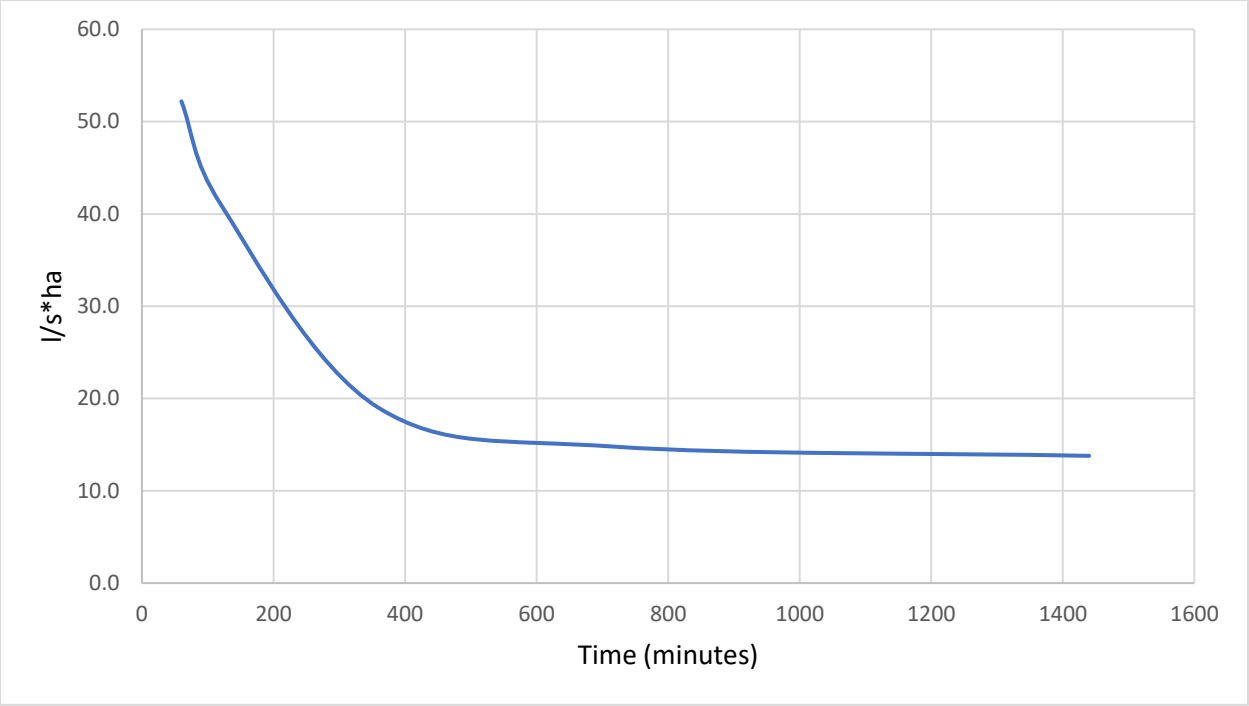

Figure E-5: The local IDF curve for 200-year return period, for P6-740 catchment.

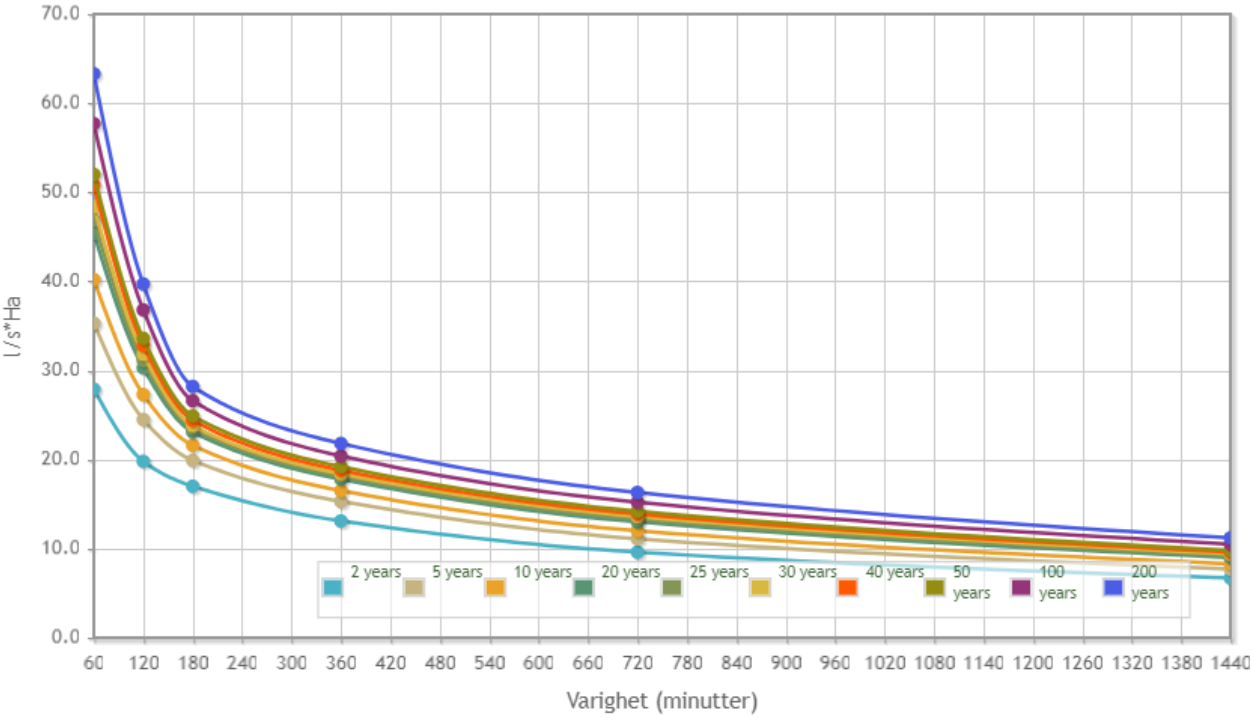

Figure E-6: The online IDF curve, for 200-year return period in blue, for P6-740 catchment.

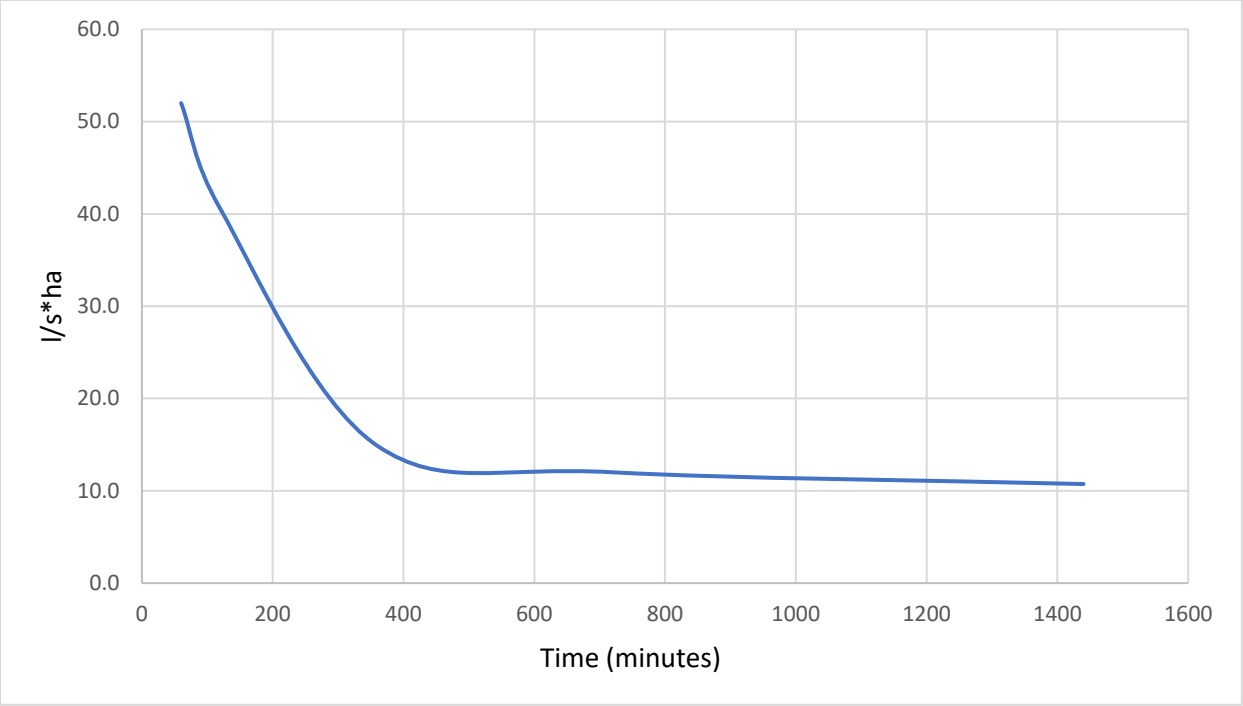

Figure E-7: The local IDF curve for 200-year return period, for P7-640 catchment.

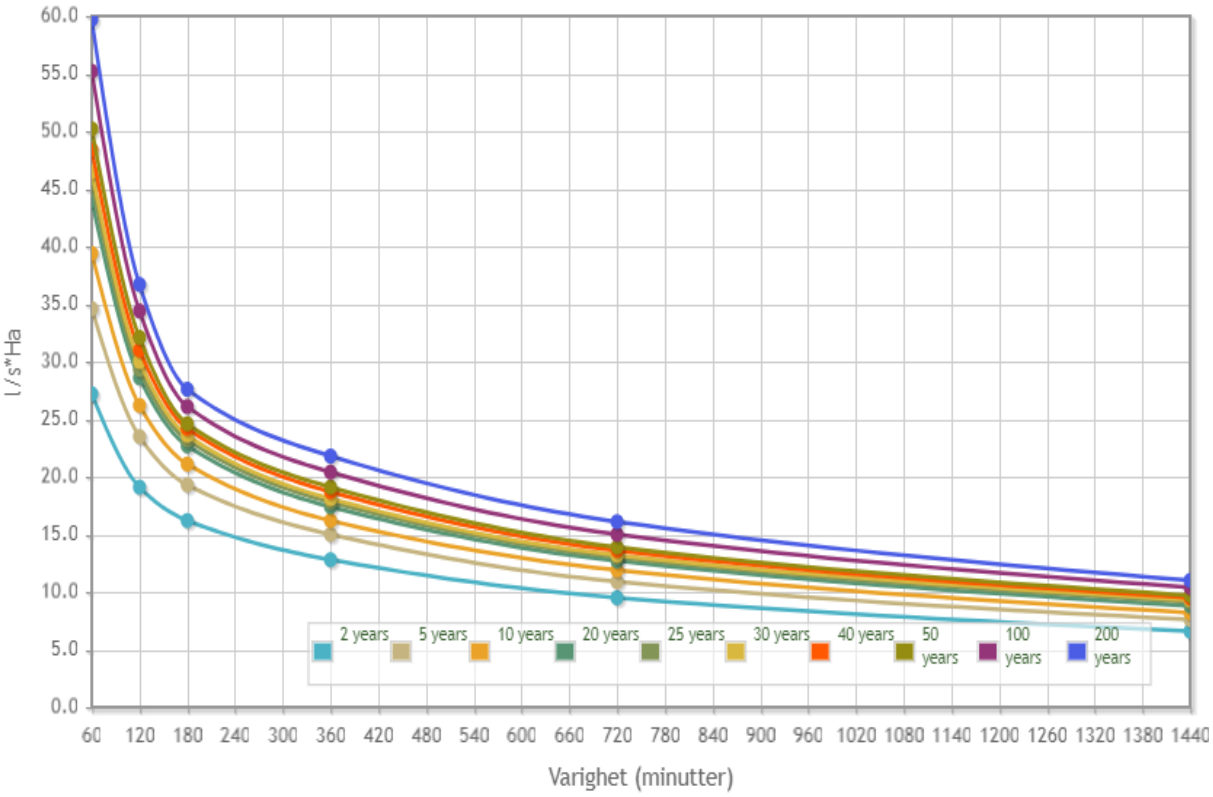

Figure E-8: The online IDF curve, for 200-year return period in blue, for P7-640 catchment.

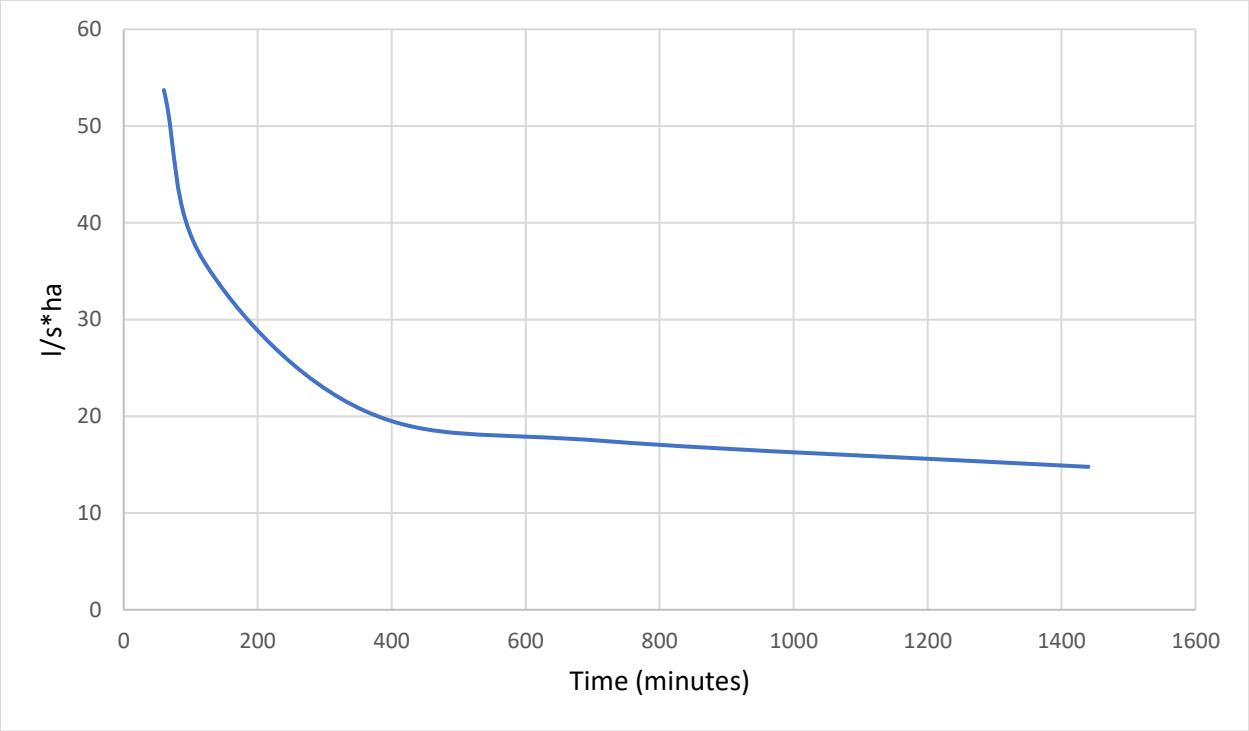

Figure E-9: The local IDF curve for 200-year return period, for P4-4970 catchment.

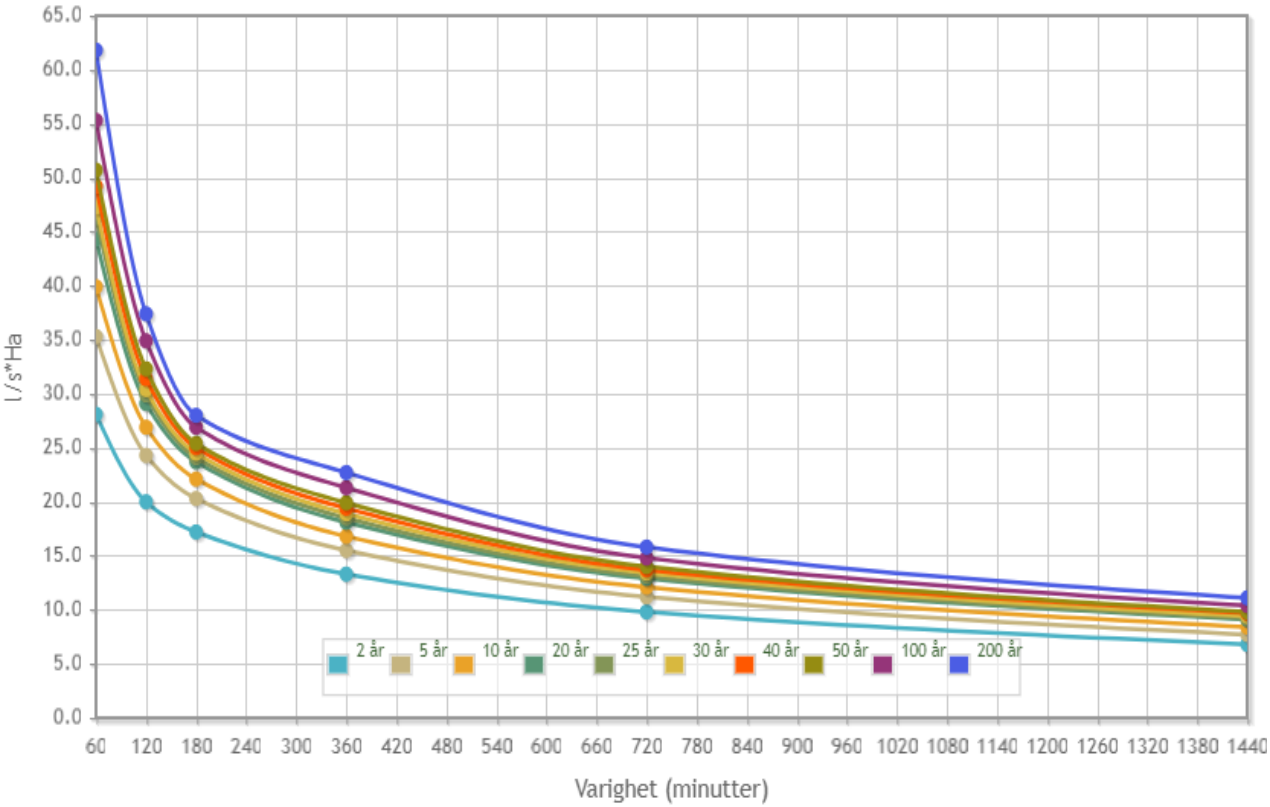

Figure E-10: The online IDF curve, for 200-year return period in blue, for P4-4970 catchment.

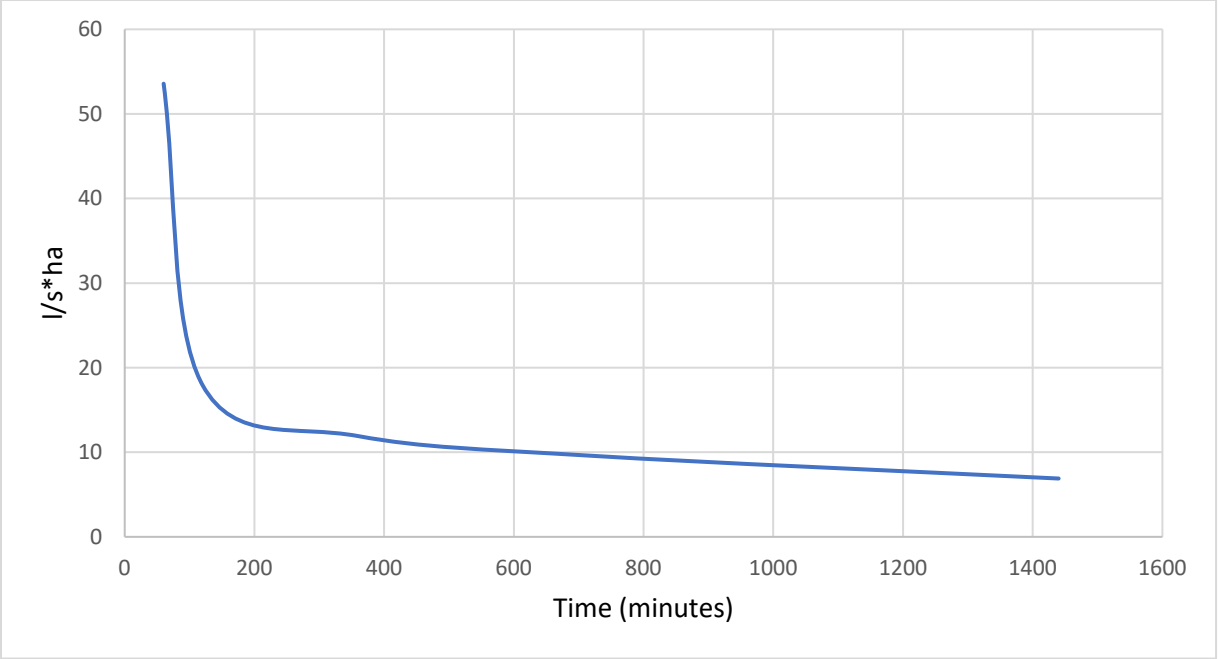

Figure E-11: The local IDF curve for 200-year return period, for P4-2680 catchment.

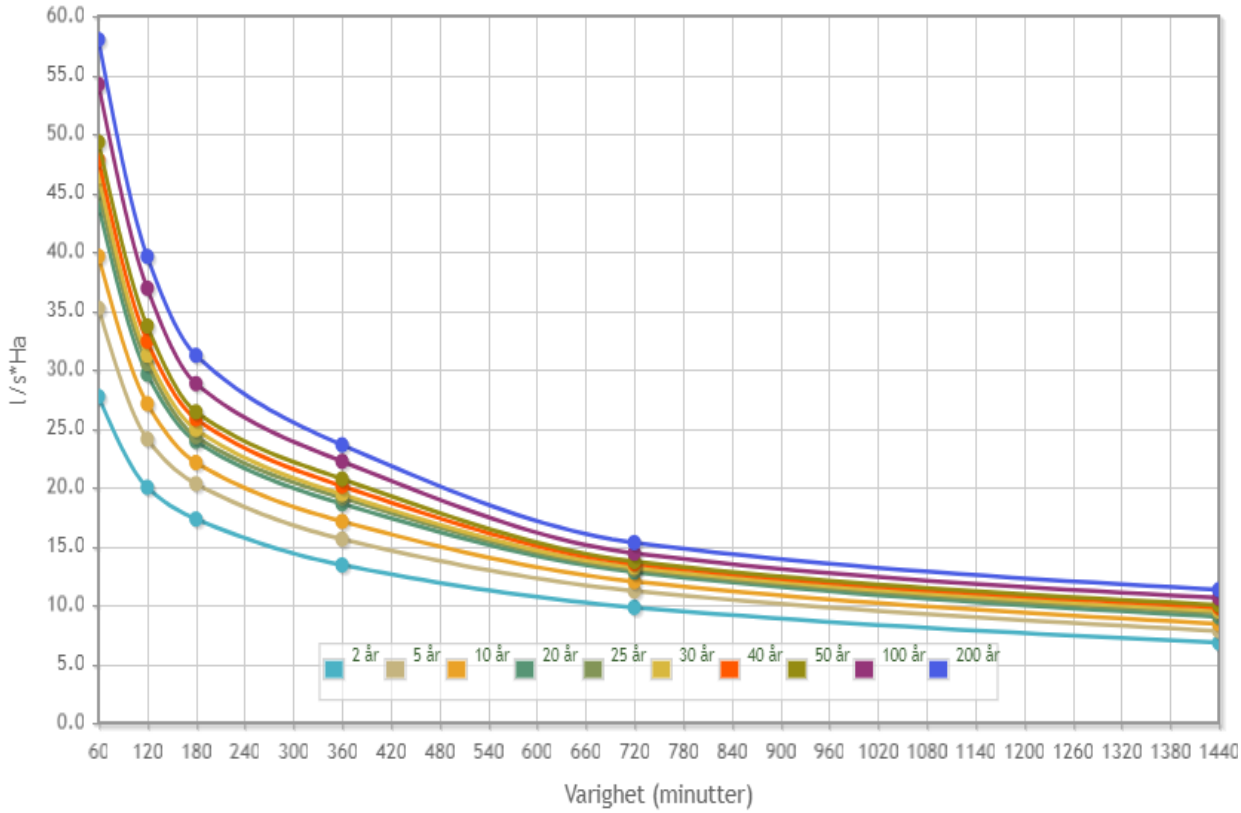

Figure E-12: The online IDF curve, for 200-year return period in blue, for P4-2680 catchment.

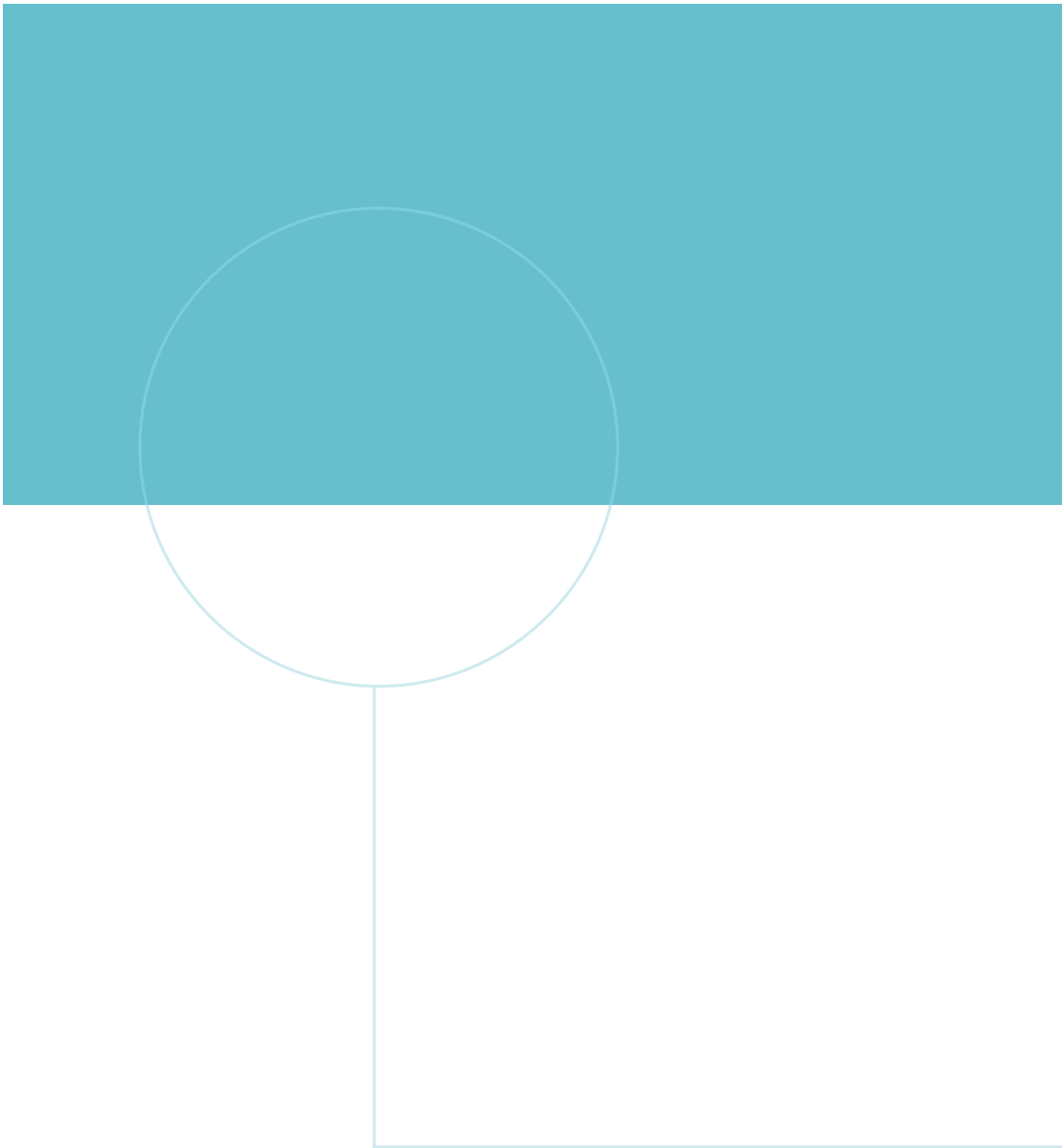

NTNU

Norwegian University of
Science and Technology